Cytosolic recognition of pathogenic nucleic acids

Dissertation

zur

Erlangung des Doktorgrades (Dr. rer. nat.)

der

Mathematisch-Naturwissenschaftlichen Fakultät

der

Rheinischen Friedrich-Wilhelms-Universität Bonn

vorgelegt von

Cristina Amparo Hagmann

aus Manhattan, KS (USA)

Bonn 2010

Angefertigt mit Genehmigung der Mathematisch-Naturwissenschaftlichen Fakultät der Rheinischen Friedrich-Wilhelms Universität Bonn

1. Referent: Prof. Dr. Albert Haas

2. Referent: Prof. Dr. Gunther Hartmann

Tag der Promotion: 22. März 2011

Erscheinungsjahr: 2011

The investigations described in this thesis were carried out at the Institute for Clinical Chemistry and Clinical Pharmacology of the Rheinischen Friedrich-Wilhelms Universität Bonn (Germany)

Erklärung

Diese Dissertation wurde im Sinne von § 4 der Promotionsordnung vom 7.1.2004 im Zeitraum von Dezember 2006 bis Juli 2010 von Herrn Prof. Dr. Hartmann betreut.

Eidesstattliche Erklärung
Hiermit versichere ich, dass ich die vorliegende Arbeit persönlich, selbstständig und unter Offenlegung der erhaltenen Hilfen angefertigt habe.

Bonn, den

Acknowledgements:

Heartfelt thanks to everyone who supported me in the years during my work for this thesis:

I would especially like to thank my advisor Professor Dr. Gunther Hartmann for accompanying me during my thesis and supplying the labs for me to work in. It is thanks to Professor Hartmann that I discovered the fascination and immediacy of clinical research. Professor Hartmann opened my eyes to the wide spectrum of the intricacies of the experimental process; it is with his help that I could familiarize myself with all the aspects of a clinical laboratory.

My most profound thanks goes to my lab head Dr. Martin Schlee. He advised me on all my projects and steered me in the right direction when I felt like I had reached an impasse. His expertise in biochemical and methodological questions were an invaluable help for the course of my thesis. He was always open for discussion and I felt like I could pester him with questions at any time.

Thanks also goes to Professor Dr. Albert Haas who listened to me and my thesis proposal and helped with various aspects of my thesis. I would not have investigated the autophagy-dependent aspect of many experiments if he hadn't suggested it.

I would have been hopeless in the face of all the paperwork if it hadn't been for Christiane Ahlemeyer, our exceptionally talented secretary. She knows all the dos and don'ts around the clinic, and her sunny disposition often brightened my day.

To Bastian Lüdenbach, Dr. Christoph Coch,, Chrissy Schuberth, Anna Herzner, Heike Prange, Jonas Doerr and Christine de Nardo, thank you for helping in the most diverse circumstances. I will always remember the mandarin cake, the editing and revising of my correspondence, the hours spent at the microscope and the countless evenings discussing research details over a glass of grapefruit beer and pizza. Thank you so, so much.

And, of course, thanks to my family. I wouldn't have gone to Bonn if it hadn't been for my mother, I wouldn't have chosen a science major if it hadn't been for my father. They helped make me what I am today.

Summary

The innate immune system senses pathogens by pattern recognition receptors (PRR) located in different cell compartments. Components of the bacterial cell wall and conserved proteins are detected by Toll-like receptors (TLRs) on the cell surface, and by NODs or NOD like receptors (NLRs) in the cytosol of cells. Viruses are recognized via their nucleic acids by TLRs in the endosome and RIG-I like helicases in the cytosol. Even though viral and bacterial DNA possess, with TLR9, a PRR in the endosome, the cytosolic type I inducing DNA receptor (DNAR) has as yet remained elusive. In the first part of this thesis, the minimal recognition motif for the cytosolic DNAR will be investigated. We dissected recognition motifs of short double stranded DNA oligonucleotides (dsODN) in primary monocytes and cell lines and identified two different types of immune stimulatory ODN: In addition to recognition of long dsDNA, including plasmid DNA, human monocytes detected concatamerized short dsODN. Surprisingly, monocytes were also able to recognize short dsODN when harboring mismatched terminal G extensions at 5' and 3' ends (G_n-dsODN). As determined by gel electrophoresis and circular dichroism (CD) spectroscopy under physiological salt and temperature conditions, the G extensions of stimulatory G_3-dsODN did not form G quartet structures, which excluded a polymerization-dependent recognition effect. Fluorescence and FRET-based analysis techniques revealed no considerable difference in uptake and degradation between G-ended and C-ended dsODNs. ShRNA-mediated knock-down experiments revealed involvement of the adaptor molecule MITA downstream of the DNAR in dsODN-mediated signaling. Our results define a new sequence-dependent recognition motif of short cytosolic dsDNA in human immune cells by an as yet unknown DNA receptor.

Like the genetic material of viruses, nucleic acids of bacteria are recognized by TLRs in the endosome. In contrast to exclusively extracellular bacteria, intracellular bacteria have evolved mechanisms to escape the endosome and penetrate into the cytosol, where they are accessible to cytosolic PRRs. *Listeria monocytogenes* infection has been linked to cytosolic nucleic acid sensor-dependent type I IFN induction. Current knowledge indicates that immune cell type I IFN response to Listeria is processed via the bacterial DNA. However, it is tempting to speculate that like DNA, RNA can enter into the cytosol. Using a novel, sensitive labeling method, we were able to show cytosolic access of Listeria RNA during infection. Furthermore, transfection of bacterial RNA into the cytosol of human monocytes or epithelial cells resulted in a type I IFN response, which was dependent on RNA phosphorylation. In contrast to monocytes, epithelial cells were not triggered by bacterial DNA, providing a non-redundant nucleic acid recognition pathway. Notably, knock-down of RIG-I in epithelial cells showed a diminished IFN response to both Listeria RNA and infection. This characteristic was only minimally evident in monocytic cells. We conclude that RIG-I mediated recognition of Listeria monocytogenes plays a role in infection of non-immune cells lacking a mechanism for a direct response to bacterial DNA.

Zusammenfassung

Das angeborene Immunsystem identifiziert Pathogene mittels Pathogenerkennungsrezeptoren (PRR), die sich in verschiedenen Zellkompartimenten befinden. Komponenten der Bakterien-Zellwand und konservierte Proteine werden durch Toll-ähnliche Rezeptoren (TLRs) auf der Zelloberfläche oder durch Nod-ähnliche Rezeptoren (NLR) im Zytosol detektiert. Viren werden über ihre Nukleinsäuren von TLRs im Endosom und RIG-I ähnliche Rezeptoren im Zytosol erkannt. Obwohl die Erkennung von bakterieller- und viraler DNA durch TLR9 im Endosom gut charakterisiert ist, konnte bisher der korrespondierende zytosolische Typ I IFN induzierende DNA-Rezeptor (DNAR) nicht identifiziert werden. Im ersten Teil dieser Dissertation wurde das Minimalerkennungsmotif des zytosolischen DNAR untersucht. Dabei wurden Monozyten und monozytäre Zelllinien mit doppelsträngigen DNA Oligonukleotiden (dsODN) stimuliert und die Typ I IFN-Antwort analysiert. Neben der Erkennung von langer DNA, wie z.B. Plasmid-DNA, reagierten Monozyten auf konkatamerisierte kurze dsODNs und kurze dsODN, wenn diese ungepaarte G_n-Überhänge ($n \geq 2$) aufwiesen (G_n-dsODN). Wie durch Gelelektrophorese und Zirkuläre Dichroismus-Spektroskopie gezeigt wurde, bildeten immunstimulatorische G_3-dsODN keine intermolekularen G-Tetraden aus, was eine Polymerisation und somit eine längenabhängige Erkennung ausschließt. Fluoreszenz- und FRET-basierte Analysetechniken zeigten keinen deutlichen Unterschied bezüglich Aufnahme und Abbau von stimulatorischen G_3-dsODN und nicht-stimulatorischen C_3-dsODN. ShRNA-vermittelte Knock-Down-Experimente zeigten die Beteiligung des Adapters MITA aus dem bisher bekannten DNAR-Signalweg bei G_n-dsODN-induzierter Immunstimulation. Die G_n-dsODN-Struktur stellt somit ein neues sequenzabhängiges Erkennungsmotiv des bisher noch nicht identifizierten DNAR dar.

Ähnlich wie das genetische Material von Viren können bakterielle Nukleinsäuren im Endosom erkannt werden. Im Gegensatz zu rein extrazellulären Bakterien haben intrazelluläre Bakterien Strategien entwickelt, aus Phagolysosomen ins Zytosol zu entkommen, wo sie für zytosolische PRRs erreichbar sind. *Listeria monocytogenes* Infektionen sind mit Nukleinsäurenabhängiger Typ I IFN Induktion assoziiert worden. Bisherige Studien zeigten, dass die Typ I IFN Induktion durch Listerien über bakterielle DNA (bacDNA) erfolgt. Der Transfer und die Erkennung von bakterieller RNA (bacRNA) sollte jedoch ebenso möglich sein. Mittels einer neuen, sensitiven Visualisierungsmethode konnte in dieser Arbeit Listerien bacRNA im Zytosol der Wirtszellen nachgewiesen werden. Die Transfektion von bacRNA ins Zytosol von Epithelzellen oder Monozyten induzierte eine Typ I IFN-Antwort. Jedoch zeigten Epithelzellen im Gegensatz zu Monozyten keine IFN-Antwort auf bacDNA. was auf die Erkennung von bacRNA als nichtredundanten Signalweg schließen lässt. Der Knock-Down von RIG-I bewirkte eine starke Verminderung der Typ I IFN-Antwort in Epithelzellen, jedoch kaum in monozytären Zellen. Dies deutet darauf hin, dass die RIG-I–vermittelte Erkennung von Listerien vor allem eine wichtige Rolle bei der Infektion von nicht-Immunzellen ohne einen Mechanismus der zytosolischen DNA-Erkennung spielt.

1. Introduction

1.1. The components of the innate immune system

The function of an organism's immune response is to protect it from pathogens that would otherwise cause disease. Most higher organisms have two immune responses; the adaptive or acquired immune response and the innate immune response. Adaptive immunity concerns the response and activation of antigen-specific immune cells to the pathogen. It is based on the presence of highly specialized lymphocytes. By contrast, the innate immune system recognizes pathogens by germ line encoded pattern recognition receptors and defends invading pathogens either directly or by activating the adaptive immune response.

1.1.1. Cells of the innate immune system

The cells of the innate immune system are not subject to the clonal selection process present in the adaptive immune system (Forsdyke 1995). Pathogens are recognized by broadly specific cells and their receptors, usually within minutes of infection. To be able to do this, the cells of the innate immune system must be ubiquitous and present in relatively high numbers throughout the organism. Mainly sup-populations of peripheral blood mononuclear cells (PBMC) were analyzed in the course of this thesis (see **Fig. 1.1.**).

1.1.1.1. Peripheral blood mononuclear cells (PBMC)

PBMC, like all leukocytes, originate in the bone marrow from multipotent hematopoietic stem cells (see **Fig. 1.1.**). They are obtained from full blood samples by ficoll density gradient centrifugation.

PBMCs, as such, do not comprise a clearly defined subpopulation of cells, but include all mononuclear cells present in the blood, such as T cells, B cells and NK cells, as well as monocytes, eosinophiles, neutrophiles, myeloid dendritic cells (MDC) and plasmacytoid dendritic cells (PDCs). For this thesis monocytes and PDC are of special interest.

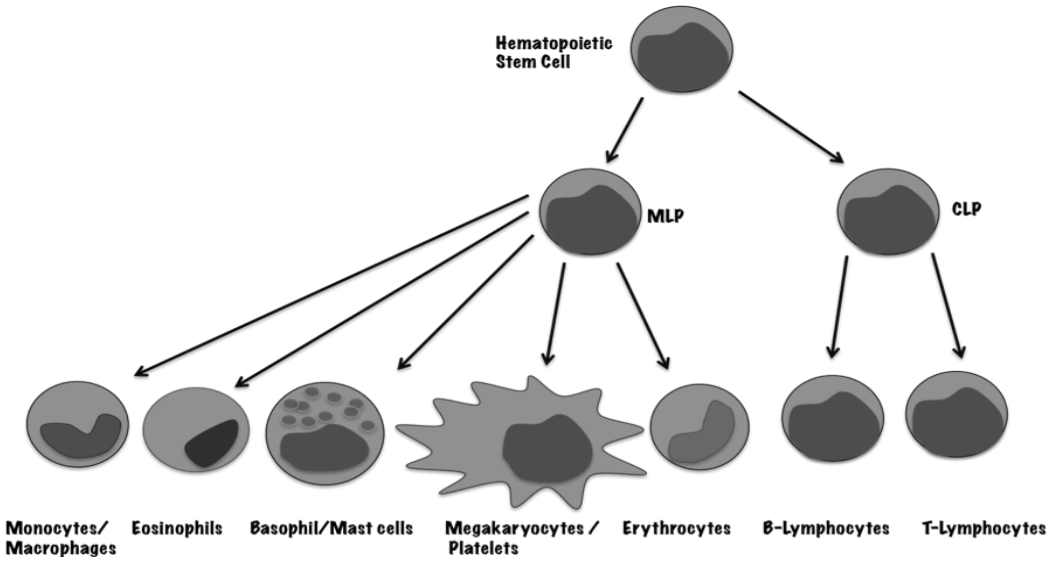

Fig. 1.1: Progenitor cells of the innate immune system. Hematopoetic stem cells give rise to all the lymphocytes of the innate and adaptive immune systems (adapted from (Kenneth Murphy 2008)). MLP= myeloid lymphoid progenitors, CLP = common lymphoid progenitors

1.1.1.2. Monocytes

Monocytes are of special interest because of their response to pathogens and pathogen associated molecular patterns (PAMP). Monocytes make up about 15- 20% of a PBMC population. They reside in the blood and are the precursor cells of macrophages. When in culture, addition of macrophage colony stimulating factor (M-CSF) to monocytes will result in monocyte differentiation to macrophages. Monocytes migrate throughout the body and are phagocytic, but usually differentiate into macrophages when an infection occurs. There are two different populations of monocytes; $CD14^{+hi}$ and $CD14^{+lo}/CD16^{+}$. $CD14^{+hi}$ monocytes differentiate into $CD14^{+lo}/CD16^{+}$ monocytes (Ziegler-Heitbrock 2007). Monocytes, but above all macrophages, migrate to sites of infection and help induce inflammation, alerting the adaptive immune system by presenting antigens to immature lymphocytes and secreting chemokines and cytokines, including IFNα, which will be discussed further on.

1.1.1.3. Plasmacytoid dendritic cells (PDCs)

PDCs are dendritic cells that accumulate in peripheral lymphoid tissues. They secrete copious amounts of type I IFN in response to certain types of DNA or RNA stimulus and are therefore of great interest when researching nucleic acid-induced immune responses. They do not play a particularly large role in presenting antigens to naive T cells. They express surface markers such as blood dendritic cell antigen 2 (BDCA-2) and CD123, but no CD11c or CD14, the markers for DCs and monocytes, respectively (Shortman and Liu 2002). They recognize DNA

sequences which contain unmethylated CpG dinucleotides (Hartmann and Krieg 2000; Krug, Rothenfusser et al. 2001) and GU-containing RNA (Heil et al. 2004, Hornung et al., 2005). CpG containing DNA functions as the ligand for Toll-like receptor 9 (TLR9), a receptor vigorously expressed in PDCs (Bauer and Wagner 2002). RNA is recognized by TLR7 (Heil et al. 2004, Hornung et al., 2005).

Blocking the PDC-derived IFN response is accomplished by inhibiting endosome maturation, the localization of TLR9. Chloroquine halts the early endosome from lowering its pH, thus preventing TLR9 and TLR7 from activation (Rutz, Metzger et al. 2004).

1.1.2. Receptors of the innate immune system

The innate immune response functions as a highly complex combination of cells and their associated receptors. As had been mentioned previously, the innate immune system is capable of broadly distinguishing bacterial from viral infection: Pattern recognition receptors (PRR) are capable of distinguishing and binding to ligands characteristic of pathogens, such as components of the cell wall, (e.g. lipopolysaccharide (LPS)) the locomotor system (e.g. flagellin), or nucleic acids with unusual structure, modification or location (Kawai and Akira). Researching these receptors and their ligands is of great interest precisely because they are part of the innate immune system and, therefore, on call practically immediately in the event of an infection. Finding out how to be able to use this characteristic for therapeutic purposes should be a fascinating endeavor.

1.1.2.1. Toll-like receptors and their ligands

Toll like receptor localization

TLRs are members of the TLR-Interleukin (IL)-1 superfamily. They are membrane-spanning receptors and reside either on the cell membrane or in cellular compartments such as the endosome. TLRs are expressed by most antigen-presenting cells (APCs) of the innate immune system, such as monocytes and macrophages, although subpopulations differ concerning which TLRs are expressed (Iwasaki and Medzhitov 2004). Ten different TLR genes have been discovered in higher organisms, each recognizing a different pathogen-associated molecular pattern (PAMP) (see Fig. **1.2.**). (Medzhitov and Janeway 2000),(Barton and Medzhitov 2002).

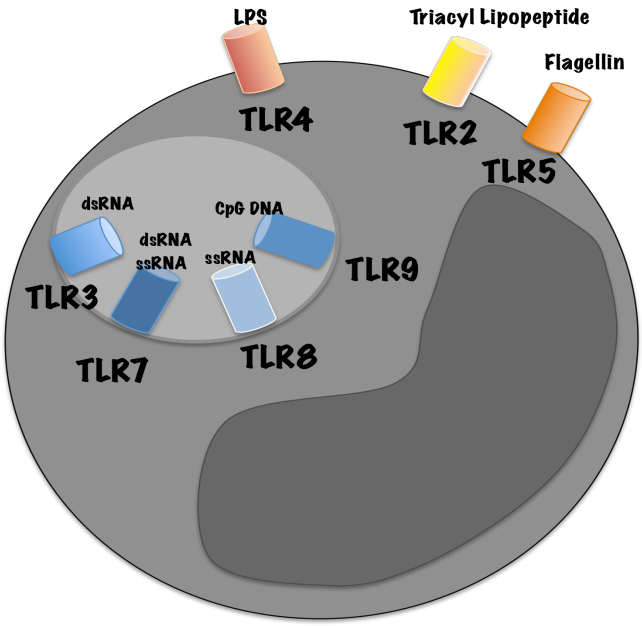

Fig. 1.2: Cellular localizations and ligands of TLRs in human cells. TLRs 2, 4 and 5 recognize bacterial lipopeptides, TLR4 recognizes LPS and TLR5 flagellin. The endosomally located TLRs 3, 7 8 and 9 recognize dsRNA, ssRNA and CpG DNA, respectively.

TLRs are comprised of a leucine-rich-repeat (LRR) ectodomain, which represents the receptor half of the protein, and a cytoplasmic domain which is homologous to the IL-1 receptor. (Xu, Tao et al. 2000).

Toll- like receptors 1, 2, 4, 5 and 6

TLRs can be classified into two main groups; the receptors that recognize pathogen cell wall components such as LPS and flagellin and are themselves located on the cell surface, such as TLRs 1, 2, 4, 5 and 6 (see **Fig. 1.2.**). The second group is composed of TLRs that bind to pathogenic nucleic acids and are situated in the endosome, such as TLRs 3, 7, 8, 9. (see **Fig. 1.2.**) (Du, Poltorak et al. 2000). Endosomally located TLRs require endosomal maturation in order for them to recognize their ligands (Ahmad-Nejad, Hacker et al. 2002).

Concerning the cell-surface TLRs, TLR2 binds to lipoteichoic acids (LTA) of gram positive and lipoproteins of gram negative bacteria (Dziarski and Gupta 2000). On macrophages, LPS is recognized by TLR4, in association with cluster of differentiation (CD) 14 and MD-2 (Medzhitov, Preston-Hurlburt et al. 1997; Dziarski and Gupta 2000; Rhee and Hwang 2000). TLR5 recognizes flagellin. (Hayashi, Smith et al. 2001), while TLR6 usually acts in concert as a heterodimer with TLR2 or TLR1. Binding of these ligands to their corresponding receptors results in the production of cytokines with very different effects; TLR2 results in tumor necrosis factor alpha (TNFα) induction while TLR4 can induce type I IFN as well as TNFα (De Trez, Pajak et al. 2005).

Toll-like receptors 3, 7, 8 and 9

In the endosome, TLR3 recognizes double stranded (ds) RNA, which is generated during viral infections (Alexopoulou, Holt et al. 2001). TLR3 binds to its ligand as a dimer (Liu, Botos et al. 2008). Activation of TLR3 results in induction of type I IFN. This PAMP is quite useful, because most viruses produce dsRNA at some point during their replication.

TLR7 and TLR8 share a high homology in humans. They reside in the endosome of PDCs (TLR7) and monocytes (TLR8) (see **Fig. 1.2.**), respectively (reviewed in (Barchet, Wimmenauer et al. 2008)). They are activated by ssRNA (TLRs 7, 8) or dsRNA (TLR7), which although also a motif naturally occurring in human cells, avoids autoimmune recognition by localization of TLR7 and TLR8 in the endosome. Human TLR7 and TLR8 had been shown to recognize the synthetic compound imidazoquinoline, which is similar to guanosine in structure (Heil, Ahmad-Nejad et al. 2003). Guanosine and uridine-rich strands, such as occur in vesicular stomatitis virus or influenza virus life cycles, are readily recognized by TLR7 and TLR8 (Diebold, Kaisho et al. 2004; Heil, Hemmi et al. 2004; Lund, Alexopoulou et al. 2004; Hornung, Guenthner-Biller et al. 2005). Activation of TLR 7 results in type I IFN induction.

Predominantly found in PDCs (Krug, Rothenfusser et al. 2001; Hornung, Rothenfusser et al. 2002), TLR9 is the only endosomal receptor to recognize DNA (see **Fig. 1.3.**). It is preferentially activated by CG containing DNA motifs (Hemmi, Kaisho et al. 2003). TLR9 is recruited to the endosome from the endoplasmatic reticulum (ER); once there, it is proteolytically cleaved and activated (Hacker, Mischak et al. 1998; Ahmad-Nejad, Hacker et al. 2002) (see **Fig. 1.3.**). Unmethylated CpG DNA is one of the characteristics of bacterial DNA (mammalian cytosine is highly methylated) and therefore an easily recognizable PAMP (Heeg, Sparwasser et al. 1998; Hartmann and Krieg 2000). CpG DNA can induce both the antiviral cytokine type I IFN, as well as the inflammatory cytokine IL-12 (Krug, Towarowski et al. 2001). TLR9 recognition of CpG DNA is, however, not restricted to bacterial CpG DNA; virally-produced CpG DNA has also been shown to induce type I IFN in PDCs (Krug, Luker et al. 2004). IgG-coupled DNA-based induction of IFN by TLR9 also has a role in autoimmune diseases; internalized chromatin binds to TLR9 and is one of the mechanisms thought to be involved in systemic lupus erythematosus (SLE) (Boule, Broughton et al. 2004).

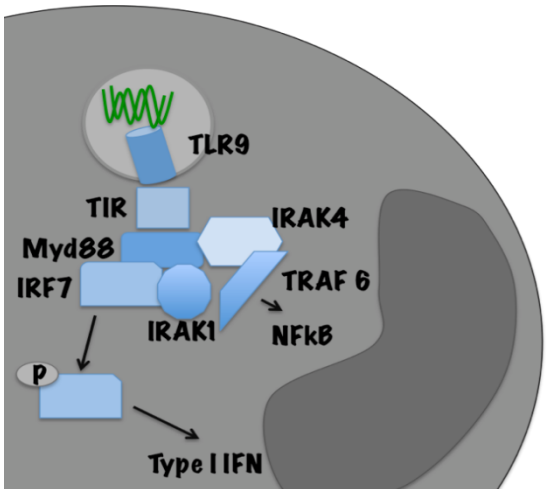

Fig. 1.3: TLR9 localization and signaling pathway. Originally situated in the ER, TLR9 translocates into the endosome. Once bound to CpG-DNA, the IFN signaling pathway is activated, recruiting MyD88, IRAK4 and IRAK 1, which in turn activate IRF7 and NFkB.

1.1.2.2. TLR signaling pathways

There are two main pathways of TLR signaling; the MyD88-depdendent and MyD88-independent pathway (see Fig. **1.4.**).

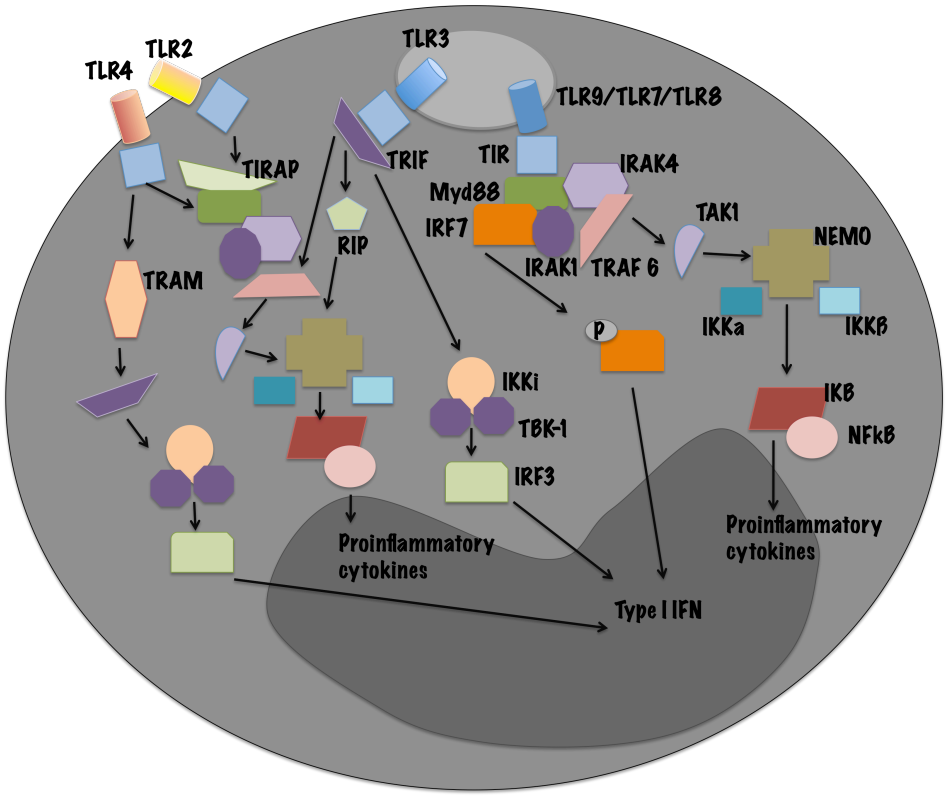

Fig.1.4: TLR signaling pathways. After a TLR binds to its ligand, two main transcription factors are activated, mostly resulting in production of inflammatory cytokines or type I IFN. MyD88 is recruited to the TIR domains of TLRs 1, 2, 4, 5 and 6. Once there, it recruits IRAK4, 1 and 2, which phosphorylate TRAF6. This leads to ubiquitinylation of TAK1, activation of IKKα and β and dissociation of IkB from NF-κB. TRIF is recruited upon TLR3 activation and interacts with TRAF6 and the IKKi/TBK1 complex, resulting in IRF3 phosphorylation and induction of type I IFN.

The MyD88-dependent pathway

TLR-mediated cytokine induction is dependent on the adaptor protein in the cytoplasm relaying the TLR signal (Rifkin, Leadbetter et al. 2005). The main adaptor molecule, MyD88, binds to all the TLRs except for TLR3 and, in some cases, TLR4 (see Fig. **1.4**.). It starts a signaling pathway inducing cytokines such as IFNα, IL-12p40 and IL-6. MyD88 recruits IL-1 receptor associated kinases (IRAK). IRAK-1, 2 and 4 are of great importance for the MyD88-dependent pathway (Suzuki, Suzuki et al. 2002); they activate the E3 ligase tumor necrosis receptor associated factor 6 (TRAF6). TRAF6 transmits the signal to TGFβ-activated kinase (TAK1). Once phosphorylated, TAK1 activates the NFkB pathway via IkB kinase (IKK). A protein similar to MyD88, TIR domain containing adaptor protein (TIRAP), has been found to function together with MyD88 in TLR 2 and 4 pathways, but not for TLRs 7, 8 and 9, affording a tidy signaling specificity for MyD88-dependent TLR pathways (Horng, Barton et al. 2002; Kagan and Medzhitov 2006) (see Fig. **1.4**.). The endosomal receptors TLRs 7 and 9 in PDC recruit MyD88, which, after activating the IRAK4-TRAF6 complex, phosphorylates IRF7. IRF7, structurally very similar to IRF3, translocates to the nucleus and induces IFNβ production (Honda, Yanai et al. 2005) (see Fig. **1.4**.).

The TRIF-dependent pathway

MyD88 is not involved in the TLR3 pathway and only partly involved in the TLR4 pathway; MyD88-deficient macrophages showed only a slight delay of the NFκB pathway when confronted with LPS (Kawai, Adachi et al. 1999). The TIR-domain containing adaptor protein inducing IFNβ (TRIF) is the cornerstone of the MyD88-independent pathway (Yamamoto, Sato et al. 2003). TRIF is recruited to TLRs 3 and 4, then recruits Tank binding kinase-1 (TBK1), which phosphorylates IRF3 (Fitzgerald, McWhirter et al. 2003; Honda and Taniguchi 2006). TRIF also recruits TRAF6, together with RIP1; they complex with TAK1, activating NFκB. This combines MyD88-independent and dependent pathways (Cusson-Hermance, Khurana et al. 2005). As TLR4 is part of both the MyD88-dependent and independent pathways, it is possible that TLR4 first induces TIRAP-MyD88 signaling at the plasma membrane and is then endocytosed and activates TRAM-TRIF signaling from early endosomes (Kagan, Su et al. 2008).

1.1.2.3. RNA helicases and their ligands

The innate immune system is comprised not only of membrane-bound TLRs, but also includes cytosolic PRRs. Some of the best-known cytosolic nucleic acid receptors are the helicases RIGI and Mda-5 (Yoneyama, Kikuchi et al. 2004; Kawai and Akira 2006). They both recognize pathogenic RNA in the cytosol, but very different motifs (see **Fig. 1.5.**).

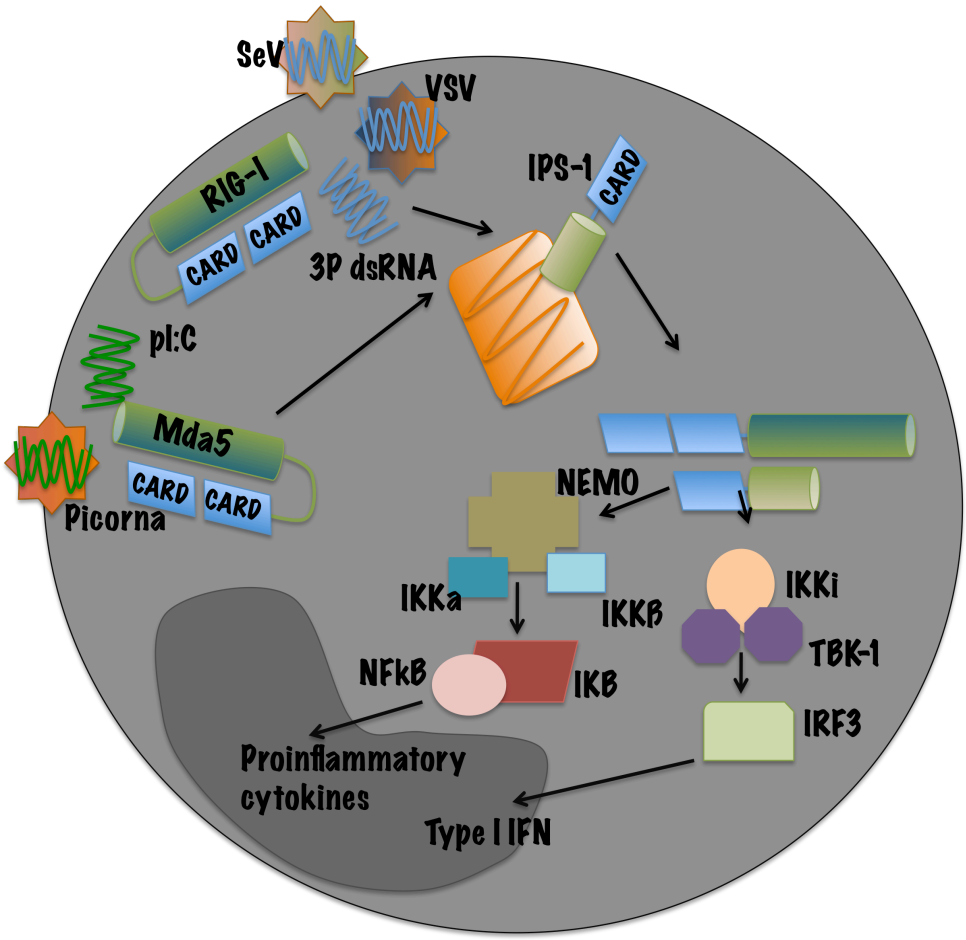

Fig. 1.5: Cytosolic recognition of RNA. RNA from picornaviruses and the synthetic RNA strand pI:C are recognized by Mda-5. Short 5' triphosphate dsRNA is recognized by RIG-I. Once activated, the CARD domains of the helicases associate with IPS-1 and induce either a type I IFN response or result in the production of inflammatory cytokines.

RIG-I

Retinoic acid-inducible gene I possesses two caspase recruitment (CARD)-like domains, which are crucial for interaction with adaptor proteins further downstream on the activation pathway. They associate with IFNβ stimulator-1 (IPS-1), located on the outer membrane of mitochondria. IPS-1, in turn, activates NFkB signaling through Fas-associated death domain protein and RIP-1 (Kawai, Takahashi et al. 2005). An alternative signaling pathway includes IKKi and TBK-1 in order to phosphorylate IRF3 for IFNβ induction (see **Fig. 1.5.**).

RIG-I is present in its inactive form in the cytosol and is activated only upon presence of dsRNA in the cytoplasm. 5'-triphosphorylated dsRNA is vitally necessary for an IFN response. 5' triphosphate, uncapped RNA is atypical for the human cell and as such well suited as a PAMP. The cellular RNAs nonetheless present in the cytosol carry modifications such as pseudouridine and 2'O methyl. They therefore do not activate RIG-I (Hornung, Ellegast et al. 2006). ATP hydrolysis is needed for the CARD domains to become accessible for IPS-I binding (Yoneyama, Kikuchi et al. 2004) (see **Fig. 1.6.**). Inactive, RIG-I is a monomer; hydrolysis leads to dimerization and the possibility of CARD-CARD interactions with IPS-I (Kawai, Takahashi et al. 2005) (see **Fig. 1.5.**). In our lab, it has recently been found that short dsRNA with a 5' triphosphate is preferentially recognized, although the main criterion is base pairing at the 5' triphosphate end and not a complete double-stranded sequence (Schlee, Roth et al. 2009). Recent publications have demonstrated that the long dsDNA sequence poly(dA-dT) is also recognized by RIG-I after having been transcribed into RNA by RNA polymerase III (Ablasser, Bauernfeind et al. 2009), therefore planting a long-thought DNA receptor ligand firmly into the RIG-I domain.

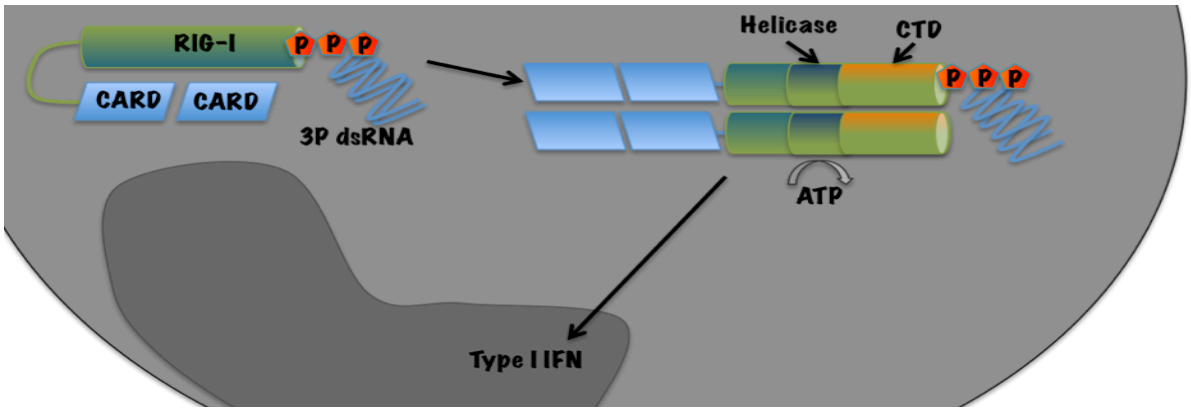

Fig.1.6 Structure and function of RIG-I. The two CARD domains associate with each other and with IPS-I upon ATP-dependent binding of short dsRNA sequences. The C-terminal regulatory domain (CTD) binds RNA, but only if it has a 5' triphosphate. It thus activates the RIG-I ATPase, enabling the CARD domains to dimerize and bind to IPS-I.

Mda-5

Melanoma differentiation associated gene 5 shows a certain amount of homology to RIG-I (Yoneyama, Kikuchi et al. 2005) (see **Fig. 1.5.**). It is the receptor that recognizes RNA from viruses which do not possess 5'triphosphorylated genomic RNA, like picornaviruses, which are not recognized by RIG-I (Gitlin, Barchet et al. 2006; Kato, Takeuchi et al. 2006). This, along with the different ligand motifs concerning either helicase, namely short 5' triphosphate dsRNA for RIG-I and long, intermittently double-stranded picornavirus RNA strands, shows that the receptors are by no means to be considered redundant (Kato, Takeuchi et al. 2008).

RIG-I and Mda-5 signaling pathways

RIG-I and Mda-5 share signaling pathways, ending in either induction of type I IFN or proinflammatory cytokines (see **Fig. 1.5.**). Once the RNA ligand of choice is bound to the receptor, the CARD domains recruit IPS-1 (Kawai, Takahashi et al. 2005; Meylan, Curran et al. 2005; Seth, Sun et al. 2005; Xu, Wang et al. 2005). IPS-1 has a CARD domain, a proline-rich-region (PRR) and a transmembrane domain at its C-terminal end. IPS-1 is therefore permanently located at the mitochondrial membrane. It recruits proteins on the NFkB signaling pathway, TRAF6 and TRAF2 (see **Fig. 1.7.**). Meanwhile, TRAF3 binds to the PRR in the middle of IPS-1 and uses ubiquitin to form a scaffold of sorts for the IKKe-TBK1 complex. This complex phosphorylates IRF3 and 7, ultimately resulting in type I IFN induction (see Fig. **1.7.**) (Kawai, Takahashi et al. 2005; Meylan, Curran et al. 2005; Xu, Wang et al. 2005).

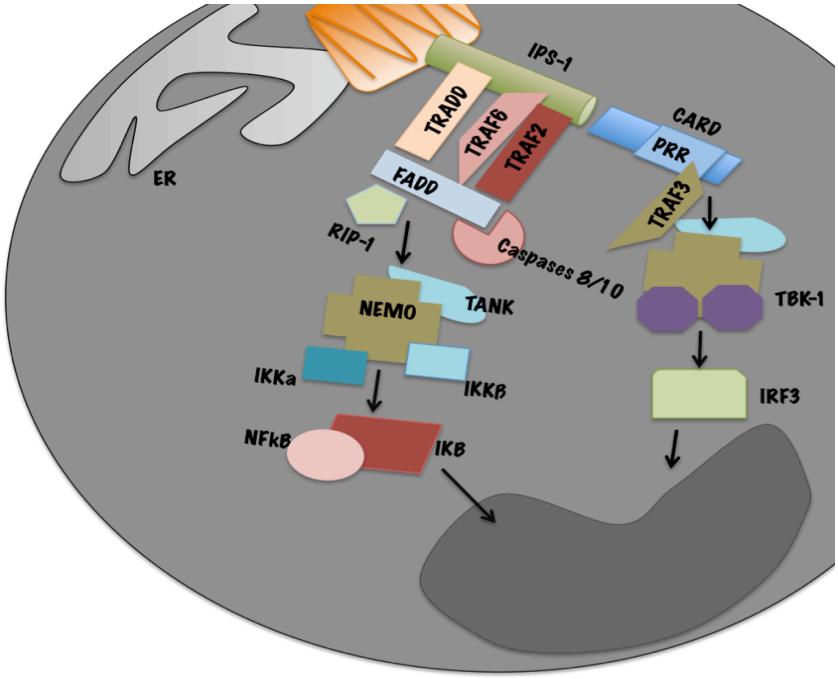

Fig 1.7.: Both arms of the signaling pathway of RIG-I/Mda-5 going via IPS-1. Upon binding, TRADD and TRAF6/2/3 associate with IPS-1 and recruit NEMO-IKK and NEMO-TBK-1 complexes. This ensures that both the NFkB and IRF3/IRF7 pathways are triggered.

1.1.2.5. DNA recognition in the cytosol

Rotem *et al* (Rotem, Cox et al. 1963) had discovered an IFN response to murine and yeast nucleic acids in chick fibroblasts, a 1963 finding which had not been further investigated until the end of the 20th century (Yamamoto, Yamamoto et al. 1992). After multiple groups discovered IRF-3 dependent recognition of DNA in the cytosol (Ishii, Coban et al. 2006; Stetson and Medzhitov 2006), the spotlight was on the cytosolic DNA receptor. The clinical relevance of cytosolic DNA recognition is self-explanatory. Cytosolic DNA can have multiple

origins, be it from apoptotic cells (Ishii, Suzuki et al. 2001), DNA viruses or certain types of bacteria (Stetson and Medzhitov 2006). Autoimmune responses to self-DNA are linked to systemic lupus erythematosus (SLE) (reviewed in (Rahman and Isenberg 2008)). In the past years, various components of cytosolic recognition of DNA have been discovered.

Z-DNA binding protein-1 (ZBP-1)

A type I IFN response dependent on a cytosolic DNA receptor was published in 2007 (Takaoka, Wang et al. 2007). Originally named ZBP-1, it had been discovered in tumor stromal cells and later also localized in immune cells (Schwartz, Behlke et al. 2001; Deigendesch, Koch-Nolte et al. 2006). As evidenced in the name, ZBP-1 was found to bind Z-form DNA. Z-form DNA possesses a left-handed double helical structure in which its helix winds clockwise with very little difference between its minor and major grooves. Some of the characteristics of ZBP-1 made it exceedingly interesting as a possible cytosolic DNA receptor: it was IFN inducible, it had similar DNA-binding domains to an RNA editing enzyme and had multiple C-terminal serine/threonine phosphorylation sites (Fu, Comella et al. 1999; Takaoka, Wang et al. 2007). Takaoka *et al* overexpressed ZBP-1 and could show an IRF-3 dependent type I IFN response to B-DNA. B-DNA presents itself as a right-handed double helical structure. It is the most common of the three DNA forms A, B and Z. ZBP-1 was demonstrated to colocalize with TBK-1 and IRF3. When ZBP-1-siRNA treated cells were infected with DNA virus or transfected with poly(dA-dT), the IRF-3 activation and subsequent type I IFN induction was reduced. DNA was shown to bind to ZBP-1 irrespective of sequence, but lengths below 100bp were poorly recognized (Takaoka, Wang et al. 2007) (see **Fig. 1.8.**).

All of these discoveries hinted at ZBP-1 being the cytosolic DNA receptor, but two later papers disproved this theory. Ishii *et al* showed that cells from ZBP-1 and MyD88/TRIF knockout mice still showed a robust IFN response in answer to B-DNA vaccination or transfection, thus rendering ZBP-1 non-essential (Ishii, Kawagoe et al. 2008). Lippmann *et al* overexpressed human ZBP-1 or ZBP-1ΔZα, a splice variant lacking one of the DNA binding domains, in human A549 cells. They found no effect on IFNβ production in A549 cells infected with bacteria or transfected with poly(dA-dT). Nor did ZBP-1 siRNAs suppress IFNβ expression in response to bacterial or poly(dA-dT) stimulation (Lippmann, Rothenburg et al. 2008). This finding is of particular interest because both poly(dA-dT) and intracellular bacteria are thought to be, in part, recognized via RIG-I (Ablasser, Bauernfeind et al. 2009). The latter will be discussed as part of this thesis later on.

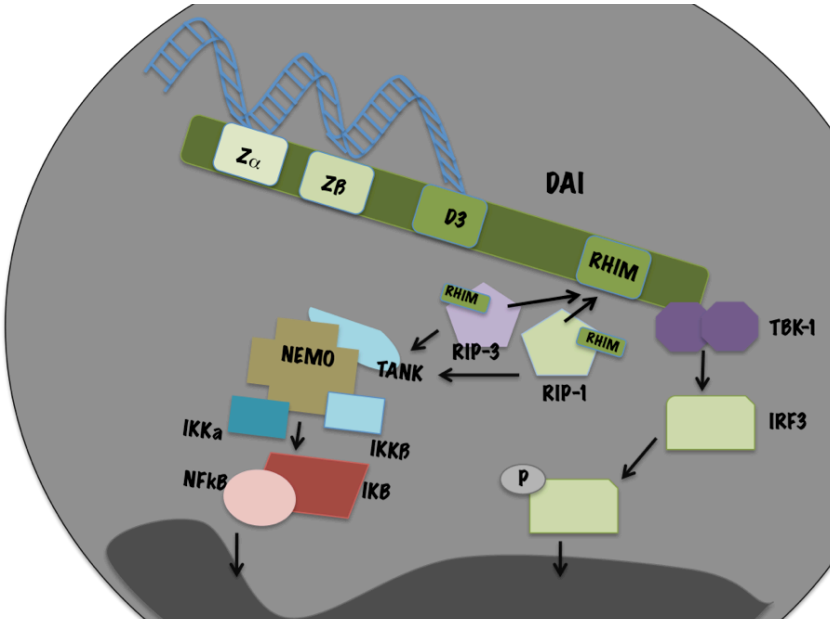

Fig. 1.8.: ZBP-1/DAI and its signaling, proposed by (Takaoka, Wang et al. 2007). The Zα, Zß and D3 domains of DAI bind to dsDNA, with the RHIM recruiting RIP3 and RIP1, which in turn initiate the NEMO and TBK-1 signaling pathway. RHIM: RIP homotypic interaction motif, RIP: receptor-interacting protein kinase 1

DNAses

Endogenous DNA is not usually found in the cytosol but rather restricted to the nuclear envelope or the mitochondria. Exceptions are replication and cell death. Mammalian DNA found where it shouldn't be is digested by the host DNases I, II and III. They degrade DNA found in the extracellular space, the endosome and the cytosol (Murai, Yamanaka et al. 1980; Mazur and Perrino 1999; Oliveri, Daga et al. 2001). Stabilizing DNA with phosphothioate modifications results in heightened type I IFN induction (Haas, Metzger et al. 2008).

DNaseI is an endonuclease that reduces long chromatin strands in necrotic cells to short, non-immunogenic dsDNA segments. DNase I deficiency in mice leads to SLE-type symptoms, an indication that mutations in the human DNAse I gene are one of the factors in SLE (Yasutomo, Horiuchi et al. 2001).

The endonuclease DNase II is involved in DNA clearance from apoptotic cells and works best in an acidic environment. Deficiency of DNase II leads to accumulation of dsDNA in macrophages and is lethal in mice. It can, however, be rescued by knocking out the IFN receptor 1 (IFNR1). Even with this rescue, though, mice develop symptoms mimicking rheumatoid polyarthritis (Yasutomo, Horiuchi et al. 2001).

The intensely studied exonuclease DNase III (or TREX1) has been tapped as having a proofreading function for the human DNA polymerase (reviewed in (Vilaysane and Muruve 2009)). TREX1 localizes to the ER and regulates accumulation of ssDNA that could initiate

an innate immune response to DNA. TREX1-deficient mice developed inflammatory myocarditis and cardiomyopathy within months (Morita, Stamp et al. 2004). When bred to IRF3 or IFNR1-deficient mice, the TREX1 knockout did not result in medium-term lethality. This demonstrated that TREX1 was intimately associated with IRF3-dependent IFN induction (Stetson, Ko et al. 2008). Although TREX1 may not be a candidate for the role of cytosolic receptor, the connection to IRF3 and the type I IFN response is not to be neglected.

Absent in melanoma 2 (AIM-2)

In addition to the TLR family and the RIG-I-like helicases (RLH), another family of innate receptors has been thoroughly investigated: the nucleotide-binding domain leucine rich repeat (NLR) family. NLRs are cytosolic PRRs, but differ from TLRs and RLH in that they do not induce a type I IFN response, mediating caspase I activation and NFκB signaling instead. The receptor family has certain similar features in its composition: LRRs, signaling and NOD domains. Some NLRs bind microbial components (Franchi, Eigenbrod et al. 2009), but most NLRs are part of inflammasomes, a collection of complexes that activate caspase 1 to cleave pro-IL1 to its active form (reviewed in (Petrilli, Dostert et al. 2007)). AIM-2 recruits the caspase-1 protease in response to binding of dsDNA (Burckstummer, Baumann et al. 2009; Hornung, Ablasser et al. 2009).

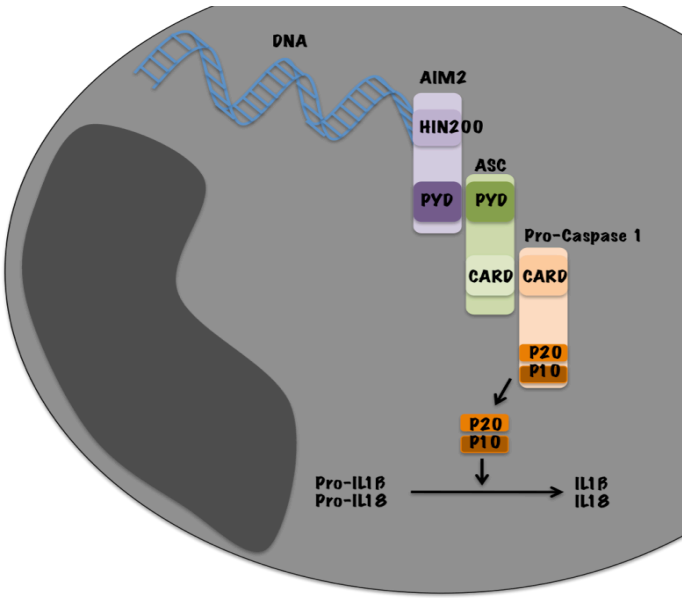

Fig. 1.9.: AIM-2 and cytosolic dsDNA. The AIM-2 inflammasome interacts with dsDNA via its HIN200 domain. The PYD domain recruits ASC, which in turn associates with Pro-caspase 1. Pro-caspase 1 cleaves pro-IL-1β and pro-IL18 to soluble IL-1β and IL-18

AIM-2 is a member of the HIN200 family and expressed in the cytoplasm (see **Fig. 1.9.**). Other HIN2000 family members, such as Ifi16 and IfiX are not cytoplasmic, but rather found

in the nucleus (Roberts, Idris et al. 2009). It binds directly to cytoplasmic DNA via its HIN200 domain, oligomerizes, and recruits the adaptor protein ASC via its PYD domain, thus initiating the pro-IL-1β cleavage process (see **Fig. 1.9.**). Caspase recruitment occurred with mammalian, synthetic, viral and bacterial DNA (Hornung, Ablasser et al. 2009) (Fernandes-Alnemri, Yu et al. 2009).

Mediator of IRF3 activation (MITA)/stimulator of interferon genes (STING)

Recently, a new adaptor protein has been discovered. Two groups had simultaneously identified a membrane protein that could activate IRF3 and, therefore, induce a type I IFN response to viral infection. Dubbed either MITA or STING, the protein was found to contain multiple transmembrane domains and to colocalize with the RIG-I adaptor protein IPS-1 (Ishikawa and Barber 2008; Zhong, Yang et al. 2008). Originally found to interact with IPS-1, it was also mentioned that the IFN response to cytosolic dsDNA was also abrogated when MITA was inhibited. Further publications then cemented the necessity of MITA presence for cytosolic dsDNA-induced IFN (Ishikawa, Ma et al. 2009).

MITA is an ER resident transmembrane protein. It interacts with IPS-1 and RIG-I, and participates in the type I IFN induction pathway (Sun et al., 2009) (see **Fig. 1.10.**). MITA was shown to not be involved in the TLR pathway (Ishikawa and Barber 2008), and did not co-immunoprecipitate with Mda-5. MITA-deficient cells could not induce type I IFN production in response to transfected poly(dA-dT), viral DNA or *Listeria monocytogenes* (Ishikawa and Barber 2008). TBK1-mediated phosphorylation of MITA was critical for virus-triggered activation of IRF3 (Zhong, Yang et al. 2008).

Ishikawa *et al* found that IFNβ production in MITA-deficient MEFs was abrogated in response to oligonucleotide dsDNA containing or lacking CpG sequences, viral DNA and *L. monocytogenes*. $MITA^{-/-}$ macrophages transfected with dsDNA revealed that MITA functioned independently of the AIM2 inflammasome. $MITA^{-/-}$ plasmacytoid dendritic cells, however, still induced a type I IFN response to exogenous CpG DNA, thus confirming the MITA-independent TLR9 response (Ishikawa, Ma et al. 2009).

The localization of MITA between the ER and the mitochondria would imply MITA to be a junction point linking RIG-I and dsDNA-mediated innate immune responses (see **Fig. 1.10.**). This way it could detect viral RNAs in translation in addition to DNAs, inducing antiviral immunity via TBK1. A MITA/TBK1 complex is formed following transfection with DNA and then shuttles to endosomal compartments leading to a robust

innate immune response (Ishikawa and Barber 2008; Zhong, Yang et al. 2008; Ishikawa, Ma et al. 2009).

Although a role for MITA as the central adaptor protein mediating both intracellular DNA and negative-stranded RNA virus IFN responses in all cell types is well established, many questions remain unanswered, first and foremost of course the receptor molecule that bridges the gap between intracellular DNA detection and type I IFN induction.

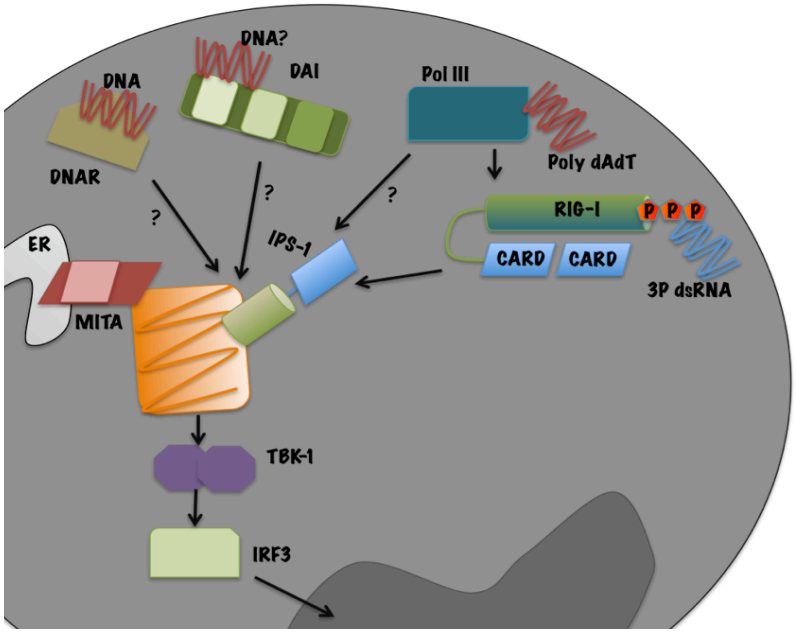

Fig. 1.10.: MITA signaling pathways. MITA has been shown to be a transmembrane protein resident in the ER. MITA interacts with IPS-1. Interactions of the DNAR, DAI, or a direct interaction with RNA polymerase III without going via RIG-I are all hypothetical and currently under investigation.

1.1.3. Clinical relevance of cytokines of the innate immune system

Cytokines are signaling substances secreted by cells of the immune system, facilitating cellular communication. They are immunomodulating agents that are of great interest for their therapeutic application, but also for further elucidation of infection pathways. Cytokines can be broadly divided into two groups, those that favor cellular immune responses and those that favor antibody responses (Cannon 2000). The following section will briefly introduce the cytokines of interest in investigating recognition of pathogens and their nucleic acids.

1.1.3.1. Interleukins 1α and 1β

The proinflammatory chemokine IL-1 was discovered to induce fever, control lymphocytes, increase the number of bone marrow cells and cause degeneration of bone joints. It consists of two isoforms, IL-1α and IL-1β (March, Mosley et al. 1985; Dinarello 1994).

IL-1α

IL-1α is a pleiotropic cytokine that plays a role in multiple immune responses, inflammatory processes, and hematopoiesis. It is manufactured by monocytes and macrophages as a proprotein, which is proteolytically processed and released in response to cell injury, inducing apoptosis (March, Mosley et al. 1985).

IL-1α in disease

Polymorphism of the IL-1A genes could be associated with rheumatoid arthritis and Alzheimer's disease (Hu, Li et al. 2009), which is of interest because rheumatoid arthritis is also associated with TREX1 deficiency and can therefore considered to be affiliated with nucleic acid-based disease. IL-1α has also been demonstrated to be essential for maintenance of skin barrier function, especially with increasing age (Hu, Wang et al. 2003; Barland, Zettersten et al. 2004).

IL-1β

The IL-1β precursor pro-IL-1β is cleaved by the cytosolic caspase 1 (as described for the AIM-2 inflammasome). A thiol protease splits the product to give mature IL-1β, which is an important mediator of the inflammatory response, and is involved in cell proliferation, differentiation, and apoptosis (March, Mosley et al. 1985). Synthesis of IL-1β is induced by, among others, TLR agonists such as LPS or nucleic acids. The precursor of IL-1β is present in the cytosol, but is transported to the lysosome, where it is combined with procaspase-1. Only after the active caspase 1 is cleaved from this procaspase-proIL-1β complex can caspase 1, in turn, cleave IL-1β into its active form (Dinarello 2005). The whole process is tightly regulated; the phospholipase A2 is necessary for the caspase activation in the lysosome, while the phospholipase C is needed for lysosomal exocytosis and secretion of IL-1β (Dinarello 2005).

IL-1β in disease

It stands to reason that a system so tightly regulated as the one of IL-1β results in complications when the signaling doesn't go as planned. Various diseases have been connected to aberrant IL-1β levels; allergy and rheumatoid arthritis, to name a few (Buchs, di Giovine et al. 2001; Um, Do et al. 2004; Hanninen, Katila et al. 2008). Blocking IL-1β secretion with IL-1 receptor antagonists prevents cold-associated acute inflammation in familial cold autoinflammatory syndrome (Hoffman, Rosengren et al. 2004), as well as mitigating neonatal

onset multisystem inflammatory disease (Lovell, Bowyer et al. 2005; Goldbach-Mansky, Dailey et al. 2006).

1.1.3.2. IL-6

IL-6 is an interleukin that acts as both a pro-inflammatory and anti-inflammatory cytokine; it is secreted by macrophages and T cells (Li and He 2006), stimulating immune response to tissue damage and leading to inflammation. Concerning the immune response to a foreign pathogen, IL-6 has been shown, in mice, to be required for resistance against the bacterium, Streptococcus pneumoniae (van der Poll, Keogh et al. 1997). IL-6's role as an anti-inflammatory cytokine is mediated through its inhibitory effects on TNF-alpha and activation of IL-1ra and IL-10. IL-6 is a prominent fever mediator and its acute phase response. It is secreted by macrophages in response to PAMPs such as LPS and nucleic acids, inducing intracellular signaling cascades that give rise to inflammatory cytokine production (Pauls, Senserrich et al. 2007). IL-6 signaling is accomplished when IL-6 binds to its receptor, which is composed of CD126 and CD130. As IL-6 interacts with CD126, it triggers CD126 and CD130 to form a complex, activating the receptor. CD130 then initiates a signal cascade through the Janus kinases (JAK) and Signal Transducers and Activators of Transcription (STAT) pathways.

IL-6 in disease

IL-6 is of great clinical interest because of its involvement in various diseases; diabetes, atherosclerosis, SLE, prostate cancer, and rheumatoid arthritis all have been shown to be influenced by IL-6 concentration (Tackey, Lipsky et al. 2004; Kristiansen and Mandrup-Poulsen 2005; Dubinski and Zdrojewicz 2007). The case for blocking of IL-6 in SLE is of particular relevance because of the nucleic-acid-associated pathology of SLE. Tackey *et al* showed that IL-6 played a critical role in the B cell hyperactivity and immunopathology of human SLE, thus mediating tissue damage. It was proposed that blocking the effect of IL-6 in humans may improve lupus by interacting with the auto inflammatory process of SLE both systemically and locally. It is also known that metastatic cancer patients have higher levels of IL-6 in their blood, doubly putting the spotlight on IL-6 research as therapy against many of these diseases (reviewed in (Smolen and Maini 2006)).

1.1.3.3. Interferons

IFNs are cytokines released by cells in response to PAMPs or tumor cells. As cytokines, they serve as communication between cells to activate the body's defense system. They are so named because of the function that caused them to be identified in the first place; their ability to "interfere" with viral replication within host cells. They do, however, have other functions: activating immune cells, such as macrophages; up-regulating antigen presentation to T cells, and increasing the ability of uninfected host cells to resist new infection by virus. Type I IFNs IFNα, IFNβ and IFNω all bind to the IFNα receptor (IFNAR). Type II IFN IFNγ binds to the IFNγ receptor (IFNGR).

Once a virally infected cell releases IFN, the neighboring cells, in response to IFN, produce large amounts of protein kinase R (PKR). PKR phosphorylates the eukaryotic translation initiation factor-2 (eIF-2) in response to new viral infections. eIF-2 forms an inactive complex with eIF2B, to reduce protein synthesis within the cell. Additionally to PKR, IFN and dsRNA also induces and activates RNase L, which cleaves RNA intracellularly to further reduce protein synthesis of both viral and host genes (Urisman, Molinaro et al. 2006). Inhibition of protein synthesis, when long enough, destroys both the virus and infected host cells. IFNs also induce production of interferon-stimulated genes (ISGs), genes that code for hundreds of proteins and can generally be classified to have roles in combating viruses. IFNs limit viral spread by increasing the activity of antitumor protein p53, which kills virus-infected or cancer cells by promoting apoptosis (Pestka 2003).

Major histocompatibility complex molecules MHC I and MHC II are upregulated in response to IFN; higher MHC I expression increases antigen presentation. IFNs also increase immunoproteasome activity; the immunoproteasome processes viral peptides for loading onto the MHC I molecule, thereby increasing the recognition and killing of infected cells by T cells. Meanwhile, higher MHC II expression increases presentation of viral peptides to helper T cells. IFNs induction occurs predominantly in response to PAMPs. PAMPs bind to their PRRs, which start a signaling cascade ending in induction and release of type I IFNs.

Type I IFNs

Together with type II IFN, type I IFNs represent one of the most important classes of cytokines. They influence a great palette of biological functions, the ones of interest here being those affecting the immune system. IFN-α/β affects the development of immunocyte lineages, innate immunity, and most aspects of the adaptive immune response. The reason for their wide range of effects lies in their receptors. Activating IFNR leads to modulation in expression of

hundreds of genes (Der, Zhou et al. 1998) (reviewed in (Pestka 2000).

Ubiquitously expressed, IFN-α and -β share a heterodimeric receptor composed of IFNAR1 and IFNAR2 subunits. Both chains are required for signal transduction. Multiple cell types display small (200 to 6000) numbers of these high-affinity receptors. Binding of IFNα/β results in receptor dimerization, and then to auto- and transphosphorylation of the two receptor-associated Janus protein tyrosine kinases (Tyk2 on IFNAR1 and Jak1 on IFNAR2). Phosphorylation of the Janus kinases leads to phosphorylation of the cytosolic domain of IFNAR1, thus making docking sites for STAT2 (connected with STAT1 on IFNAR2). STAT2 is then phosphorylated and serves as a platform for recruitment of STAT1. The activated STAT1/STAT2 heterodimers then translocate into the nucleus, where they associate with IRF9 to form the heterotrimeric complex IFN-stimulated gene factor 3 (ISGF3). ISGF3 then binds to upstream regulatory consensus sequences of IFN-α/β-inducible genes, also known as ISRE, and initiates transcription (reviewed in (Stark, Kerr et al. 1998)). Most cells can produce type I IFNs, although pDCs are considered the main IFNα producing population (Colonna, Krug et al. 2002). IFN-α/β activate several other pathways, including transcription of genes containing IFN stimulated regulatory elements (ISRE) and Gamma-activated sites (GAS) (reviewed in (Platanias 2005)). Negative regulation of type I IFN signaling is accomplished by various mechanisms, including receptor internalization and degradation, dephosphorylation of Jaks and STATs by several phosphatases, induction of suppressors of cytokine signaling (SOCS), and repression of STAT-mediated gene activation by protein inhibitors of activated STATs (PIAS)(reviewed in (Theofilopoulos, Baccala et al. 2005)).

Type I IFNs in disease

Type I interferon (IFN) is produced by the innate immune system in several autoimmune diseases, such as systemic lupus erythematosus (SLE), polymyositis, and systemic sclerosis. In these diseases, immune complex (IC)-containing DNA or RNA may act as endogenous IFN inducers. The abilities of these ICs to reach the endosomes in the plasmacytoid dendritic cells (PDC) cause the intracellular toll-like receptor (TLR) to initiate a cascade of transcription factors - a critical step in triggering type I IFN production. A special configuration of the nucleic acid (NA), such as CpG-rich non-methylated DNA or GU-rich RNA, appears crucial. However, other components of the IC, like HMGB1, may also be necessary. Studies regarding the genetic background of autoimmune diseases suggest that variants of genes involved in both IFN production and response are associated with disease susceptibility. This knowledge is important for the development of new therapeutic strategies in autoimmune diseases. Infection

induces the production of type I IFNs, resulting in fever and aching muscles. The beneficial effects of IFNs, i.e. the induction of IFN-stimulated genes (ISG) in cells with IFNR, have been extensively used for therapeutic uses. The TLR7 agonist imidazoquinoline is the main ingredient of Aldara cream, which is used for actinic keratosis, basal cell carcinoma, papilloma and external genital warts. Instead of inducing IFN production with administration of PRR agonists, synthetic IFNs can also be given as antiviral, antiseptic and anticarcinogenic drugs, as well as treating autoimmune diseases. IFNβ, for example, is used for treatment of multiple sclerosis (Hafler 2004).

Effects, both detrimental and beneficial, of IFN-α/β in several other autoimmune diseases have been reported, such as Sjögren's syndrome, myasthenia gravis, autoimmune hemolytic anemia, thyroiditis, uveitis and Behcet's disease. IFNβ reportedly inhibited collagen-induced arthritis in mice and rhesus monkeys and had some beneficial effects in rheumatoid arthritis and Sjögren's syndrome (Tak, Hart et al. 1999; Cummins, Papas et al. 2003). A negative side effect of IFNα treatment is autoimmune hemolytic anemia. Hemolytic anemia was significantly reduced in IFNAR1-deficient NZB mice (Andriani, Bibas et al. 1996). It is of great interest that IFNα/β have a major effect on a high percentage of autoimmune diseases. They are, therefore, an excellent candidate on which to start a treatment (Reviewed in (Biggioggero, Gabbriellini et al.)).

IFN therapy can also be administered as cancer treatment, when accompanying chemotherapy and radiation. IFN therapy is most effective for treating hematological malignancy; leukemia and lymphomas including hairy cell leukemia, chronic myeloid leukemia, nodular lymphoma and cutaneous T-cell lymphoma. Recombinant IFNα is used to treat patients with recurrent melanomas as well as in hepatitis B and hepatitis C infections. Some patients with hepatitis subjected to IFN therapy have a sustained virological response and can clear the virus. Some studies demonstrate giving IFN immediately following infection can prevent chronic hepatitis C. Once infected, chronic hepatitis C treatment by IFN is associated with reduced hepatocellular carcinoma (Reviewed in (Rong and Perelson). IFN therapy can also cause immunosuppression. This manifests itself via neutropenia and can result in uncommon infection progression (Bhatti and Berenson 2007).

1.2. Response of the innate immune system to cytosolic pathogens

1.2.1. Viruses

Viruses are ubiquitous pathogens. The immune system blocks the infectious process of the majority of them; however, a small fraction succeeds at evading the host immune response or subverting it to their own purposes.

1.2.1.1. DNA Viruses

DNA viruses, such as Adenoviruses, Herpesviruses, Poxviruses, Parvoviruses, Papovaviruses and Hepadnaviruses possess a DNA strand encoding their genome. Their infection pathway follows, broadly speaking, a common pathway: The virus attaches to a susceptible cell, mostly through recognition of a cell surface receptor or receptors. The virus enters the cells and the gapped DNA strand is repaired and translocated to the nucleus in a circular form, CCC DNA (Mosevitskaia 1978; Bourne, Dienstag et al. 2007). The negative strand of the CCC DNA is then used as the template for RNA polymerase II. RNA polymerase II produces longer RNA strands, called the pregenome, and shorter mRNAs. The viral mRNAs are translated in the ER and the surface antigens of the virus enter the secretory pathway (reviewed in (Chow and Broker 1994; Boehmer and Lehman 1997; Sugden 2002). The pregenome RNA is translated at low efficiency to produce a reverse transcriptase that binds to the pregenome, synthesizing viral DNA fit for packaging. Mature nucleocapsids bud out of the ER and are released by exocytosis.

DNA virus evasion strategies of the innate immune response

DNA viruses, as all viruses, are subject to certain restrictions where their capacities of interfering with the immune response are concerned. Their strategies are dependent on inhibition of antiviral signaling pathways in the host cell. Karposi's sarcoma-associated herpesvirus encodes a viral homolog of the IRF proteins, vIRF3. This inhibits transcriptional IRF7 activity and, therefore, activation of ISGs (Zhu, King et al. 2002). KSHV also encodes the K-bZIP, a transcription factor that binds to the regulatory domain of the IFNβ promoter, thus competing with IRF3 for the binding site. This results in abrogation of the RANTES and CXCL11 response (Lefort, Soucy-Faulkner et al. 2007). The genome of the human herpesvirus Epstein-Barr virus encodes the protein BZLF-1. BZLF-1 interacts with IRF7 and

therefore inhibits the type I IFN response induction (Hahn, Huye et al. 2005). The vaccinia virus VACV encodes the inhibitory proteins A46R and A52R. A46R possesses a homotypic TIR domain allowing it to interfere with MyD88, TRIF and TRAM signaling. This obstructs IRF3 activation and, therefore, type I IFN induction (Stack, Haga et al. 2005). A52R, on the other hand, binds to TRAF6 and IRAK2, both components of the NFκB pathway (Harte, Haga et al. 2003; Bonjardim, Ferreira et al. 2009).

1.2.1.2. RNA Viruses

Recognition of RNA from RNA viruses by RIG-I has been extensively explored and investigated. Although a focus of this thesis will be on recognition of bacterial RNA by RIG-I, the viral infection mechanism concerning said receptor will be briefly introduced to portray possible points of overlap in the signaling pathway between the pathogens. There are various types of RNA viruses, divided into the polarity of their RNA. The main groups are dsRNA, negative strand RNA and positive strand RNA viruses. The dsRNA viruses include the rotavirus and the bluetongue virus. The (-) strand RNA viruses are composed of, among others, the measles, mumps, hanta, rabies and influenza viruses. The (+) strand RNA viruses include corona, SARS, Hepatitis A, picorna and Hepatitis C viruses. Viruses with a dsRNA genome enter the cell using receptor-mediated endocytosis. The virus undergoes proteolytic cleavage and subsequently leaves the vacuole.

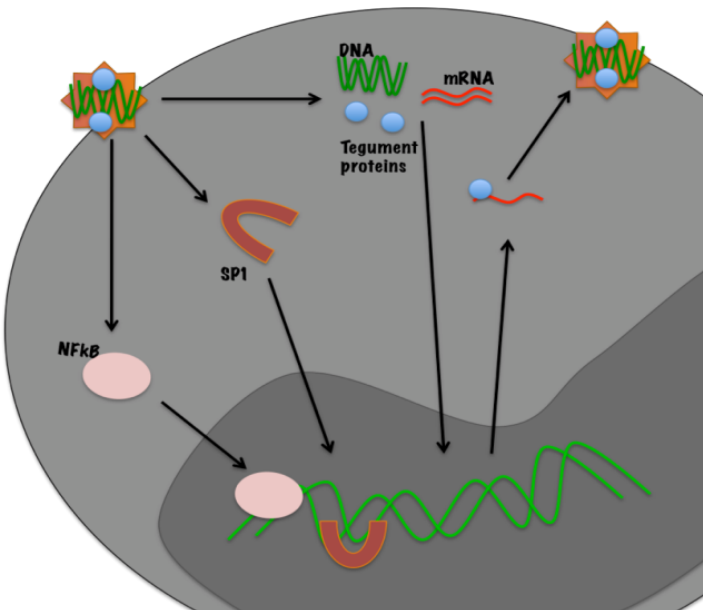

Fig. 1.11: DNA Human cytomegalovirus infection cycle. HCMV enters the host cell and associated PAMPs can either activate the NFkB pathway or transcription factor SP1. Viral DNA and mRNA, as well as relevant proteins, are released into the cytosol and used for transcription of virion components. Once assembled, the virion then exits the host cell (adapted from (Huang and Johnson 2000).

Multiple capped viral mRNAs are then synthesized from the core particle and associate with newly translated viral proteins. Each of the small mRNAs is a template for negative strand synthesis. The mRNAs code for an RNAse-resistant subviral particle that serves as location for assembly of additional virus particles. The preformed viral capsid proteins are added at the end of the assembly process. The virus exits the cell via lysis.

The rabies virus reproductive cycle will be briefly explained representing the (-) ssRNA virus infection. The virion enters the host cell via receptor mediated endocytosis. It fuses with the endosome, releasing the viral nucleocapsid, composed of negative strand RNA, which is copied into 5 subgenomic mRNAs by the L and P proteins also contained in the nucleocapsid. The mRNAs code for, among others, more L and P proteins. Viral RNA replication is started with synthesis of the positive strand RNA of the viral genomic RNA, which is used for further production of negative strand RNA, reinitiating the reproductive cycle. Glycosylated viral membrane proteins are transported to the host cell membrane, as are nucleocapsids, thus enabling budding off of virions from the host cell membrane (reviewed in (Chazal and Gerlier 2003)).

RNA virus infection evasion of the innate immune response

Confronted with the broadly responsive innate immune system, viral pathogens have developed evasion and inhibition mechanisms allowing them to multiply and survive in theoretically hostile environments. Various strategies have been developed, ranging from inhibition of IFN synthesis, binding of secreted IFN molecules, interference with IFN-induced proteins or obstruction of IFN-dependent signaling (reviewed in (Bonjardim, Ferreira et al. 2009)). The viral protein VP35 offers itself as a rival substrate for IKKξ and TBK-1, thus obstructing the signaling pathway to IFN induction (Prins, Cardenas et al. 2009). VP35 also induces SUMOylation of IRF7, blocking its transfer to the nucleus (reviewed in (Basler and Amarasinghe 2009)). The protein VP24, as encoded by the Ebola virus obstructs the nuclear import of STAT1. The same protein encoded by the Marburg virus, however, simply blocks STAT 1 and 2 phosphorylation (Valmas, Grosch et al. ; Basler and Amarasinghe 2009).

It was discovered that the flavivirus Hepatitis C encodes a protease complex that targets IPS-I for cleavage as part of its immune evasion strategy; bioinformatic analysis revealed that two flaviviruses encode a viral product that exhibited strong homology with the amino terminus of MITA. This product inhibited the type I IFN response induced by MITA, probably due to direct interaction (Ishikawa et al., 2009).

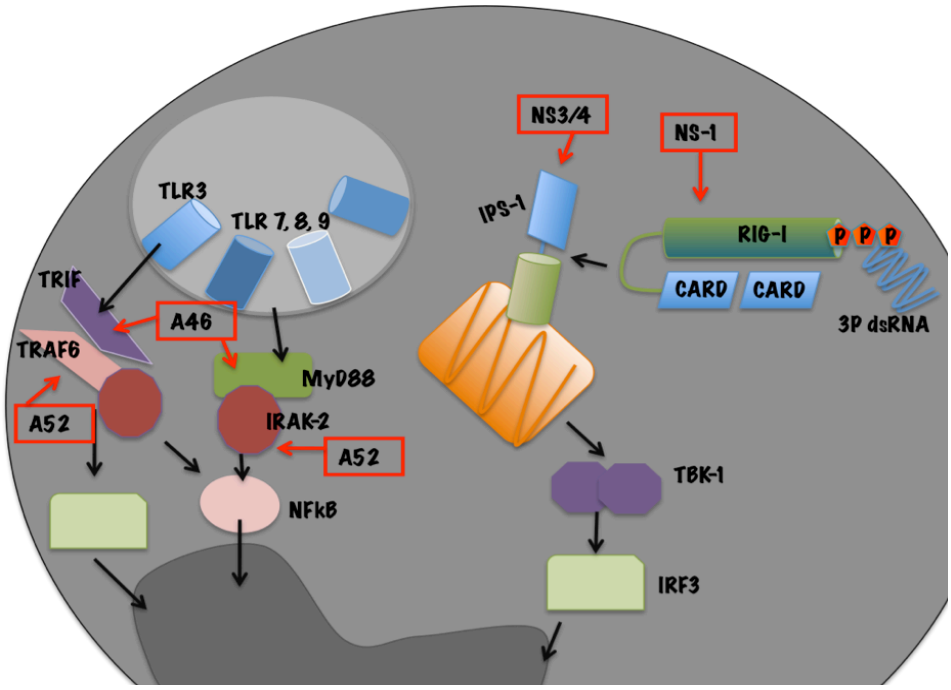

Fig. 1.12: Viral evasion techniques. RNA and DNA viruses have both evolved strategies to avoid or block the innate immune system. A52, for example, inhibits TRAF6 and IRAK2 signaling, while A46 possesses as TIR homology domain and therefore blocks the MyD88 and TRIF pathway (adapted from (Schroder and Bowie 2007)).

1.2.2. Bacteria

Most bacteria are not, like viruses, obligate intracellular pathogens, but those that can, or must, replicate intracellularly, are of course of particular interest to intracellular PAMP research. TLRs such as TLR2 and 4 cannot induce IFN or IL-1β induction to cytosolic pathogens, while RIG-I and the DNAR can readily mount an innate immune response to intracellular pathogens such as *Legionella pneumophila* and *Listeria monocytogenes*.

1.2.2.1 Legionella pneumophila

Legionella pneumophila is a gram-negative bacterium. It replicates in host macrophages and causes Legionnaires' Disease, a severe kind of pneumonia. *L. pneumophila* is acid labile, does not sporulate, and is a not capsulated rod-like bacteria. In humans, *L. pneumophila* invades and replicates in alveolar macrophages (Horwitz and Silverstein 1980). Macrophage phagocytosis of the bacteria can be enhanced by the presence of antibody and complement but is not strictly necessary. A pseudopod coils around the bacterium in this unique form of internalization. Once phagocytosed, the bacteria surround themselves in a membrane-bound vacuole, preventing fusion with lysosomes that would otherwise degrade the pathogen. The bacteria multiply in this protected compartment. A Type IVB secretion system known as Icm/Dotis inject effector Ank proteins into the host, increasing the bacteria's ability to survive inside the host cell (Isberg,

O'Connor et al. 2009): They interfere in the fusion process of the *Legionella*-containing vacuole with the host's degradation endosomes (Pan, Luhrmann et al. 2008).

1.2.2.2. Listeria monocytogenes

Listeria monocytogenes is a facultative intracellular bacterium that is the causative agent of Listeriosis. It is a foodborne pathogen and especially dangerous for immunocompromised individuals, such as the elderly, the young, or pregnant women (Ramaswamy, Cresence et al. 2007).

Primarily, *Listeria* infects the host via the intestinal epithelium where the bacteria invade non-phagocytic cells. Induction of uptake occurs by the binding of listerial internalins (Inl) to host cell adhesion factors such as E-cadherin. This, in turn, results in activaton of certain Rho-GTPases which, then bind and stabilize Wiskott Aldrich Syndrome protein (WASp). WASp can serve as an actin nucleation point. Subsequent actin polymerization extends the cell membrane around the bacterium, eventually engulfing it (Dykes and Dworaczek 2002). *L. monocytogenes* uses internalins only for invasion of non-phagocytic cells; invasion of macrophages, their preferred host cell, does not require internalin use.

The bacterium must then escape from the phagosome before fusion with a lysosome can occur: the three main virulence factors which allow the bacterium to escape are listeriolysin O (LLO - encoded by hly) phospholipase A (encoded by plcA) and phospholipase B (plcB) (Leimeister-Wachter, Haffner et al. 1990) (Schmid, Ng et al. 2005). Briefly, secretion of LLO creates holes in the vacuolar membrane and allows the bacterium to escape into the cytoplasm, where it can reproduce.

Once in the cytoplasm, ActA proteins associated with the bacterial cell pole are capable of binding the Arp2/3 complex, and thus induce actin nucleation at a specific area of the bacterial cell surface. Actin polymerization can then be used by the bacterium for transport, either into the extracellular space or directly into another host cell.

Immune recognition of Listeria

The innate immune response to *Listeria* infection has been investigated under the aspects of Nod1, Nod2 and TLR2 activation. Nod1 and Nod2 were found to be involved in bacterial recogniton of TLR ligands such as LPS and LTA. Experiments showed that bacterial clearance in mice previously challenged with LPS or *E.coli* was critically dependent on Nod1 and Nod2 upon systemic infection with *L. monocytogenes* (Kim, Y.G. Immunity 2008). Another group investigated the mutation in the Nod2 gene and its role in Crohn's disease. Nod2-deficient

mice were, interestingly, also susceptible to orally administered *Listeria*: Recognition of *Listeria* infection in the intestinal tract involves Nod2 (Kobayashi, K.S. 2005). Nod1 involvement of the intracellular innate immune response to *Listeria* was cemented using RNAi and Nod1 overexpression. Endothelial cells with Nod1 respond to *Listeria* infection with secretion of IL-8 in a p38-dependent manner (Opitz, B. 2006). The antimicrobial innate response in mesothelial cells, which line the outer surface of interior organs, is regulated by Nod1 and TLR receptors, as measured by chemokine output. Park *et al* infected mesothelial cells with *Listeria* and observed a CXCL1 response dependent on the presence of Nod1 (Park, J.h. 2007). *Listeria*, however, can also induce IFN in an IRF-3 dependent manner bypassing TLR and Nod2. IRF3 was proposed as a convergence point for immune response signals to *Listeria* infection, as IRF3-dependent signal transduction occurred independently of MyD88, TRIF and TRAM (Stockinger, S. 2004). Ipaf and Nalp3 were shown to activate caspase 1 in the event of *Listeria* infection. A dose-dependent response to *Listeria* flagellin via Ipaf. The inflammasome component ASC activated caspase 1 in the presence of cytosolic *Listeria*. (Warren, S.E. 2008, Reviewed in Tsuji, N.M. 2004). After comparing host responses to *Listeria* infection in wt and TLR2-deficient mice, it was found that TLR2-deficient mice succumb easier to *Listeria* infection. The response of cytokines such as TNF and IL-12, or the expression of costimulatory molecules, was reduced in TLR2-deficient macrophages (Torres, D. 2004).

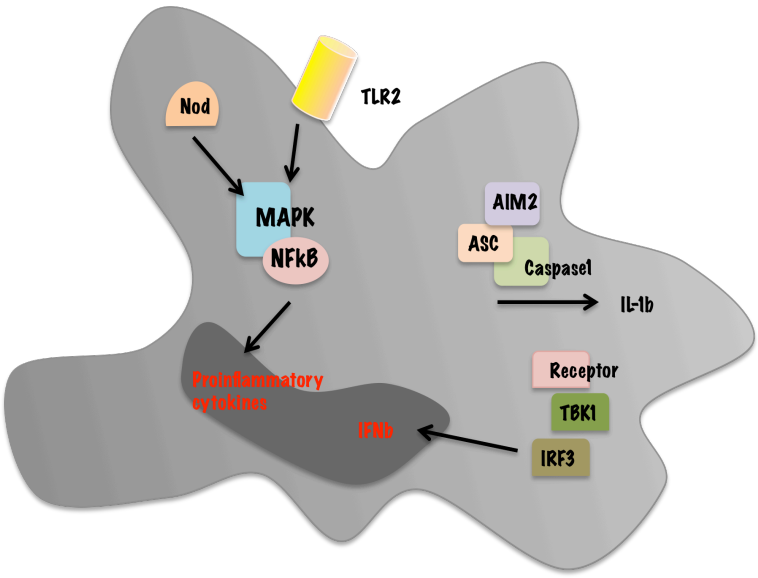

Fig. 1.13.: Pathways of innate immune recognition to *Listeria* in macrophages. *Listeria* enter the cell using Internalins. Components of the bacterial cell wall can either interact with TLR2 on the cell membrane or with NLRs in the cytosol. Bacterial nucleic acids can interact with AIM-2 or an as yet unknown receptor of the TBK-1/IRF3 pathway.

Interestingly, recent investigations have shown *Listeria* to be sensed by the NLRP3 and AIM2 inflammasomes in murine macrophages. *Listeria*-triggered cell death was reduced in cells

without AIM2 and NLRP3, indicating a role for sensing of intracellular bacterial DNA in the cytosol of macrophages (Kim et al, 2010).

Investigations in the labs of Decker and Portnoy suggested TLR-independent pathways leading to induction of type I IFN in mouse macrophages infected with *Listeria monocytogenes* (O'Riordan, Yi et al. 2002; Stockinger, Materna et al. 2002). Elucidating the host response to *Listeria* had been though to have been explained in 2006, when Decker *et al* described an IPS-1 independent response to *Listeria*. IPS-1 relays signals from RIG-I and Mda-5 to the IRF3 kinase complex, resulting in a type I IFN response. Using siRNA-mediated knock-down in macrophages, it was shown that *Listeria* infection targeted the IFNβ gene without detectable IPS-1 requirement (Soulat, Bauch et al. 2006). Furthermore, type I IFN induction depended on cytosolic localization of the bacteria (O'Riordan, Yi et al. 2002; Stockinger, Materna et al. 2002) but was shown to be Nod2 independent (Stockinger, Reutterer et al. 2004).

Later on, Medzhitov *et al* could show that DNA represents the type I IFN inducing agent in the lysate of *Listeria monocytogenes* when transfected into murine monocytes. From their experiments, they concluded that intracellular bacteria (*L. monocytogenes* and *L. pneumophila*) with cytosolic shuttle mechanisms induce a type I interferon response by the recognition of bacterial genomic DNA in the cytosol. The transfer of bacterial RNA, however, should also be possible in the same way and recognition mechanisms as observed for RNA viruses should be triggered by intracellular bacteria. In contrast to eukaryotic RNA, *bacterial* mRNA is not capped but contains 15% 5'triphosphorylated RNA (Bieger and Nierlich 1989), a primary requirement for recognition by RIG-I. IL-1β is an indicator for *Listeria* infection; blocking the IL-1R exacerbates murine listeriosis (Havell, Moldawer et al. 1992). Observing the correlation of IL-1β and IL-6 induction to the type I IFN response after *Listeria* infection might help characterize the innate immune response to *Listeria*; IL1 and IL6 collaborate to protect the host from *Listeria* (Dalrymple, Lucian et al. 1995; Liu, Simpson et al. 1995). As will be shown in this thesis, evidence exists to suggest that *Listeria*, like *Legionella*, also take the RIG-I pathway. Maybe not uniquely, but RNA definitely plays a role in the innate immune response.

1.3. Aim of this thesis

PRRs and their signaling pathways will be investigated in this thesis. As it is known that components of the bacterial cell wall and conserved proteins are detected by TLRs on the cell surface, and by NLRs in the cytosol of cells. Experiments were conceived to investigate the type I IFN response to bacterial presence in the cytosol. *Listeria* are considered the model organism for cytosolic invasion by bacteria. To this end, *Listeria* with and without the ability to enter the cytosol were used for infection of cell lines with differing cytosolic nucleic acid receptors. This would allow a differentiated approach to infection pathways and provided cell-line specific innate immune responses.

Along with the abovementioned experimental setup to determine bacterial type I IFN recognition pathways, another approach was designed to establish the minimal recognition motif of cytosolic DNA ligands. In order to allow for experimental readout under controlled conditions, synthetic oligonucleotides (ODNs) were constructed with minute differences in sequence. With RIG-I so acutely dependent on 3-P ends, it would stand to reason that a cytosolic DNA receptor is equally dependent on small changes in sequence for IFN induction. This thesis will explore the influence of structure and sequence of short dsODNs on type I IFN induction in monocytic cells.

2. Materials and Methods

2.1 Materials

2.1.1 Equipment

Analyzer for Agarose gels	
Cell culture incubators Herasafe KS-15	Thermo, Langenselbold
Centrifuge 5424	Eppendorf, Hamburg
Centrifuge 5810R	Eppendorf, Hamburg
Herafreeze HFU 586	Thermo, Langenselbold
Horizontal Gel Electrophoresis SGE-020-02	CBS Scientific, Del Mar, California
Horizontal shaker DOS-10L	Neolab, Heidelberg
Lumistar Luminometer	BMG Labtech, Offenburg
Magnetic Stirrer	VWR, Batavia, Illinois
Microplate Reader Apollo 8 LB-912	Berthold Technologies, Bal Wildbad
Microscope Wllovert 30	Hund, Wetzlar
pH-meter, digital	
PowerStation 300 Plus	Labnet International, Berkshire
Precision Balance 440-47N	Kern, Balingen
Precision Bench Scale EG-420-3NM	Kern, Balingen
Premium nofrost	Liebherr, Kempten
Shaking Incubator for bacteria 311DS	Labnet, Edison, New Jersey
Spectrophotometer Nanodrop ND-1000	Peqlab, Erlangen
Sterile Workbench Heracell 240	Thermo, Langenselbold
Thermal Cycler Px2	Thermo Electron Corporation, Langenselbold
Thermomixer 5350	Eppendorf, Hamburg
Vertical Blotting System EBX 700	CBS Scientific, Del Mar, California
Vertical Gel Electrophoresis MGV 202	CBS Scientific, Del Mar, California
Western Blot developer	

2.1.2 Chemicals

Unless otherwise stated, all chemicals were obtained from the following companies; DiagonalFluka, Gibco, Invitrogen, Merck, Roche Diagnostic GmbH, Serva, Carl Roth and Sigma. Solutions were prepared using deionized water.

2.1.3. Media and antibiotics for bacterial cultures

Media were sterilized by autoclaving for 20 min at 121°C.

LB-Mediums	Bacto-Trypton 10g/L
(Luria-Bertani)	Bacto yeast extract 5g/L
	NaCl 10g/L
	pH 7.5
LB-Agar	Bacto-Trypton 10g/L
	Bacto yeast extract 5g/L
	NaCl 10g/L
	Bacto-Agar 15g/L
	pH 7.5
Columbia Agar	Casein-peptone 10g/L
	Meat peptone 5g/L
	Heart Peptone 3g/L
	Yeast extract 5g/L
	NaCl 5g/L
	Corn starch 1g/L
	Agar 15g/L
	pH 7.3
Antibiotics stock solutions	50µg/mL Ampicillin 1:1000 in LB
filter sterilized	50µg/mL Kanamycin 1:1000 in LB
	50µg/mL Puromycin 1:4000 in RPMI
HTM medium and agar	100mM MOPS
	4.82mM KH2PO4
	11.55mM Na2HPO4
	1.70mM MgSO4
	55mM Glucose
	2.96mM Thiamine

	1.33mM Riboflavine
	2.05mM Biotine
	24pM Lipoic acid
	0.1mg/mL Cysteine
	0.1mg/mL Methionine
	0.6mg/mL (NH4)SO4
	15g/L Agarose

2.1.4. Mediums and Solutions for Cell Culture

Trypsin/EDTA	0.05% Trypsin/EDTA (w/v) Invitrogen
PBS	1xPBS (Invitrogen)
Pharmlyse	10x BD Pharm Lyse Lysing Buffer (Pharmingen)
RPMI Culture Medium	1x RPMI 1640 (Invitrogen) 2mM Glutamine 100 U/mL Penicillin 100 U/mL Streptomycin 10% Heat-inactivated fetal calf serum (FCS)
DMEM	1x Dulbecco's modified Eagles Medium (Invitrogen) 100U/mL Penicillin 100U/mL Streptomycin 10% Heat-inactivated FCS
Opti-MEM	Opti-MEM, Invitrogen
Cryo-medium	FCS:DMSO 9:1 (Dimethylsulfoxide, Roth)

2.1.5. Solutions for use in molecular biology

Plasmid preparations (Jetstar Maxiprep)

Sol E1	Resuspension	50mM Tris 10mM EDTA 100µg/mL RNase A pH 8.0

Sol E2	Lysis buffer	200mM NaOH 1% SDS (w/v)
Sol E3	Neutralization buffer	3.1M $C_2H_7NO_2$ pH 5.5
Sol E4	Equilibration buffer	600mM NaCl 100mM $C_2H_3NaO_2$ 0,15% Triton-X 100 pH 5.0
Sol E5	Wash buffer	800mM NaCl 100mM $C_2H_3NaO_2$ pH 5.0
Sol E6	Elution buffer	1250mM NaCl 100mM Tris pH 8.5

Gel extraction(JetQuick Protocol)

Sol L1	Gel solubilization buffer	$NaClO_4$ $C_2H_3NaO_2$ TBE-solubilizer
Sol L2	Wash buffer	EtOH NaCl EDTA Tris/HCl
Tris Buffer	Elution buffer	10mM Tris HCl pH 8.0

DNA Agarose Gel Electrophoresis

10xTBE	1M Tris-HCl 890mM Boric acid 10mM EDTA pH 8.0
6x DNA sample buffer	15% (w/v) Ficoll 0.25% (w/v) bromophenol blue 0.25% (w/v) xylene cyanol
1kb Ladder, 10kb Ladder	New England Biolabs, Fermentas

Ethidiumbromide solution	10mg/mL in TBE

PCR Purification Kit (Jetquick column)

Sol H1	Binding buffer	Guanidine Hydrochloride
		Isopropanol
Sol H2	Wash buffer	EtOH
		NaCl
		EDTA
		Tris/HCl

2.1.6. Materials in molecular biology

Unless otherwise stated, all materials used were obtained from Invitrogen (Darmstadt, Germany), Roth (Karlsruhe, Germany) and Metabion (Martinsried, Germany)

2.1.7. Bacterial strains

XL1-Blue
Listeria monocytogenes 11919
Listeria monocytogenes 43251
Listeria monocytogenes Δhly
Listeria monocytogenes Δprf
Listeria monocytogenes EGD
DH10ß
Sure

2.1.8 Cell lines

HEK 293T	Human embryonal kidney fibroblasts with a stable integration of the large T-antigen of the SV-4 virus.
Vero	African green monkey kidney epithelial cells
A498	Human epithelial cell kidney carcinoma
FaDu	Human epithelial squamous cell carcinoma.
HaCat	Human ceratinocytes
NIH 3T3	Mouse embryonic fibroblast cells

THP-1	Monocytic cell line
THP-1 505	Monocytic cell line, RIG-I knock-down
A549	Lung epithelial cell line
A549 505	Lung epithelial cell line, RIG-I knock down
THP-1 MITA	Monocytic cell line, MITA knock-down
THP-1 MITA-Inv	Monocytic cell line, MITA knock-down
THP-1 Atg5	Monocytic cell line, Atg5 knock-down

2.1.9. Primary cell cultures

Peripheral blood mononuclear cells (PBMCs)	Isolated from leukocyte-rich buffy coats of healthy blood donors
Human pDCs	
Human monocytes	
Murine glia cells	Isolated from healthy C57/BL6 mice
Murine bone marrow-derived dendritic cells	

2.1.10. Plasmids

The plasmids used in this thesis are listed in Table 2.1.

Table 2.1: Vectors used in this thesis. Fusion proteins, cDNAs with complete reading frames and mutants used for eukaryotic gene expression were cloned into MIRTOP and pLuc

pBKs
IFNb-gLuc
IRF 1
IRF 3
IRF 7
RIG-I Flag
RIG-I GFP
DAI
MDA-5
IPS-1
pATTR
pSUPER

pLV
pLKO-MITA
pLKO-Atg5

2.2. Methods used in molecular biology

Unless otherwise stated, most of the methods described are adapted from those characterized in Sambrook et al (2000).

2.2.1. Preparative methods

2.2.1.1. Isolation of DNA by alkaline lysis

A reliable and fast way to isolate small amounts of plasmid DNA from E. Coli is alkaline lysis. The extracted DNA can be used for restriction analysis and transformations.

Bacteria from 1.5mL of overnight bacterial cultures (LB supplemented with appropriate antibiotics) were pelleted for 30sec at 13,200 rpm at room temperature in an Eppendorf Biofuge. The pelleted bacteria were lysed with 200µL lysis buffer. After 5 min at room temperature, 150µL neutralization buffer were added and the lysate centrifuged for 15 minutes at 13,200 rpm, pelleting denatured proteins and genomic DNA. The clear supernatant was transferred to a new Eppendorf tube. Addition of 1mL ice-cold 100% EtOH, followed by 2min incubation at room temperature, led to DNA precipitation. After centrifugation (of 10min at 13,200 rpm), the supernatant was discarded and the resulting pellet was washed in 70% EtOH (v/v) and was then resuspended in 10-20µL H_2O-RNase.

2.2.1.2. Isolation of DNA on a preparative scale

A kit from the Genomed company was used to obtain larger quantities of plasmid DNA. Bacteria were cultured overnight in 250mL LB-medium with antibiotics and pelleted for 15min at 6000rpm (4°C, Eppendorf centrifuge). All traces of medium were carefully removed. The pellet was resuspended in 10mL Solution E1 until the suspension was homogenous. 10mL of Solution 2 were added and the suspension gently mixed by inversion, then incubated at room temperature for 5min. After the incubation period was over, 10mL of solution E3 were added and the suspension immediately mixed through multiple inversions until the suspension appeared homogenous and no remainders of viscous matter were visible. The mixture was centrifuged for 10min at 12,000g. During the last centrifugation step, the columns were equilibrated with 30mL solution E4. The supernatant was then applied to the equilibrated

column and the lysate allowed to pass through by gravity flow. The flow-through was discarded. The column was washed with 60mL of solution E5 and the flow-through discarded. The DNA was then eluted with 15mL of solution E6.

2.2.1.3. Isolation of DNA fragments

To isolate DNA fragments, DNA was digested with restriction enzymes and appropriate fragments separated by agarose gel electrophoresis (10V/cm distance between the electrodes). The sample was loaded onto an agarose gel and the relevant band excised. The DNA in the gel band was then isolated by using the gel extraction protocol from the Genomed company. Briefly, the gel slice was transferred into an Eppendorf tube and 300µL solution L1 added for every 100mg gel slice, then incubated for at least 15 minutes at 50°C. A JetQuick spin column was placed into a 2mL Eppendorf tube and the L1-gel slice mixture loaded onto the silica matrix, then centrifuged at 12,000g for 1 minute. The flow-through was discarded and the column replaced onto the Eppendorf tube. 500µL of solution L2 were then added to the column and then centrifuged for 1minute at 12,000g. The flow-through was discarded and the empty column centrifuged again for 1 minute at 12,000g. The JetQuick spin column was placed in a new Eppendorf tube and 50µL sterile water or TE buffer pipetted directly onto the silica matrix, then centrifuged at maximum speed for 2 minutes.

2.2.1.4 Phenol-Chloroform extraction of DNA

1 Vol (up to 700µL) of aqueous DNA solution was pipetted into an Eppendorf tube, with an equal volume of phenol:chloroform:isoamyl alcohol (25:24:1) added on top. The mixture was then vortexed vigorously to mix the phases. The suspension was centrifuged at top speed for 2 minutes to separate the phases. The aqueous upper phase was removed to a new tube and an equal volume of phenol:chloroform (1:1) added. The suspension was vortexed and centrifuged for 2 minutes at top speed. The aqueous phase was then removed to a new tube and the DNA precipitated with EtOH.

2.2.1.5. Purification and isolation of DNA from aqueous solutions

In order to precipitate DNA from an aqueous solution, 0.1Vol 3M sodium acetate (pH 5.2) and 2 Vol ice-cold 100% EtOH were added to the solution. The mixture was incubated for 30 min at -20°C. DNA was precipitated by centrifugation for 15 min at 13,200rpm. The pellet was washed with 70% EtOH (v/v), air-dried and subsequently dissolved in an appropriate

volume of H_2O. Alternatively, to keep the total volume small, 1 Vol of isopropanol was used for precipitation.

2.2.2. Analytical methods

2.2.2.1. DNA restriction digest

Plasmid restriction digests were performed according to the manufacturer's instructions. 2 to 10 units of the restriction enzyme were used per µg DNA. The digest was performed for 1 to 12 hours at 37°C.

2.2.2.2. Oligo dA-dT elongation

Oligo dA-dT elongation was performed according to previous publications (Hanaki *et al.*, 2004). Briefly, 85µL H2O were added to 10µL 10x Klenow fragment buffer, 5U Klenow fragment, 1µg dAdT and 200µM each of dATP and dTTP. The mixture was incubated for 4 hours at 37°C and the DNA extracted with EtOH precipitation.

2.2.2.3 Measurement of DNA concentration

To determine the concentration and purity of DNA samples, the optical density (OD) was measured at 260nm and 280nm. An OD260 corresponds to a concentration of 50µg/mL double-stranded DNA. The OD260/280 ration indicates the amount of protein impurities in the sample. This ratio should be between 1.8 and 2.0 for pure nucleic acids.

2.2.2.4 Electrophoretic separation of large DNA (> 100bp) fragments

The preparative and analytical separation of DNA fragments according to size was done by agarose gel electrophoresis. In order to obtain an optima DNA separation, agarose concentration varied between 0.8% and 2%. 1xTBE was used as gel and electrophoresis buffer. The gel was prepared by heating the agarose in 1xTBE buffer and pouring the clear solution into a horizontal gel chamber with inserted comb. Ethidiumbromide was added to the still-fluid solution in a final dilution of 1:2000. Before the samples were loaded onto the gel, they were combined with 1/6 vol 6x loading buffer. The gel electrophoresis was run at 10V/cm2 and took, depending on the agarose concentration, 1-2 hours. Afterwards the gel was photographed on an UV-transilluminator.

2.2.2.5. Electrophoretic separation of small (<100bp) DNA fragments

The analytical separation of synthetic oligonucleotides according to size was done by acrylamide gel electrophoresis. In oder to obtain an optimal DNA separation, acrylamide concentration varied between 6% and 10%. 1xTBE was used as gel and electrophoresis buffer. The gel was prepared by mixing (for an 8% gel) 4mL 30% acrylamide, 1.5mL 10xTBE, 9.5mL H2O, 150µL 10% APS and 15µL TEMED and pouring the solution into a vertical gel chamber. The gel was pre-run for 30min at 200V. The samples were combined with 1/6vol 6x loading buffer and the gel was run for 1 hour at 200V. The gel was then stained for 30 minutes with 0.02% methylene blue solution (w/v).

2.2.3. Plasmid construction

2.2.3.1. Phosphorylation of PCR fragments

To subclone PCR fragments into the desired vector, they were phosphorylated by adding 12µL of purified synthetic oligonucleotide to 5x T4 DNA-Polymerase buffer (Boehringer), 2µL 10 x PNK (polynucleotide kinase) buffer (Boehringer), 1µL 2mM ATP/1mM dNTPs, 0.5µL PNK at 10U/µL (Boehringer) and 0.5µL T4 DNA polymerase (Boehringer). The mixture was incubated for 30 min at 37°C, fragments isolated and ligated with the vector.

2.2.3.2 Ligation of DNA fragments and synthetic oligonucleotides

DNA ligase catalyzes the ligations of a vector with a passenger fragment. This ATP-dependent enzyme covalently joins a 3' OH end with a 5' phosphate group, producing a phosphodiester bond. In order to insert one or more DNA fragments into a vector, 12µL insert and 5µL vector were mixed with 3µL ligation buffer, 5µL T4 DNA ligase (1U/µL), 1.5µL 10mM ATP and 3µL 50% PEG (polyethylene glycol). The solution was incubated overnight at 16°C. Subsequently, the ligated DNA was precipitated by adding 1µg tRNA, 10µL 3M sodium acetate (pH 5.2), 275µL -20°C EtOH and 60µL H2O to the ligation mixture. After an incubation period of at least two hours at -20°C, the DNA was pelleted for 15 min at 13,2000rpm, the pellet washed with 150µL 70% EtOH, centrifuged for 5 min at 13,200rpm and then dissolved in an appropriate amount of H2O.

2.2.3.3. Cultivation of bacteria

E.coli and *L.monocytogenes* strains were grown overnight at 37°C on LB and Columbia agar plates, respectively. A single colony was used to inoculate LB medium in order to obtain suspension cultures, and then incubated overnight on a shaker at 220rpm and 37°C. Glycerol stocks were prepared for permanent storage at -80°C. To this end, glycerol was added to a final

concentration of 20° (v/v) to an overnight culture. In oder to inoculate from glycerol stocks, a glass pipette was dipped into the stock solution and then transferred to an appropriate volume LB medium, which was then incubated overnight on a shaker at 37°C.

2.2.3.4. Preparation of competent cells for chemical transformation

As described in Chung *et al* (1989), an 5mL overnight culture of bacteria was rediluted into 25mL of fresh LB medium. This suspension was grown to an OD600 of 0.2-0.5, then centrifuged for 10 minutes at 3000rpm and 4°C. The supernatant was removed and the pellet resuspended in 1/10 volume cold TSS buffer. 100µL aliquots were then pipetted into pre-chilled Eppendorf tubes and stored at -80°C.

2.2.3.5. Chemical transformation of bacteria

Chemically competent E.coli were taken out of -80°C storage and defrosted for 5 minutes on ice. The desired amount of DNA dissolved in 10µL TE buffer was then added and the bacteria incubated for 15 minutes on ice, then heated to 42°C for 90 seconds. The transformed bacterial suspension was then resuspended in 1mL LB medium and incubated for 30 minutes at room temperature before plating onto LB agar plates.

2.2.4. Enzyme-Linked-Immuno-Sorbent-Assay (ELISA)

2.2.4.1. Conventional ELISA method

The ELISA method is used in order to measure cytokines found in the supernatant of stimulated cells.

To this end, a primary antibody is used to coat the 96-well ELISA plate. Cytokines present in the examined substrate bind to this antibody. A second antibody, whose Fc domain is coupled to a substrate-specific enzyme (peroxidase), binds to the cytokine in question. A colorless substrate is added to the well and turns blue in dependence of the concentration of the second antibody. The reaction is stopped with 2N H_2SO_4, which turns the blue substrate yellow. The intensity of the coloring is measured with an ELISA reader and allows deductions as to the cytokine concentration.

The ELISA plate was coated with 50µL of diluted primary antibody per well and incubated overnight at 4°C. The primary antibody solution was removed and the plate washed with 100µL wash buffer (1xPBS with 0.05% Tween-20).

50µL blocking buffer (10% FCS (v/v) in 1xPBS) were added to the wells in order to block the unspecific binding sites and the plate incubated for 30 minutes at room temperature. The plate

was washed three times with wash buffer and the samples pipetted into the wells in the desired dilution. A serial dilution was performed with a known concentration of the cytokine in question and pipetted onto 8 microwells.
The plate was incubated for two hours at room temperature and then washed three times. The conjugated second antibody/HRP solution, diluted in assay buffer, attached to the bound cytokine in the microwells. The plate was incubated for one to two hours at room temperature and then washed seven times.
The ELISA was then developed. To this end, 50µL of combined substrate solution A and B were pipetted per well and the plate incubated for 20 minutes at room temperature out of the light. As soon as the five strongest concentrations of the diluted standard could be seen, the reaction was stopped with 50µL 2N H_2SO_4.
The intensity of the dye was measured in the ELISA reader at 450 and 570nm. The difference in absorption was used to calculate the cytokine concentration in the supernatants used. The hIFNa ELISA was performed in a generally similar manner, except for the fact that the secondary antibody/HRP conjugate could be added directly to the supernatant.

2.2.4.1. murine IFNa ELISA

Murine IFNa was measured with a kit made of self-assembled ingredients. The coating antibody RMMA-1 was diluted 1:2000 in coating buffer and the plate incubated overnight, then washed once with washing buffer and the samples added to the wells. The standard protein was diluted to 10^3U/mL, the plate incubated overnight at 4°C. The next day, the plate was washed 3x with wash buffer and the detection antibody (polyclonal rabbit anti-mouse IFNa), diluted 1:1000 in assay buffer, pipetted into the microwells. The plate was incubated overnight, then washed 15 times. 50µL HRP-conjugated secondary antibody (donkey anti-rabbit, dilution 1:10000) was added to the wells and the plate incubated overnight. The wells were washed 12x and 50µL substrate reagent pipetted per well.

2.3. Cell culture

2.3.1. Cell culture conditions

All procedures with cell cultures were performed under the laminar hood and using sterile utensils.

2.3.2. Thawing cells

Cells stored in liquid nitrogen were transported on dry ice. After rapid thawing in a 37°C water bath, the cells were transferred to a sterile 15mL tube. 10mL culture medium was added dropwise, the tube then centrifuged to 7 minutes at 400rcf (Eppendorf centrifuge), the pellet dissolved in 10mL culture medium and transferred to a 10mL culture dish.

2.3.3. Cell cultivation

The culture of the abovementioned cell lines occurred at 37°C in a controlled atmosphere at 5% CO_2. In order to passage confluent cells (Lindl and Bauer, 1989), they were washed once with PBS, dissociated from the dish with 2mL 0.5% Trypsin-EDTA and transferred at an adequate dilution to new 10cm dishes. HEK 293T, HaCat, RAW and Vero cells were cultured in RPMI medium and diluted every 3-4 days. FaDu and A498 cells were cultured in DMEM and diluted every 3 days.

2.3.4. Preparation and cultivation of PBMCs

Isolation of human PBMCs occurred through density gradient centrifugation using Leucosep® tubes (Greiner Bio-One, Germany). These tubes possess a porous barrier of polyethylene, preventing mixture of the sample material with the separation medium. 15mL Biocoll® sucrose gradient were poured onto the barrier and the tubes then shortly centrifuged so the separation medium could pass through. Buffy coats were diluted 1:2 with 0.9% NaCl and poured on top of the barrier, then centrifuged for 20 minutes at room temperature and 800g with the brake turned off. This resulted in the separation of the Buffy coat into different phases.

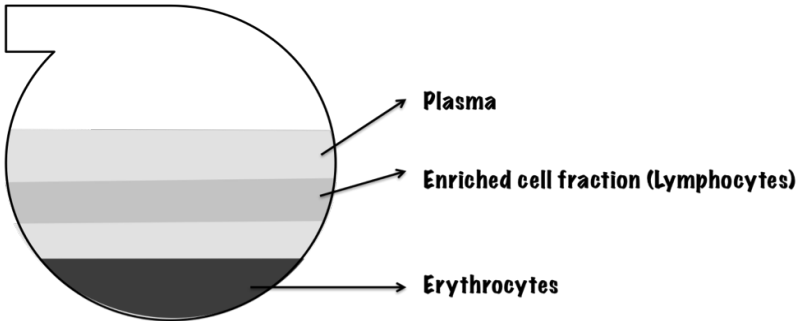

Fig. 2.1: Isolation of PBMCs through gradient centrifugation (adapted from Greiner Bio-One GmbH)

The cells contained in the enriched cell fraction were carefully removed with a pipette and deposited into a new 50mL centrifuge tube. The volume was filled to 50mL with 0.9% NaCl and centrifuged for 15 minutes at 400g and 4°C. The supernatant was removed and the pellet

resuspended in 1x Lysis buffer, then incubated for 5 minutes at room temperature. The lysed suspension was then filled to 50mL with 0.9% NaCl and centrifuged for 15 minutes at 400g and 4°C. The supernatant was removed and the lysis step repeated if erythrocytes remained visible. PBMCs were resuspended in 10mL RPMI and counted; 200µL PBMC suspension containing $4x10^5$ cells were pipetted per well.

2.3.5. Determination of cell count

1µL of cell suspension was mixed with 99µL of 0,04% trypan blue in order to determine cell vitality. Cell count was obtained using the Neubauer counting chamber. (See Fig. 2.2) The cells in 3 1mm squares were counted and the average then multiplied by 10^6 to obtain the cell concentration in 1mL.

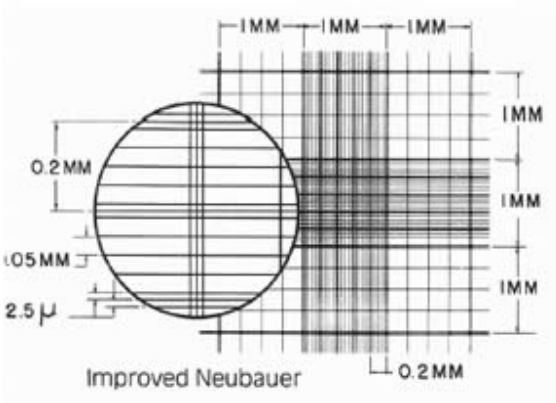

Fig. 2.2: Counting chamber. Depth of the chamber is 0.1mm, so 10x number of cells in one 1mm square would equal the concentration of cells in $1mm^3$ (Adapted from Emdiasum, Hatfield)

2.3.6. Isolation of plasmacytoid dendritic cells (PDC) from PBMCs

PDCs were isolated from human Buffy coats using the MACS (magnetic cell sorting, Milteyni) system and PDC-specific antibodies. They make up 0.5-1% of the PBMC population.

To this end, 10^8 PBMCs were resuspended in 150µL MACS buffer (1xPBS, 0.5% PSA, 2mM EDTA) together with 50µL FcR blocking reagent and 50µL Anti-BDCA-4 microbeads (blood dendritic cell antigen 4). The anti-BDCA-4 microbeads solely recognize CD304, which is specifically expressed on PDCs, and the FcR blocking reagent impedes unspecific binding of the microbeads. The suspension was incubated for 15 minutes at 6-12°C and then filled to 10mL with MACS buffer. The mixture was centrifuged to 7 minutes at 400g and the supernatant removed completely. The pellet was resuspended in a final volume of 500µL

MACS buffer. During the centrifugation step, the precooled LS columns were placed into the magnetic holder and equilibrated by pipetting 3mL MACS buffer onto the matrix.
The suspension was applied on top of the column and the flow-through, i.e. the CD304-negative cells, was either discarded or used for further experiments. The column was washed 3 times with 3ml buffer, the flow-through collected in the same tube as the negative cells. The column was then removed from the magnetic holder, 3mL buffer applied on top and the flow-through collected in a new centrifuge tube. Without the magnetic field keeping the CD304-positive cells in the column matrix, the PDCs were flushed out. In order to achieve higher purity of the resulting cell population, the cell suspension was then loaded onto precooled and equilibrated MS columns. The PDCs remaining in the column were washed once with MACS buffer, the MS column removed from the magnetic holder and the cells flushed out, then resuspended in RPMI medium and counted for viability.

2.3.7. Isolation of monocytes

Monocyte isolation was performed by depleting the cell fraction from all cells except for monocytes using the Monocyte Isolation Kit II. Monoclonal antibodies against CD3, CD7, CD16, CD19, CD56, CD123 bound to NK cells, T cells, B cells, dendritic cells and basophile granulocytes. This way, all non-monocytes would be kept in the column matrix and the non-labeled flow-through would contain the monocyte fraction. 10^7 cells were resuspended in 15µL of MACS buffer and mixed with 5µL FcR blocking reagent and 5µL Biotin-antibody cocktail. After incubation for 10 minutes at 4-8°C, another 15µL buffer were added, as well as 10µL Anti-Biotin microbeads. The suspension was mixed and incubated for 15 minutes at 4-8°C. 2mL MACS buffer were added and the mixture centrifuged for 7 minutes at 400g and 4°C The supernatant was removed and the pellet resuspended in 500µL buffer.
The precooled LD column was inserted into the magnetic holder and equilibrated with 500µL MACS buffer. LD columns are used for depletion isolation of cell populations because they have a superior microbead binding area, ensuring a higher purity of the monocyte population. The cell suspension was applied to the column and the effluent collected in a centrifuge tube. The column was washed twice with 1000µL buffer and the flow-through also collected in the same tube. The suspension was centrifuged, the supernatant discarded and the pellet resuspended in RPMI medium; a working concentration of 10^6 cells/mL was used for stimulation experiments.

2.3.8. Isolation of CD14 negative cells

CD14 is a surface receptor primarily found on monocytes and macrophages (Lacroix *et al*). It works in cooperation with TLRs in order to recognize bacterial endotoxins. Its specificity of location facilitates isolating CD14 negative cell populations.

To this end, 10^8 PBMCs were resuspended in 800µL MACS buffer and 200µL CD14 MicroBeads added. The mixture was then incubated for 15 minutes at 4-8°C. The cells were washed by adding 8mL MACS buffer, then centrifuged for 7 minutes at 300g and the supernatant removed. The pellet was resuspended in 1mL buffer and then loaded onto equilibrated LD columns. The flow-through consisting of CD14 negative cells was pelleted, then resuspended in RPMI medium and counted for viability.

2.3.9. Isolation of murine bone marrow derived dendritic cells (mDCs)

The hind leg bones of mice were used for obtaining mDCs. Bone marrow cells were isolated and differentiated into dendritic cells (DC).

The knee joint of the hind leg was overstretched, the femur separated from the tibia and fibula. The bones were cleaned from any remaining tissue and the epiphyses removed in order to have free access to the bone marrow. The bone marrow cells were flushed from the hollow into a 50mL centrifuge tube using a syringe filled with medium, then pelleted by centrifugation. The supernatant was removed , the pellet resuspended in 10mL Lysis buffer and incubated for 5 minutes at room temperature. 30mL NaCl were added and the suspension centrifuged, the pellet resuspended in medium and the cells counted.

In order to differentiate the cells to DCs, $2x10^5$ cells were pipetted per well in a 6-well plate, then incubated for seven days with 3mL medium supplemented with 3% GMCSF (Granulocyte-Macrophage Colony Stimulating Factor). After seven days, the cells were counted and seeded at a concentration of $2x10^5$ cells per well in a 96-well plate in preparation for transfection experiments.

2.4. Transfection and stimulation of cells with transfection reagents

2.4.1. Transfection of DNA and RNA with poly-L-arginin

Combining RNA with the polycationic polypeptide poly-L-arginine results in easily endocytosed particles. The size of the particles is time-dependent; longer incubation times were

performed in order to achieve larger particles. DNA or RNA can enter into the endosome and initiate TLR recognition.

Per well in a 96-well microtitre plate, 15µL PBS were combined with 0.18µL 2mg/mLPoly-L-Arginin. 0.2µg RNA or DNA were added and the solution was pipetted to the cell suspension, then incubated for 20-24 hours and analyzed for cytokine content.

2.4.2. Transfection of DNA and RNA with Lipofectamine

The cationic lipid Lipofectamine binds to DNA and facilitates its entry into the cytosol. Transfections were usually carried out in 96-well microtitre plates. Per well, 0.5µL Lipofectamine were resuspended in 25µL Opti-MEM and then combined with 0.2µg DNA/RNA, also resuspended in 25µL Opti-MEM. The mixture was incubated for 20 minutes at room temperature, then added to the cell suspension. The supernatants were removed after 20-24 hours.

2.5 Flow cytometry analysis

Fluorescence activated cell sorter (FACS) analysis is of great help where cell populations have to be differentiated and counted in a high throughput manner. In FACS analysis, cells can be separated and measured according to their size and surface or cytosolic proteins. FACS can simultaneously measure various characteristics of different subpopulations in one sample. Cells are squeezed through a capillary with an inner diameter of 50 to 100µm. Cells are forced to pass through it in single file and are thus available for selective measurement. The FACS laser is focused on the middle of the capillary and the light scattered in an acute angle, also called forward scatter (FSC). Surface smoothness scatters the light in an obtuse angle, also called sideward scatter (SSC). A combination of these two factors allows the gating, or selection, of a cell population of the desired size. Coupling the cells or molecules of interest to certain fluorochromes such as FITC, PE or FAM allows further distinction via emission of the fluorochrome in question. It is detected and converted into a digital signal for the appropriate software analysis. In this thesis, the flow cytometer LSRII and the associated software FACS Diva and FlowJo were used.

2.6.Fluorescence microscopy

Fluorescence microscopy is of great help when wanting to analyse the exact localization of cell processes. For this thesis cells were fixed for 15 minutes with 4% PFA at 4°C, then washed

three times with PBS. If a primary antibody was used the cells were first permeabilized with 0.1% saponin and 5% BSA in PBS for 30' at room temperature, then washed with PBS. The cells were blocked for 30 minutes with 10% FCS in PBS. After renewed washing with PBS, the primary antibody was incubated with the cells overnight at 4°C in a wet box. The next morning, the cells were washed with PBS and then incubated with DAPI or Hoechst 33452 and the appropriate secondary antibody for 20 minutes on ice. The cells were washed 3 times with PBS and one time with H2O, then mounted on glass slides and kept away from light until the mounting medium had dried.

2.7. Lentiviral transduction of cell lines

2.7.1. Transfection of eukaryotic cells using $CaPO_3$

HEK cells were used for transfection of the three plasmids containing the viral building blocks. The culture medium of the cells used for viral production was changed 30 minutes prior to transfection. The cells were then transfected using the BBS-Ca_2PO_4 method (Chen and Okayama 1988). In it, DNA forms crystalline structures with $CaPO_3$, which can be endocytosed into the cell, where the DNA is then expressed. For one 10cm dish, 10-12µg DNA were diluted with H_2O to a final concentration of 2µg/100µL transfection solution. The diluted DNA was combined with ice-cold $CaCl_2$ to obtain a 250mM transfection buffer that was mixed 1:1 with 2x BBS. This was incubated for 10 min at room temperature and then added, drop-wise, to the cells. The medium was replaced the next day.

2.7.2.Production of stable knock down cell lines

In order to establish polyclonal cell lines constitutively expressing shRNA, cell lines possessing the IFN response properties of interest were transduced using a lentiviral vector (A549, THP-1). The production of a lentiviral vector for transfer of the shRNA expression cassette necessitated its insertion into a lentiviral expression plasmid already carrying a puromycin cassette. The vector manufacture occurred in the abovementioned HEK293T cells: 6.5µg pMDL (encodes the Gag-Pol proteins), 3.5µg pMD.G (encodes the capsid protein VSV-G of the VSV, and 2.5µg pRSV-Rev (Rev expression plasmid) were transfected together with 10µg of the shRNA vector plasmid (pLKO). Medium was replaced the next day, and the virus-containing supernatant filtered on day two.

For the transduction of the cell lines, $2x10^6$ cells were resuspended in 2mL virus-containing RPMI, together with 1:250 diluted polybrene. The cells were seeded in 6-well plates and centrifuged for 2 hours at 400g and 30°C. After two days, the cells were washed, the medium replaced and puromycin added for selection.

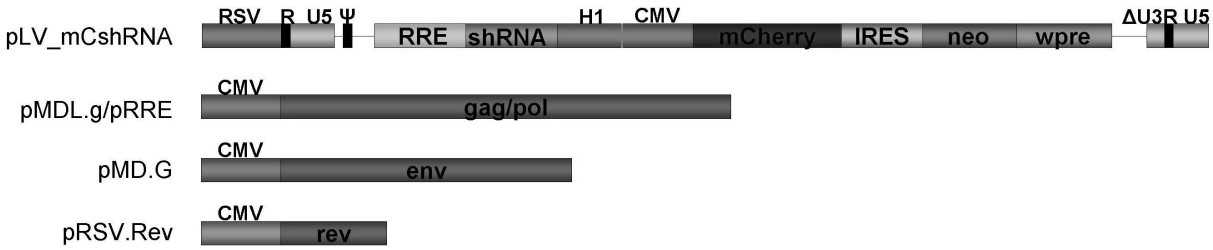

Fig. 2.3: Plasmids used for production of shRNA lentiviral vectors. This system is based on four vectors: a gag/pol-expression plasmid, an Env-Plasmid for packaging, a Rev-coding plasmid for optimization of the lentiviral export out of the nucleus and the vector genome plasmid. CMV = Cytomegalovirus Promoter, H1 = human promoter of rRNA-genes, puro= puromycin resistance, RRE = Rev-responsive element, RSV = Promoter of the Rous-Sarkoma Virus, IRES = internal ribosomal entry site, wpre = woodchuck post-transcriptional response element for the export of mRNA, □ = packaging signal. (Figure kindly supplied by C. Schuberth)

2.8. siRNA-mediated knock-down of THP-1 and A549 cells

THP-1 cells were electroporated with annealed siRNA sequences containing both sense and antisense strands. Sequences were annealed for 1hr.

Table 2.1. List of sequences used for shRNA and siRNA experiments

Name	Sequence
shRNA	
MITA 1 sense	GATCTCCCGCAACAGCATCTATGAGCTTCTTCAAGAGGAAGCTCATAGAT GCTGTTGCTTTTTGGAAA
MITA 1 antisense	AGCTTTTCCAAAAAGCAACAGCATCTATGAGCTTCCTCTTGAAGAAGCTC ATAGATGCTGTTGCGGGA
MITA 2 sense	GATCTCCCGCATCAAGGATCGGGTTTACATTCAAGAGTGTAAACCCGATC CTTGATGCTTTTTGGAAA
MITA 2 antisense	AGCTTTTCCAAAAAGCATCAAGGATCGGGTTTACACTCTTGAATGTAAACC CGATCCTTGATGCGGGA
siRNA	
MITA 1	GCAACAGCATCTATGAGCTTCTGGAGAAC
MITA 2	GTGCAGTGAGCCAGCGGCTGTATATTCTC
Luciferase sense	CGUACGCGGAAUACUUCGATT
Luciferase antisense	GAAGUAUUCCGCGUACGTT
RIG-I sense	AATTCATCAGAGATAGTCA
RIG-I antisense	GGAAGAGGTGCAGTATATT

10µg RNA were used for $2x10^6$ cells. THP-1 cells were washed with PBS and resuspended in Opti-MEM. 10µL RNA was combined with 100µL cell suspension. The electroporator was set to 300V, 150µF and 100Ω. After electroporation, cells were rapidly pipetted into 3mL RPMI in a 6-well plate. Two hours later, cells were pooled and washed. The next day, cells were replated in 96 wells and antibiotics added. Proteins were knocked down in time spans ranging from 48 to 72 hours. New medium was added prior to transfection experiments.

2.9. Circular dichroism spectra

Circular dichroism (CD) is the differential absorption of left- and right-handed circularly polarized light. Linearly polarized light is polarized in a certain direction (that is, the magnitude of its electric field vector oscillates only in one plane, similar to a sine wave). In circularly polarized light, the electric field vector has a constant length, but rotates about its propagation direction. Hence it forms a helix in space while propagating. If this is a left-handed helix, the light is referred to as left circularly polarized, and vice versa for a right-handed helix. Measurements are reported in degrees of ellipticity. This relationship is derived by defining the ellipticity of the polarization as:

$$\tan\theta = \frac{E_R - E_L}{E_R + E_L}$$

where E_R and E_L are electric field vectors of the right-circularly and left-circularly polarized light, respectively. When ER = EL, θ is 0°, meaning linearly polarized light. When either ER or EL is equal to zero, θ is 45° and the light is circularly polarized. It is known that G-tetrads have a unique melting curve at 295nm (reviewed in (Huppert 2008)).

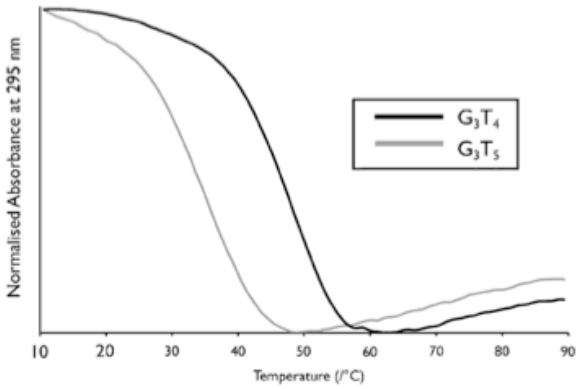

Fig. 2.4: Melting curve of G quadruplexes (Adapted from (Huppert 2008)).

2.10. HEK-Blue IFNβ reporter cell system

HEK-Blue™ Cytokine Cells from Invivogen is an engineered HEK293 cell line for detection of biologically active cytokines. They are based on the inducible expression of an optimized secreted embryonic alkaline phosphatase (SEAP) reporter gene and its quantitative detection using QUANTI-Blue™,or pNpp (p-Nitrophenyl Phosphate). HEK-Blue™ cells express the SEAP reporter gene under the control of the IFNβ-inducible ISG54 promoter.

Therefore, in the presence of IFNβ, the ISGF3 pathway is activated, modulating the SEAP activity. The amount of SEAP secreted in the cell supernatant can be measured spectrometrically with pNpp at 405nm. These cells were generated by stable transfection of HEK293 cells with the human STAT2 and IRF9 genes to have a maximally active type I IFN signaling pathway. HEK-Blue™ cells are resistant to the selectable markers blasticidin and Zeocin™ and are usable for about 30 passages.

2.11. Click-it system for RNA synthesis and infection of *Listeria*

Invitrogen has developed a system for tracking and observing nucleotide, sugar, or amino acid synthesis. RNA synthesis using ethynyl uridine was used in this thesis.

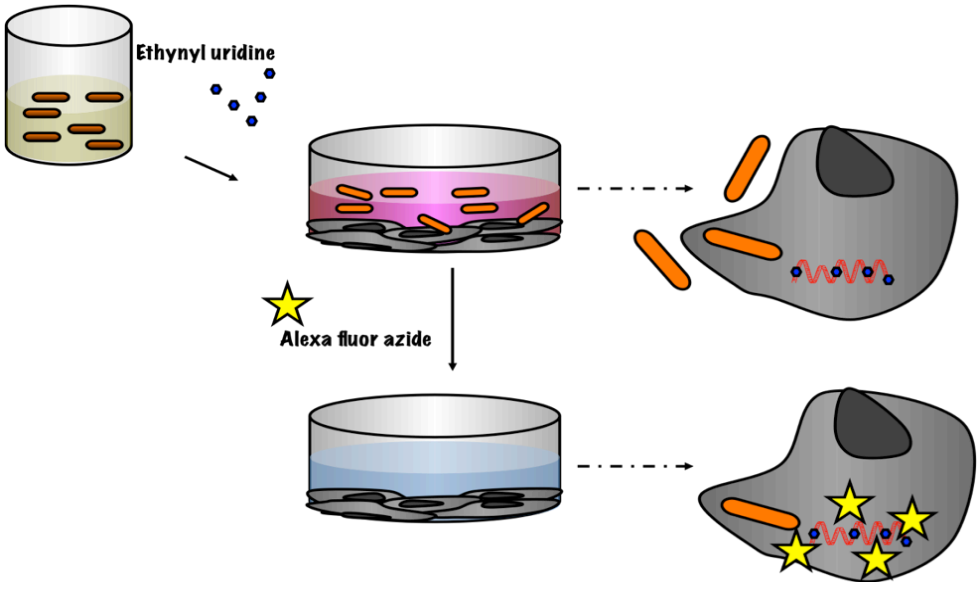

Fig. 2.5: Experimental setup of the Click-it Listeria infection. Listeria were incubated during their log growth phase with EU at the appropriate Molarity. EU-labeled Listeria were then allowed to infect host cells for various infection time points. Cells were washed and fixed with PMA. Listeria visible under fluorescence microscopy were therefore inside the host cells and red fluorescence had to be due to EU staining from Listeria, as host cells had not been fed with EU.

Click chemistry describes a class of chemical reactions that label and detect a molecule of interest using a two-step procedure. The two-step click reaction involves a copper-catalyzed

triazole formation from an azide and an alkyne. One can be used to tag the molecule of interest, while the other is used for subsequent detection. The azides and alkynes are inert, stable, and extremely small. The label is small enough that tagged ethynyl uridines are acceptable substrates for the RNA polymerases (Jao and Salic 2008). In addition to the azide and alkyne labeled molecules, copper (I) is required to catalyze the reaction. The click reaction can occur at pH values ranging from 3 to 12, at temperatures from room temperature to 37°C. In the case of *Listeria* infection, 100µL of an overnight culture of *Listeria* were grown in BHI dissolved in HTM (20% vol/vol), a minimal medium for *Listeria* (Tsai and Hodgson 2003). 20mM EU was added to the medium and the cells grown for 2-4 hours, or until the log phase had been attained. The cells were washed once with PBS to remove all traces of non-absorbed EU, then resuspended in opti-mem and added to host cells plated on coverslips at differing MOIs. After 2-4 hours of infection, the coverslips were washed, fixed with 4%PFA and permeabilized. The Alexa fluor 594 azide was resuspended in the click-it reaction cocktail (according to manufacturer's instructions), then added to the coverslips and incubated for 30 minutes at room temperature. The coverslips were washed with PBS and mounted on microscope slides, then let dry overnight.

3. Results

The work to characterize cytosolic recognition of nucleic acids encompasses three categories in this thesis (**Fig. 3.1**). The approaches to determine and detail the mechanisms and recognition motifs of cytosolic nucleic acid recognition can be divided into the search for a recognition motif, the interaction of PAMPs from pathogens such as *Listeria monocytogenes* with cytosolic receptors and the roles of MITA and autophagy with the type I IFN induction pathway.

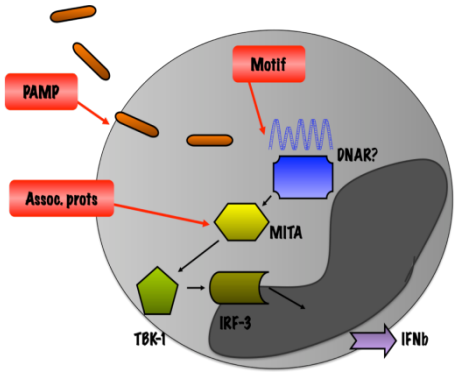

Fig. 3.1: Different approaches to characterization of cytosolic recognition of nucleic acids. In this thesis, three different methods to further understand cytosolic recognition of nucleic acids were performed. The motif for the as yet unknown DNAR will be discussed, as will the effect of RIG-I on the type I IFN and proinflammatory cytokine response. The involvement of MITA and autophagy in the monocytic IFNα pathway after transfection with nucleic acids will also be investigated.

3.1. Cytosolic recognition of DNA

Immune recognition of cytosolic nucleic acids plays a central role during the innate immune response. Cytosolic dsDNA induces a strong type I IFN response in a TLR9 independent manner. The exact mechanisms of the cytosolic dsDNA response, however, are poorly determined, the receptor unidentified. Recognition motifs of short dsDNA ODNs were analyzed in monocytes, as well as assorted cell lines, and two classes of immune stimulatory ODNs characterized. In addition to long dsDNA including plasmid DNA, human monocytes detected concatemerized short dsDNA ODNs. Surprisingly, monocytes were also able to recognize short dsDNA ODNs harboring mismatched terminal G extensions (a so-called bar-bell structure). As determined by gel electrophoresis and CD spectroscopy under physiological salt and temperature conditions, the G extensions of stimulatory dsODN did not form G tetrad structures, which excluded a polymerization dependent effect. The recognition of small dsDNA ODNs was restricted to monocytes and monocytic cell lines. This would implicate a new sequence-dependent recognition motif of short cytosolic DNA in human immune cells.

3.1.1. PBMCs recognize DNA dependent of its localization

Several recent works succeeded in showing the long DNA sequence poly dAdT a ligand for RIG-I (type I IFN induction) and AIM-2 (IL-1β induction) (Ablasser, Bauernfeind et al. 2009; Burckstummer, Baumann et al. 2009; Fernandes-Alnemri, Yu et al. 2009).

This advance, however, did not shed the expected amount of light on the subject of cytosolic dsDNA-type I IFN induction pathway. Although Burckstummer et al performed a proteomic approach, the type I IFN DNAR remained elusive. Trying to characterize the DNAR by way of its ligand has resulted in confusing discoveries, because the descriptions of possible recognition motifs differed in cell lines, organisms or readouts. Suzuki et al had shown in 1999 that mammalian DNA, bacterial DNA, double-stranded linear DNA polymers, double-stranded ODNs and double-stranded PTO-modified ODNs induced TLR9-independent expression of type I IFN inducible genes in rat thyroid cells after lipofection (Suzuki, Shiratori et al. 1999). Seven years later, Medzhitov discovered a minimal length requirement of 25bp in dsDNA ODN for type I IFN induction in murine monocytes. Medzhitov et al, however, also found a complete inhibition of IFN induction after PTO modification of the ODN backbone (modification of only the ends, however, was tolerated) (Stetson and Medzhitov 2006). Ishii et al. expanded the definition of immunestimulatory cytosolic DNA to include all B-form DNA, as long as it was transfected. Poly dAdT was strongly IFN-inducive (in contrast to pdGdC) in MEFs (Ishii, Coban et al. 2006).

In this work, recognition motifs of dsDNA ODNs and associated polymers in human monocytes were dissected. Two different types of immune stimulatory ODN, sequence or length dependent, were discovered.

The main part of the cytosolic dsDNA- induced type I IFN response is produced by monocytes.

One of the first experiments was performed in order to characterize the induction of IFNα in different cell populations of human blood. Therefore, different types of DNA were transfected in freshly isolated PBMCs before and after depletion of pDCs or monocytes. Transfected A type CpG (CpG 2216), genomic DNA (genDNA) and plasmid DNA (pDNA) all induced comparable amounts of IFNα in whole PBMCs (see **Fig. 3.2 - Fig. 3.4**)).

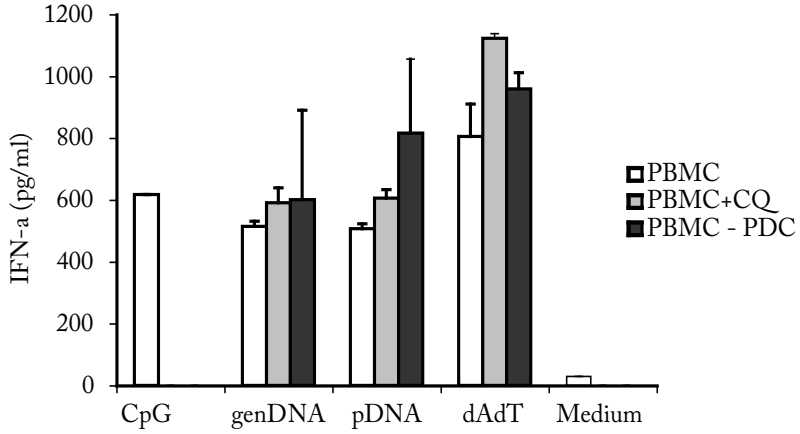

Fig. 3.2: The main part of cytosolic dsDNA-induced IFNα is produced by monocytes. PDCs were depleted from PBMC and transfected with CpG 2216, genDNA and pDNA. TLR9 activity was blocked in PBMCs with chloroquine (CQ). PBMCs with chloroquine showed the same IFNα response as PBMCs with PDC depletion.

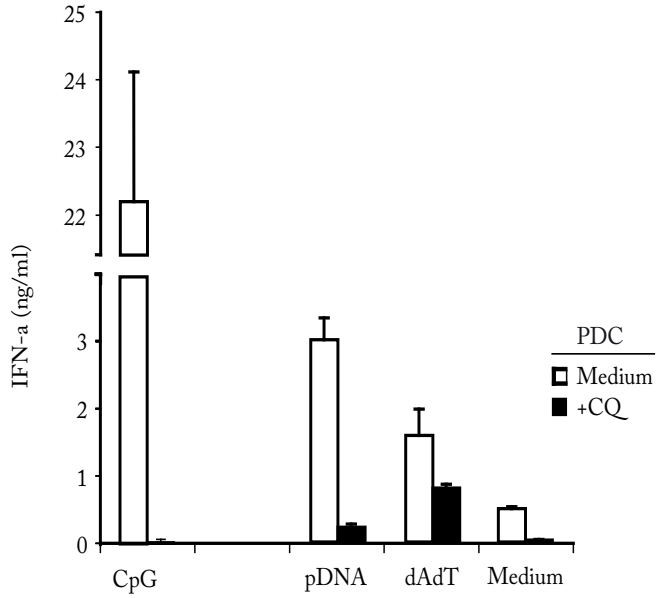

Fig. 3.3: PDCs supply the IFNα response to CpG. PDCs were isolated from PBMCs and transfected with CpG2216, genDNA, pDNA, or medium. Only PDCs that had not been treated with the endosomal acidification reagent CQ could respond to CpG2216 stimulation. The bacterial origin of pDNA is visible in the IFN response of PDCs to it.

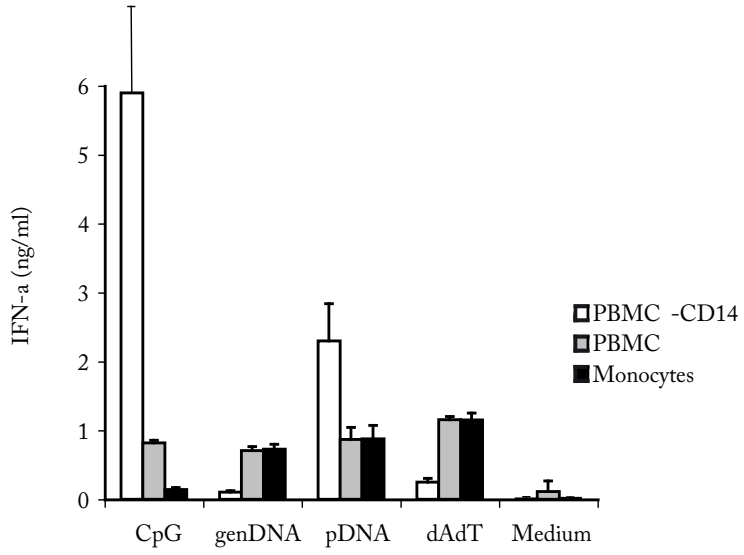

Fig. 3.4: Monocytes are the source of cytosolic dsDNA IFNα in PBMCs. PBMCs were stimulated as a whole population, or PBMCs were depleted of monocytes using CD14 beads, or the pure monocyte population was used. The amount of IFNα produced by PBMCs and monocytes was near identical, while PBMCs depleted of $CD14^+$ cells produced IFNα solely in response to TLR9 stimuli.

However, blocking of TLR9 with CQ or depletion of PDCs abrogated the induction of IFNα by type A CpG, while the induction of IFNα by genDNA and pDNA was not disturbed. In contrast, depletion of monocytes nearly completely abolished the induction of IFNα by genDNA, while the induction of IFNα by CpG2216 and pDNA was enhanced. Pure monocytes responded with the virtually same amount of IFNα as PBMCs to stimulation with genDNA. These experiments clearly show that the presence of monocytes is essential for the IFNα response to genDNA. As pDNA contains CpG motifs, pDNA represents both a TLR9 ligand and a ligand for the DNAR. According to Krieg, mammalian genDNA is not recognized by TLR9 due to its modifications (McCluskie and Krieg 2006). Further experiments in pure human PDCs show that the induction of IFNα by genDNA is only partially sensitive to CQ. This indicates that, similar to monocytes, PDC also recognize DNA in a TLR9-independent manner. However, as PDCs are infrequent in PBMCs, TLR9-independent IFNα from PDC only plays a minor role overall. With this knowledge, further experiments were done with CQ-suppressed PBMCs, assured that the IFNα response could be interpreted as coming from the monocyte population.

3.1.2. Tandem dsODN are recognized by the DNAR

So far, dsDNA ODNs, but not ssDNA ODNs, have been tested in only the murine system (Stetson and Medzhitov 2006). In order to systematically analyze the innate immune response

to dsDNA ODNs in the human system, various synthetic palindromic ODNs of different lengths were transfected into human PBMCs. The ODN sequence GC(AT)nGC was used, with n=10, 13, 20, 30, 40. IFNα production was analyzed 24h after stimulation. In addition to human PBMCs, human cell lines were used, as well as murine bone marrow-derived DCs (BMDCs) (see **Fig. 3.5**).

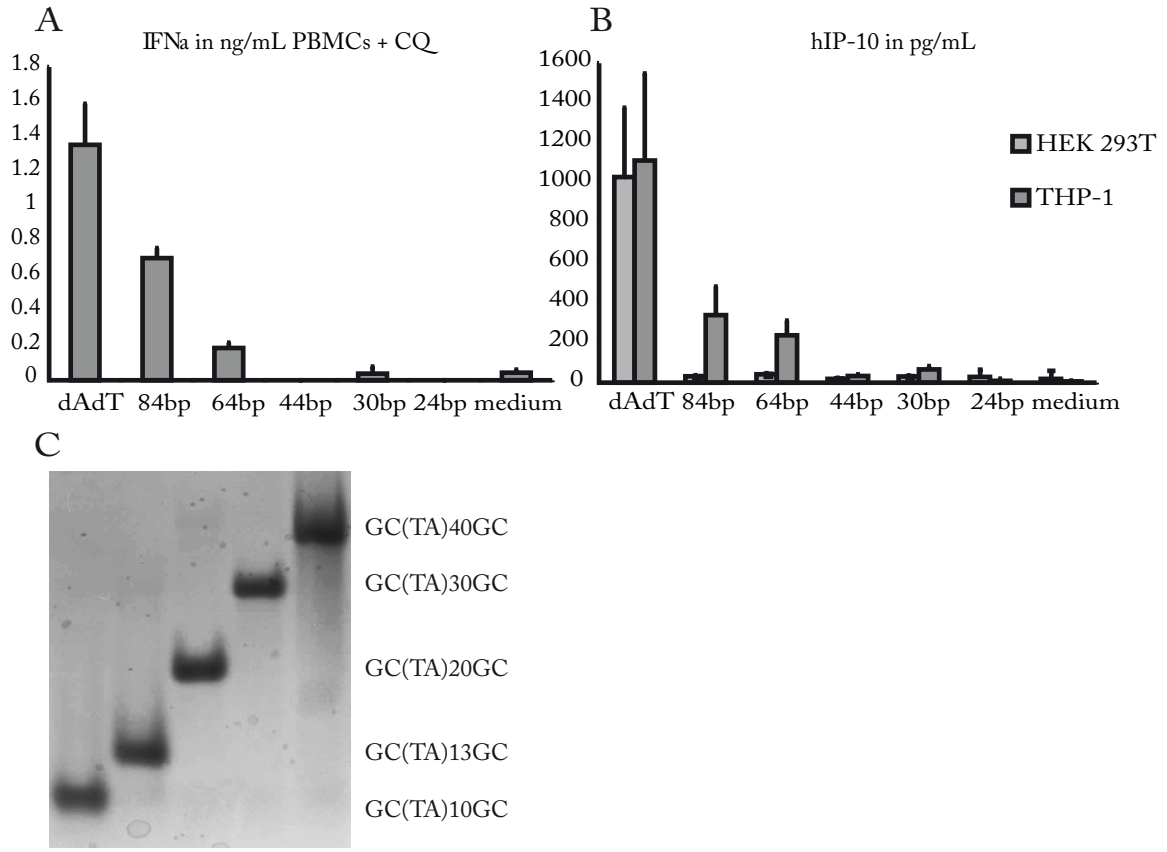

Fig. 3.5: Length-dependent induction of type I IFN in PBMCs. dsODNs were transfected into cells of different origins and different species. A) IFNα ELISA of PBMCs blocked with CQ. A robust IFNα response to dsDNA only starts after 84bp. $2x10^5$ PBMCs were plated per well of a 96-well plate and then transfected with 0.5µL Lipofectamine complexed with 0.2µg DNA. Supernatants were removed after 24 hours incubation and IFNα measured. B) hIP-10 ELISA of human cell lines HEK293T and THP-1. Only THP-1, a monocytic cell line derived from professional immune cells, seems to express a DNA recognition system. C) PA-gel of the dsDNA. 0.4µg DNA was loaded onto the gel and run for 40 min at 90V. The dsDNA ODNs traveled through the gel according to size, but showed various forms of their molecular weight because of their palindromic sequence.

PBMCs blocked with CQ were used because it had been established that the use of CQ allows for an almost purely monocyte-derived cytokine response (see **Fig. 3.2**). No considerable induction of hIFNα was obtained after transfection of ODN smaller than n=20. Various cell lines were tested for their ability to respond to transfection of cytosolic DNA with production of type I IFN; THP-1 and HEK 293T cells are shown here exemplarily. Of all the cell lines tested, only the monocyte-derived cell line THP-1 mounted a type I IFN response to DNA transfection, showing that cytosolic DNA recognition is restricted to certain cell types. As

highly repetitive, palindromic sequences could form unpredictable undusual structures, we also evaluated length-dependency of type I IFN production for non-palindromic sequences (**Fig. 3.5D**) yielding similar results.

3.1.3. Long DNA sequences are recognized regardless of sequence

Once the minimal sequence length had been determined, it was tested whether sequence specificity was a part of the type I IFN response.

Concatemerized DNA sequences resulting in long dsDNA fragments induce a type I IFN response

As earlier studies suggested a sequence independent but length dependent mechanism of DNA recognition, it was attempted to design small but self-polymerizing ODN. The concept of the motif design was to combine a pair of DNA ODNs with self-polymerizing properties. Double-stranded DNA ODNs were constructed using overlapping sense and antisense strands so that long dsDNA strands would result from hybridization of both ODNs together. CAAACCAAAGAATGGCATCATAAATAGTGGAGAGGGTGAAGGTGA (ODNs Nr 126) and its counterpart, the antisense strand with the staggered sequence TATGATGCCATTCTTTGGTTTGTCACCTTCACCCTCTCCACTATT (ODN Nr 153) give a concatemerizing double strand with a molecular weight a multiple of the single strand. (see **Fig. 3.6C**).

The 5' half of the sense strand hybridizes with the 5' half of the antisense strand, while the 3' half of the sense strand hybridizes with the 3' half of the antisense strand. Sequences leading to self-hybridization of either sense or antisense ODN had to be avoided. This is why nonpalindromic sequences based on the GFP sequence were used. In theory, hybridizing the two sequences together would result in a self-replicating dsDNA strand of varying length, while using only each ODN by itself would show a single band on a PA gel. The hybridization of both ODNs together induced substantial secretion of IFNα, while single ODN did not induce IFNα secretion when transfected. After loading the single ODNs, as well as the hybridized dsODN mixture, distinct bands were visible for the single ODNs and a long smear, as well as a solitary band, were visible for the hybridized ODN mixture, indicating that long dsDNA of a high MW had been formed.

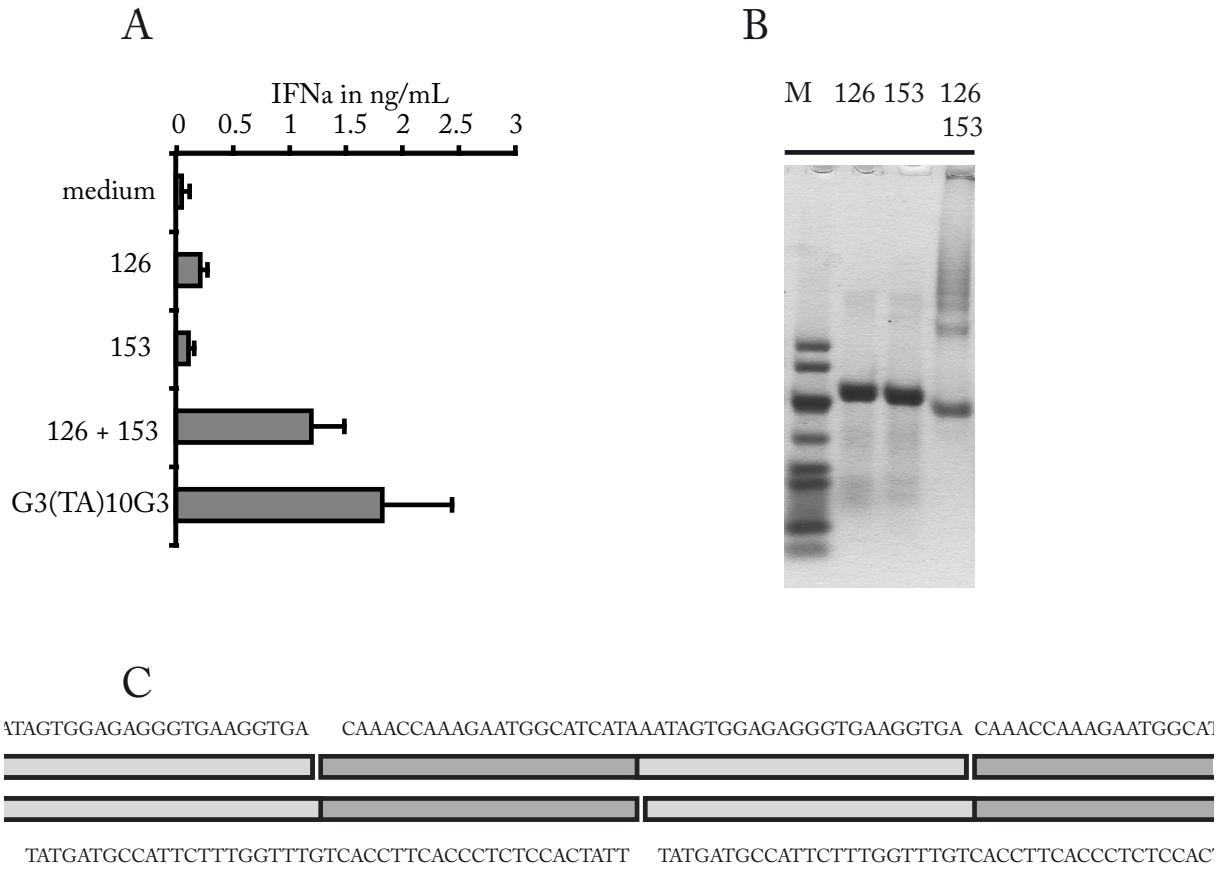

Fig. 3.6: Concatemerizing ODNs induce type I IFN only when transfected together. IFNα ELISA of PBMCs blocked with CQ and stimulated with concatemerizing ODNs. To this end, the sequence 126 and the ODN sequence numbers 153 ((TATGATGCCATTCTTTGGTTTGTCACCTTCACCCTCTCCACTATT) and its staggered partner (CAAACCAAAGAATGGCATCATAAATAGTGGAGAGGGTGAAGGTGA), respectively) concatemerize to large double-stranded DNA strands, which they do not do when single-stranded or unhybridized, as can be seen in the PA gel. A) CQ-blocked PBMCs were transfected with either the single stranded ODNs or the double-stranded hybridized version. Only the concatemer induces IFNα; ssODNs transfected alone do not induce IFNα. B) PA-gel of both ODNs alone and concatemerized. Both ODNs alone only gave a single band, while when hybridized together, they result in a smear of DNA with a larger molecular weight than either strand alone.

3.1.4. Short DNA sequences need to concatemerize for type I IFN induction

Single-stranded ODN sequences were designed, with the anti-sense strand giving a concatemerizing double strand when hybridized to the corresponding sense strand: $(AT)_6ACGGCT(AT)_6$ and $CG(TA)_{13}GC$, together with the C-G-switched pair $(AT)_6AGCCGT(AT)6$ and $GC(TA)_{13}CG$, were hybridized with each other and their corresponding strands (**Fig. 3.7A**). ODNs, when self-hybridized, failed to induce an IFNα response; only when hybridized as concatemers without gaps in the strand was an IFNα induction visible. In the next step, the ODN sequences were altered to $C_2(TA)_{13}C_2$, $(AT)_6AG_4T(AT)_6$, $G2(TA)_{13}G_2$, and $(AT)_6AC_4T(AT)_6$ (**Fig. 3.7B**). Transfection of the self-hybridized ODNs $C_2(TA)_{13}C_2$ and $(AT)_6AG_4T(AT)_6$ did not result in induction of IFNα in

CQ-blocked PBMCs, while transfection of the double strand did induce IFNα (see **Fig. 3.7B**). Transfection of self-hybridized G2$(TA)_{13}G_2$, and $(AT)_6AC_4T(AT)_6$ yielded an unexpected result; the single ODN $G_2(TA)_{13}G_2$ could induce a remarkably strong IFNα response (**Fig. 3.7B**), which was the reason for further investigation of the G-ended motif. Curiously, the single stranded $(AT)_6AG_4T(AT)_6$ showed two bands when run on a PA gel, one at the ssDNA height and one significantly further up. This band did not disappear once $(AT)_6AG_4T(AT)_6$ was hybridized to $C_2(TA)_{13}C_2$ (**Fig. 3.7C**). The IFNα induction was still dependent on the double-stranded structure; $(AT)_6AG_4T(AT)_6$ by itself, even though it multimerized into a higher-MW band, did not result in an IFNα response.

Murine BM-DCs have a lower sensing threshold for cytosolic ODNs

Murine immune cells have long been used for investigations concerning cytosolic nucleic acid recognition (Hemmi, Takeuchi et al. 2000; Takaoka, Wang et al. 2007). As differences in PRR expression such as TLR9 are already known to exist between human and murine immune cells (reviewed in (Barchet, Wimmenauer et al. 2008)), ODNs shown to induce IFNα in PBMCs were transfected into murine BM-DCs. Cells were isolated from C57BL/6 and cultivated for 7 days in media containing GM-CSF. As can be seen in **Fig. 3.8A**, the ODN ladder of 24-84bp induced a mIFNα response starting from 44bp instead of 64-84bp, as for PBMCs (**Fig. 3.5A**). In **Fig. 3.8B**, ODNs $C_2(TA)_{13}C_2$ and $(AT)_6AG_4T(AT)_6$ induced mIFNα when transfected as a concatemer, similarly to IFNα induction in PBMCs. $(AT)_6AG_4T(AT)_6$, however, also induced a mIFNα response without hybridization with $C_2(TA)_{13}C_2$. This induction could not be observed in PBMCs (**Fig. 3.7B**). This species-derived difference in length-dependent sensitivity to dsODN transfection is an example of why results obtained in using murine parameters cannot be transferred to the human system. Curiously, the single stranded $(AT)_6AG_4T(AT)_6$ showed two bands when run on a PA gel, one at the ssDNA height and one significantly further up. This band did not disappear once $(AT)_6AG_4T(AT)_6$ was hybridized to $C_2(TA)_{13}C_2$ (**Fig. 3.7C**).

3.1.5. dsODN with protruding G ends induce IFNα in PBMC

As discussed in section 3.1.4., the IFNα-inducing activity of $G_2(TA)_{13}G_2$ was similar or better than tandem matching ODN combinations. Further analysis of length and composition revealed strong IFNα inducing activity of ODNs with two mismatched protruding G at the 5' and 3' ends (see **Fig. 3.7.B**).

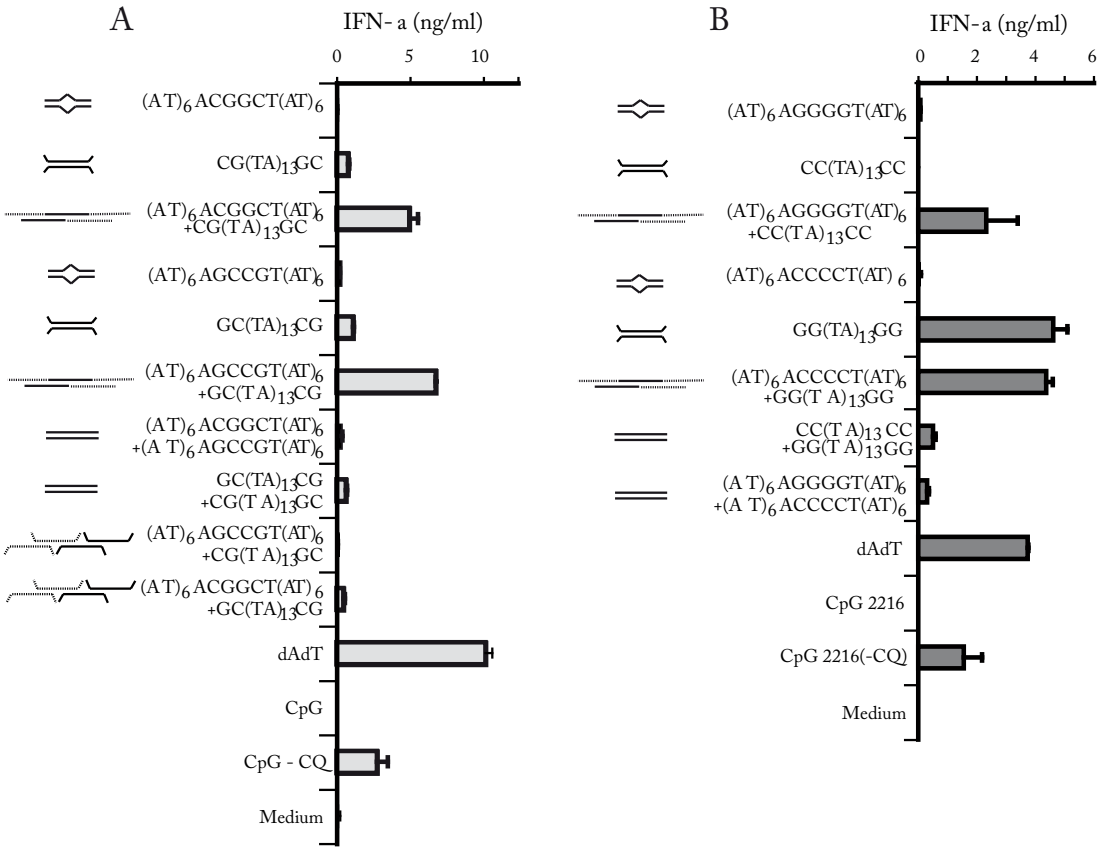

Fig. 3.7: ODNs need to be double-stranded for IFNα induction. A) CQ-blocked PBMCs were transfected with hybridized ODNs $CG(TA)_{13}GC$, $(AT)_6ACGGCT(AT)_6$, $(AT)_6AGCCGT(AT)6$ and $GC(TA)_{13}CG$. Each ODN transfected by itself did not induce an IFNα response, while the concatemerizing ODNs transfected together did induce a strong IFNα response. B) IFNα response after replacing GC pairings with only G or C sequences. The $G_2(TA)_{13}G_2$ ODN induced and IFNα response when self-hybridized, the other pairings only induced IFNα when concatemerized.

G3 induces a robust IFNα response, although C_3, A_3, T_3 do not

Three protruding Gs exhibited the most robust IFNα inducing activity. Substitution of G_3 with A_3, T_3 or C_3 led to the complete loss of IFNα activity. Interestingly, the effect of G_3 overhangs could be neutralized by pairing the G_3 ODNs with their C_3 complements. Permutation of unpaired overhangs showed that substitution of single Gs by A, T or C are gradually tolerated but confirmed that G_3-ended ODNs mount the most robust type I IFN response (**Fig. 3.10C**).

The crucial element of IFNα induction in the G-ended nucleotides is the barbell end

Sequences based on the core sequence of $G_2(TA)_{13}G_2$ were transfected onto CQ-blocked PBMCs in order to assess the length dependence of the stimulatory motif. $G_2(TA)_9G_2$ still induced a substantial amount of IFNα (see Fig. 3.9 B). This would indicate that the length of the (TA) sequence is not the section of the ODN critical for recognition.

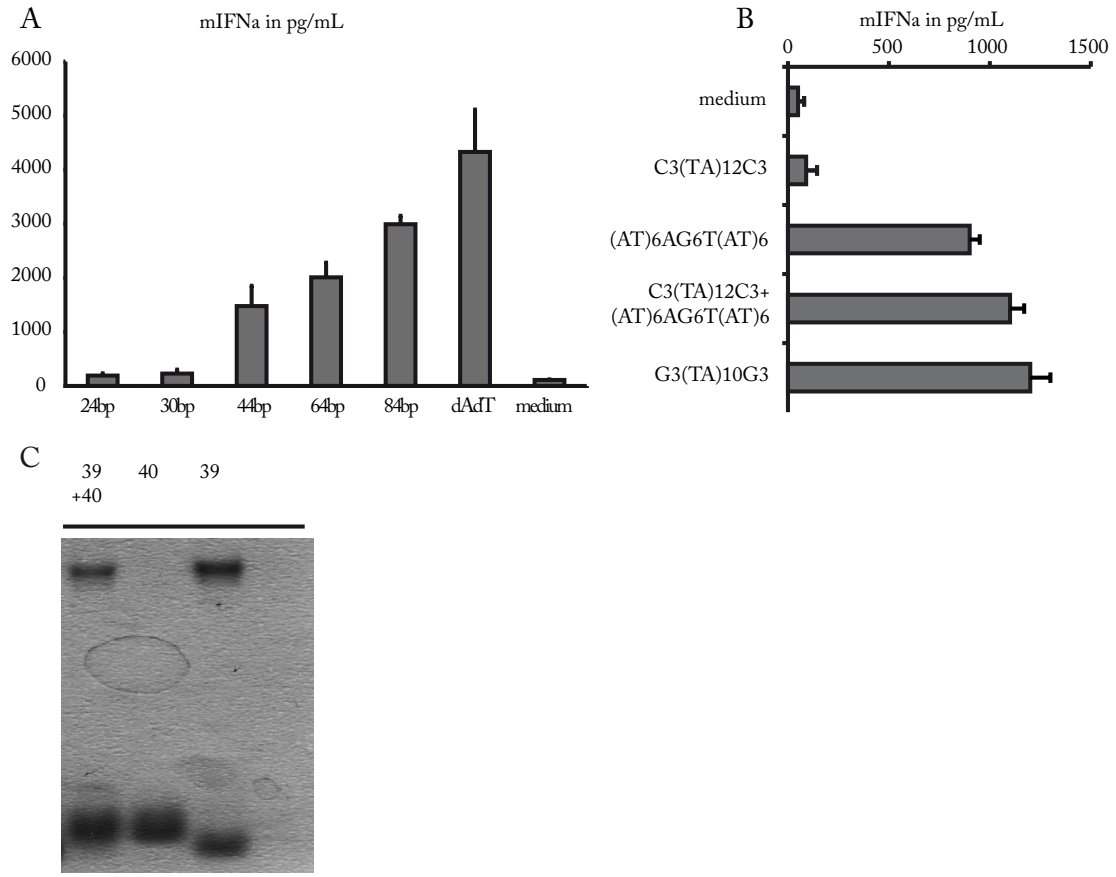

Fig. 3.8: Murine BM-DC mIFNa response to DNA ODNs. A), B): mIFNα ELISA of BMDCs stimulated with the dsDNA ODNs. BM-DCs from C57BL/6 mice were isolated and cultivated for a week in RPMI supplemented with GM-CSF. Cells were plated at 10^5 cells per well in a 96-well plate, then transfected with 0.5µL Lipofectamine complexed with 0.2µg DNA. Supernatants were removed after 24 hours incubation and mIFNα measured. A) Transfection of 24bp-84bp ODN ladder. The cutoff point for cytosolic dsDNA recognition starts much lower in murine BMDCs, indicating that results obtained in the murine system cannot be blindly transferred into the human one. B) ODNs $C_2(TA)_{13}C_2$ (40) and $(AT)_6AG_4T(AT)_6$ (39) were self-hybridized or concatemerized, then transfected on BM-DCs. $(AT)_6AG_4T(AT)_6$ induced a mIFNα response without hybridization to its C-ended counterpart.C) An indication for this induction of mIFNα may lie in the fact that $(AT)_6G_6(AT)_6$ complexes by itself into a multimer: ODNs 139 and 140 were loaded and run on a 8% PA-gel.

PBMCs were also transfected with variations of the $G_3(TA)_4NNNN(TA)_4G_3$ core sequence: As can be seen, no homogeneous (TA) sequence is needed of IFNα induction. All combinations of nucleotide pairings in the sequence between the (TA) segments induced type I IFN.

3.1.6. Bar-bell dsODNs are recognized by DNAR

Since the (TA) sequence can not be present as ssDNA strands, a nonpalindromic core sequence was designed, together with its equally nonpalindromic counterpart (G_3NonPalin1G_3 and G_3NonPalin1G_3', respectively). This way, double-stranded ODNs would occur only in presence of both ODN strands and self-hybridization could be ruled out.

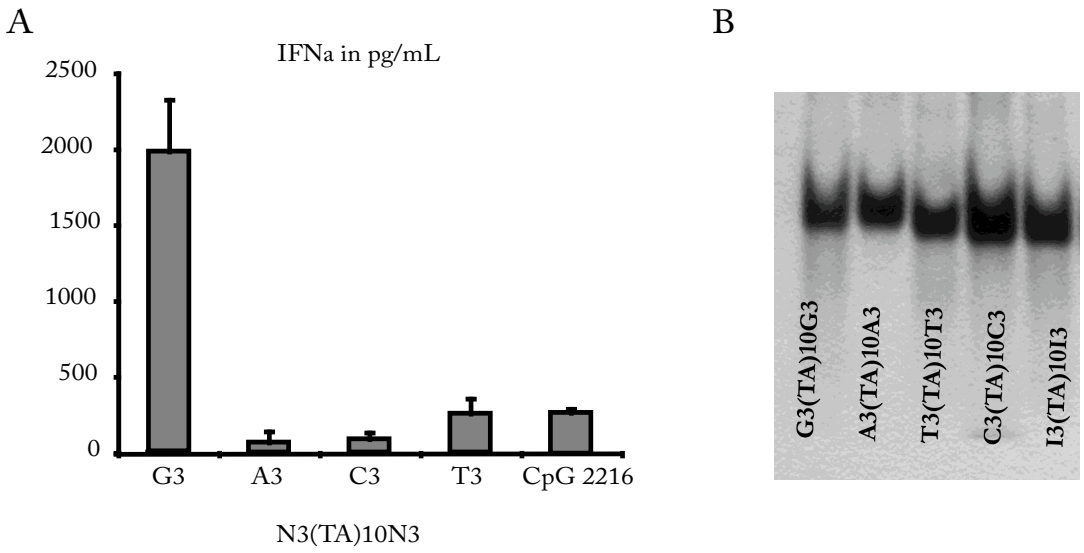

Fig. 3.9: Only G-ended oligos induce type I IFN in CQ-blocked PBMCs. A) CQ-blocked PBMCs were transfected with ODNs containing a core sequence of $(TA)_{10}$ and end sequences of G_3, A_3, T_3 and C_3, respectively. Only $G_3(TA)_{10}G_3$ transfection resulted in a type I IFN response. B) PA-gel of ODNs with a $(TA)_{10}$ core sequence and G_3, A_3, T_3 and C_3 ends, respectively. As can be seen, no structural or multimerization differences can account for the disparate IFNα induction.

Nonpalindromic DNA sequences

PBMCs were blocked with CQ and then transfected with different combinations of the nonpalindromic core sequence. When transfected with these nonpalindromic ODNs, PBMCs responded with IFNα induction only in the case of dsDNA ODNs. Each strand for itself did not induce IFNα (**Fig. 3.10A**). Human cell lines THP-1, HEK293T, A498, A549, FaDu and HepG2 were transfected with various RNA and DNA stimuli and IP-10 quantities measured. RIG-I ligand 3P-dsRNA, RIG-I and DNAR ligand dAdT and DNA stimuli genDNA, pDNA, phage DNA, CpG 2216 and G3NonPalinG3 showed a varied cytokine response. Apart from THP-1, no human cell line induced IP-10 in response to G-ended barbell ODN (**Fig. 3.11C**).

IFNα induction by nonpalindromic DNA with missing G_3 barbell ends

Hybridizing two complementary core sequences with different 5' and 3' ends was done in order to identify on which end, if any, the G_3 overhang or mismatch is essential. The experiments showed that at least one 5' and one 3' G_3 overhang per double strand must be present for IFNα induction to proceed. In general, the amount of G_3 overhangs corresponded to the IFNα response. Interestingly, two mixed ODN with either a single 5' G_3-overhang or a single 3' overhang cooperated inducing IFNα in monocytes (**Fig. 3.12B**).

Nonpalindromic DNA with inosine insertion

In order to test if the IFN induction was purely due to the structural singularities of guanosine, new ODNs were designed incorporating inosine at their 5' and 3' ends. The inosine nucleoside has a ribose ring attached to hypoxanthine using a β-N9-glycosidic bond. It can pair with adenine, cytosine, and uracil. The DNA ODNs designed with inosine continued to use the nonpalindromic core sequence mentioned previously.

Inosine-containing barbell double strands induced IFN in a comparable amount to $G_3(TA)_{10}G_3$ ODNs. Inosine replacement of only one strand did not abrogate the effect that the G ends on the other strand had on IFN induction (**Fig. 3.13B**). The nonpalindromic core sequence and its corresponding antisense sequence were outfitted with I, G, A, T or C overhangs on both 5' and 3' ends, in addition to an ODN without overhangs, i.e. the naked core sequence. All nonpalindromic sequences were hybridized with their antisense sequences, meaning IINonPalinII was hybridized with GGNonPalinGG, AANonPalinAA, and so on. This showed that inosine had a stimulatory effect comparable to guanosine; as long as only one of the strands contained inosine overhangs this resulted in an IFNα response in CQ-blocked PBMCs. Hybridization of IINonPalinII with NNNonPalinNN induced even more IFNα when N was T, A, or C.

The only exception to this was when IINonPalinII was hybridized with the ODN sequence without overhangs; this hybridization induced no IFNα. Guanosine overhangs induced at least a modicum of IFNα as long as no blunt ends resulted in the pairing (**Fig. 3.13B**).

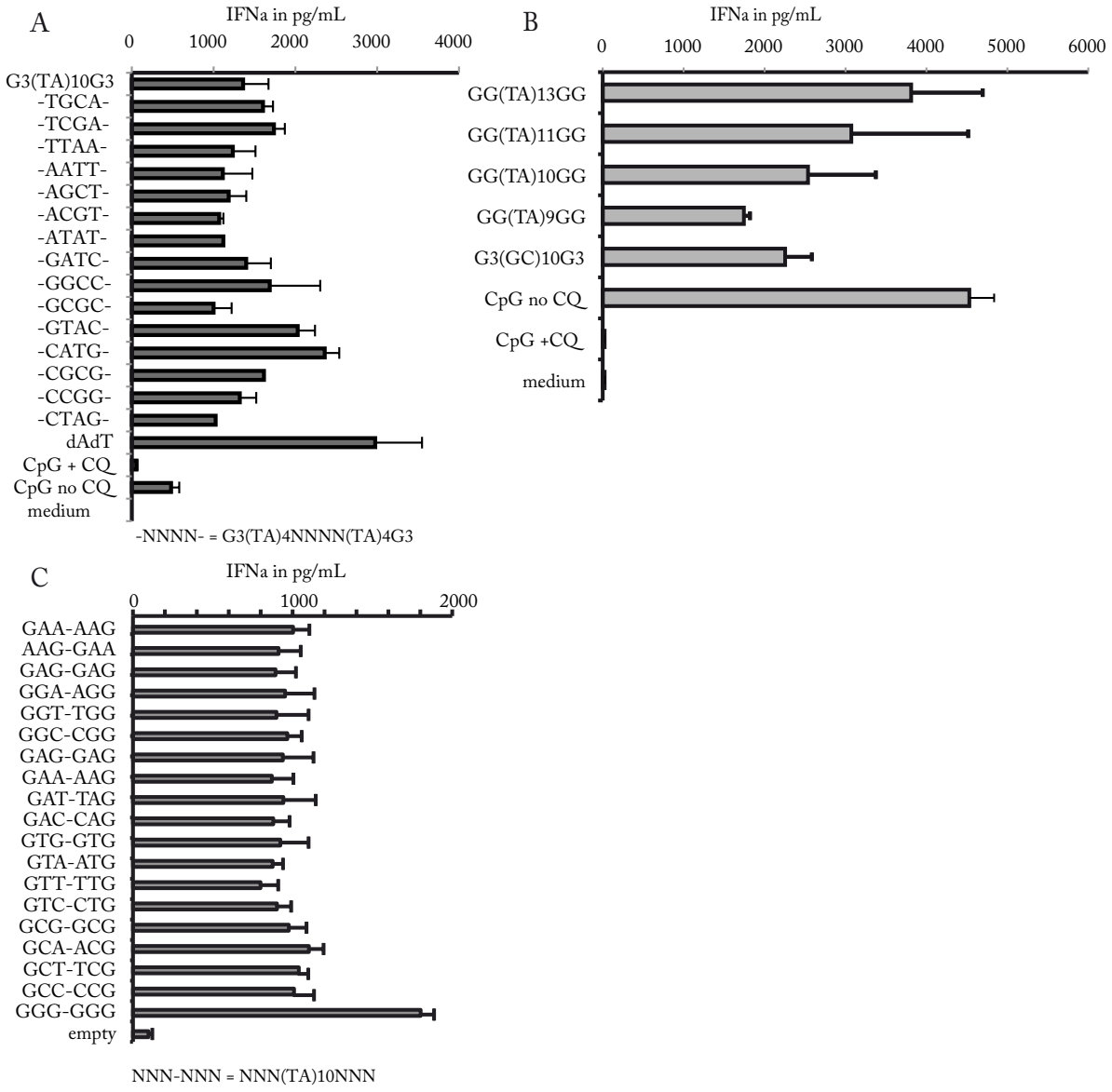

Fig. 3.10: Evaluation of (TA) length dependency on IFNα induction. A) The (TA) core sequence was further decreased by inserting different 4nt sequences. An unbroken (TA) length was therefore not necessary for an IFNα response in CQ-blocked PBMCs. Even though the TA-rich central repeat sequence appears to represent an excellent recognition motif, non-palindromic central sequences with low TA-content also induce substantial amounts of IFNα. B) Length of (TA) sequence is not important as long as Gs present on the ends. PBMCs were blocked with CQ and transfected with ODNs containing 2 guanosines on the ends but differing lengths of the (TA) core sequence. Differing lengths of the core sequence were diminished at $(TA)_9$ concerning the amount of type I IFN induced. An ODN containing no TA sequence, but G_3 ends, was also transfected and induced IFNα in the range of the (TA) sequence-containing ODNs. C) Substitution of one or more Gs by A, T, or C did not result in abrogation of the type I IFN response.

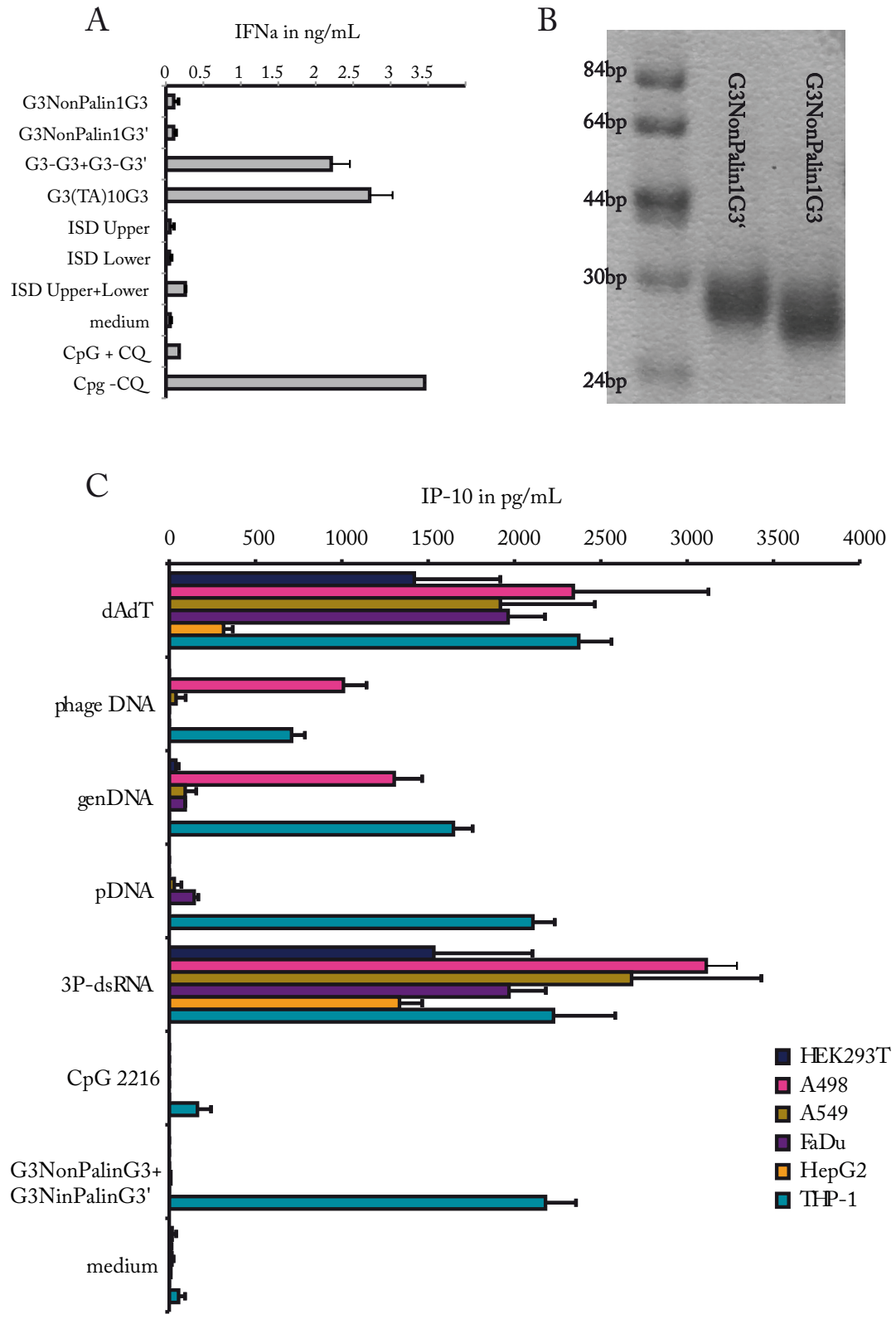

Fig 3.11: Analysis of G3NonPalin1G3 ODN characteristics. Because the sequences used previously could not guarantee a single-stranded state due to their palindromic sequences, ODNs were developed using the nonpalindromic core sequence of GGGCAATGGTCCTGCTGGAGTTCGGG (G_3NonPalin1G_3) and its corresponding antisense strand, GGGGAACTCCAGCAGGACCATTGGGG (G_3NonPalin1$G_{3'}$). They would not be able to form double strands by themselves, only when hybridized to their counterparts. A) CQ-blocked PBMCs were transfected with either only one half of the NonPalin couplet or with both strands hybridized. Only the double strand managed to induce an IFNα response, indicating that the IFNα measured after earlier transfections could be due to palindromic double-stranded sequences. Transfection of CQ-blocked PBMCs with

either one of the two ISD strands or the double strand hybridized showed only mild induction of IFNα. B) PA gel of G_3NonPalin1G_3 and G_3NonPalinG_3'. No multimeric complexes were formed. C) IP-10 ELISA of cell lines THP-1, HEK293T, A498, A549, FaDu and HepG2 transfected with RNA and DNA stimuli. Although all cell lines reacted to RIG-I ligand 3P-dsRNA and DNAR/RIG-I ligand dAdT, none reacted to DNA ODNs and CpG 2216. Although A498 responded to lambda phage DNA and genomic DNA, only THP-1 responded to G_3-barbell ODNs.

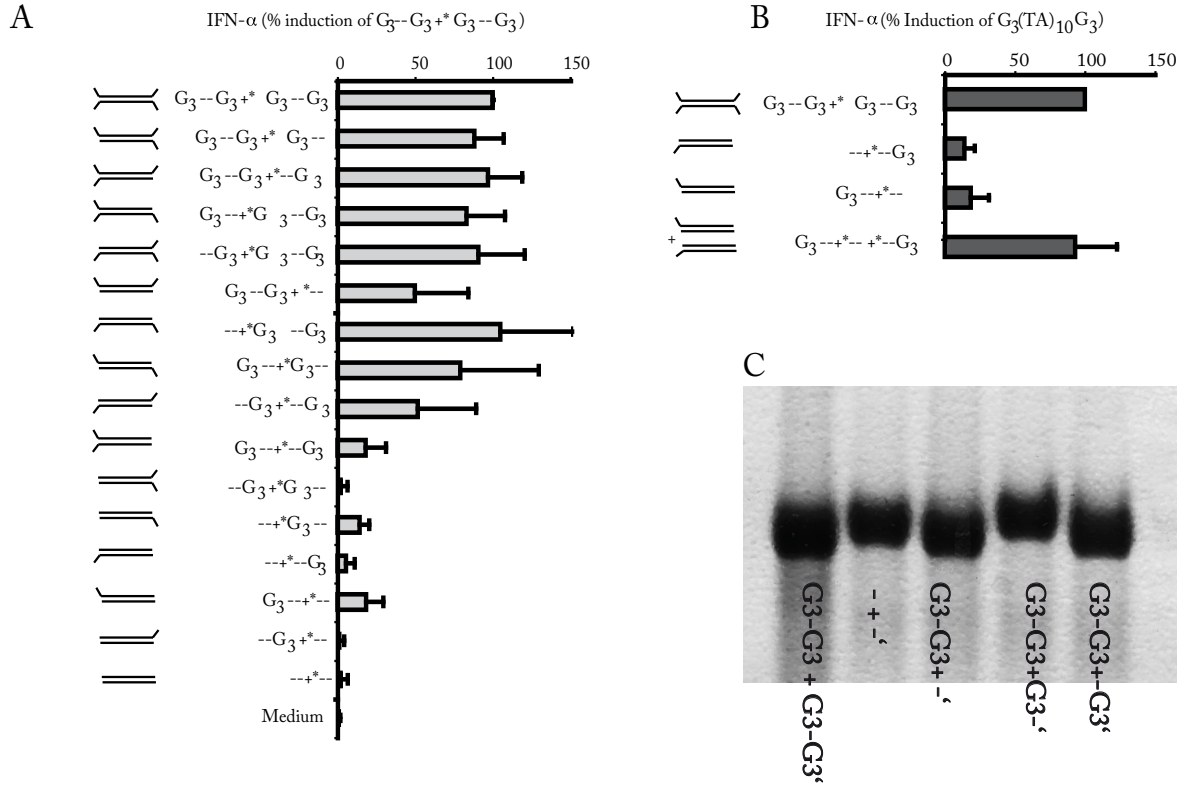

Fig. 3.12: Nonpalindromic barbell oligos induce IFN in CQ-blocked PBMCs in a barbell dependent manner. A) Double-stranded ODNs were transfected according to their G-ended overhangs. Blunt-ended nonpalindromic double strands do not induce IFN, so even if one of the strands of the double-stranded sequence has G ends, if the whole double strand has a blunt-ended motif, the IFN induction is abrogated. B) ODNs transfected together in order to assure a 5' and 3' overhang induce type I IFN; when tranfected alone, this effect could not be observed. C) Gel of the different G3-ended double stranded permutations. The double strands do not form concatemers.

3.1.7. Bar-bell ODN are active as monomers

Multiple nucleotides are capable of interacting via a quadruplex formation. There was, therefore, a distinct possibility that ODNs with overhanging G-rich ends interact via intermolecular G-quadruplex interplay, forming long chains recognized by virtue of their length. These so-called G tetrads are also present in telomeres: in mammalian cells, telomeres consist of hexanucleotide (TTAGGG) repeats, thus providing a possible answer for the immunogenicity of G-ended overhangs (Wallace, Salonen et al. 2000; Gursel, Gursel et al. 2003). Using native gel electrophoresis, it could be shown that ODNs with G_4 and G_5 ends

form high molecular weight bands typical for G quadruplexes, while G_2 and G_3-ended ODNs migrated as a simple low molecular weight band (see **Fig. 3.14B**).

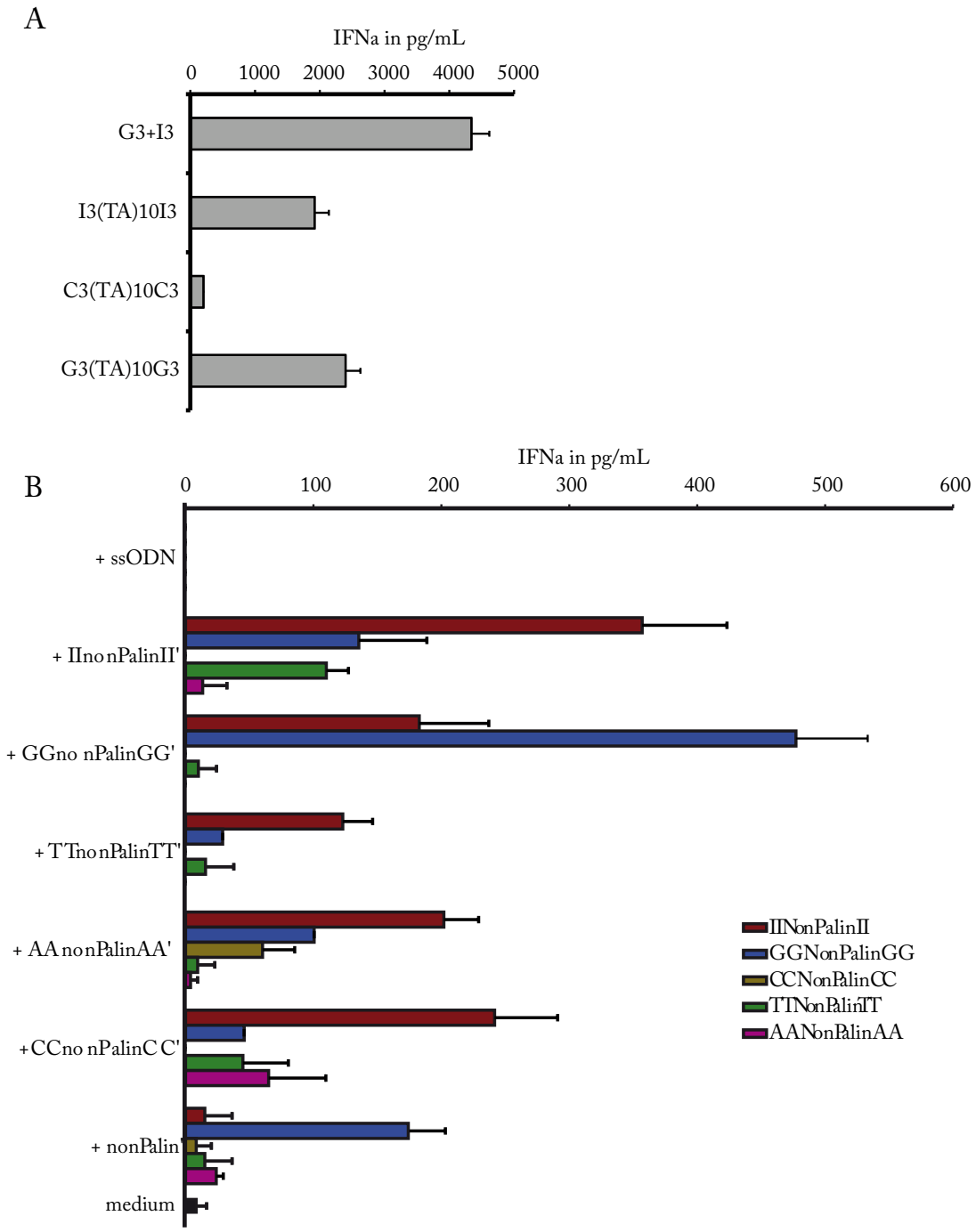

Fig, 3.13: Effect of Inosine on nonpalindromic ODN sequences. A) PBMCs were transfected with the abovementioned ODN sequences. G_3- and I_3-ended ODNs induced IFNα. B) Nonpalindromic core sequences with I, G, C, T or A ends were paired with the corresponding strands. Inosine-containing barbell double strands induced IFNα in a comparable manner to G-ended barbell double strands.

PAGE gels show a single band of G_2, G_3

Oligonucleotides were loaded on a non-denaturing PA-gel using KCl as a buffer instead of TBE. The gel was run for 14 hours at 4°C, so any complex formation of the ODNs would not

be disturbed. Two different core sequences were used; G overhangs were added to core sequences of $(TA)_4TGCA(TA)_4$ and $(TA)_{10}$. As can be seen in **Fig 3.14**, ODNs $G_2(TA)_{10}G_2$, $G_3(TA)_4TGCA(TA)_4G_3$ and $G_3(TA)_{10}G_3$ did not show multiple bands on PA gels. ODNs with longer overhangs such as $G_5(TA)_4TGCA(TA)_4G_5$, $G_4(TA)_4TGCA(TA)_4G_4$ and $G_4(TA)_{10}G_4$ did. The power of multimer formation did not, however, have any influence on IFNα induction in CQ-blocked PBMCs. All G-ended ODNs had similar IFNα-inducing properties (see **Fig 3.14A**).

Circular Dichroism spectra show no tetramer formation

Because a native electrophoretic gel may interrupt weak interactions because of its strong electric field, the molecular interactions were investigated in a physiological solution; 150mM NaCl, 30°C starting temperature. To this end, CD spectroscopy was used. A G quadruplex is arranged chirally (**Fig. 3.15A**), which enables it to be detected by CD spectroscopy, where the difference of absorption between circularly left and right polarized light is measured. In contrast to dsDNA, G tetrads show a unique optically active melting curve at 295nm (**Fig. 2.4**). CD spectra melting curves were measured from 30°C to 70°C using the ODNs listed in table 6.4. While G4 and G5-ended ODNs showed a clear melting curve, all of the other ODNs, including the G2 and G3-ended ones, exhibited no optical activity at 295nm (**Fig. 3.15C**). This is a strong indication that these immune stimulatory ODNs are also present as monomers under physiological conditions. In order to exclude a G quartet interaction under unknown parameters, ODNs were tested with the protruding 5' and 3' Gs subsequently replaced by 7-deaza-guanosine (**Fig. 3.15D**). Replacement of N7 by a C-H group disables tetrad formation. As the non-modified ODN demonstrates the same immune stimulatory ability as the modified ODN (**Fig. 3.15E**), it is to be assumed that G quartet formation, and, accordingly, polymerization is not necessary for immune recognition. This could, therefore, be considered a new sequence motif.

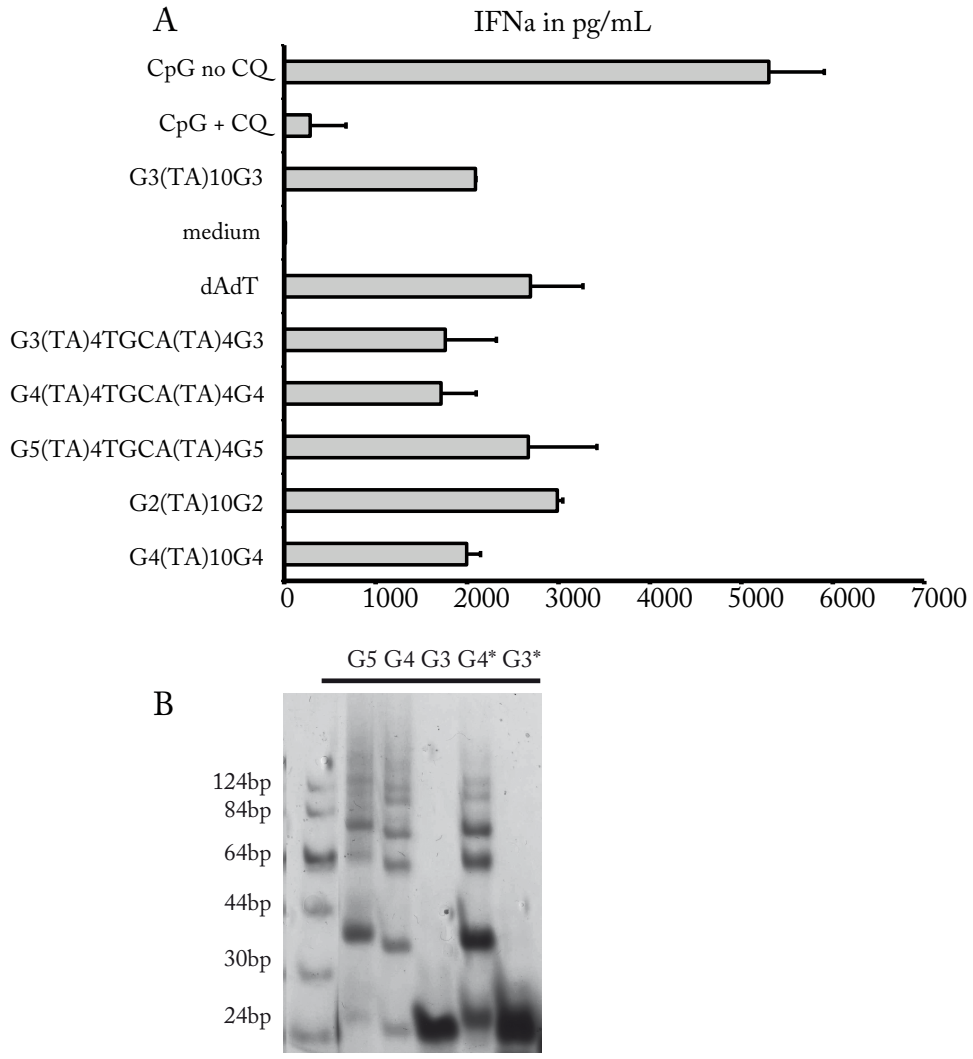

Fig. 3.14: G-ended ODNs induce IFNα in CQ-blocked PBMCs regardless of tetramer formation. A) CQ-blocked PBMCs were transfected with ODNs containing G ends of different lengths. All ODNs proceeded to induce a type I IFN response independent of tetramer formation. B) PA-gel of ODNs with different lengths of G ends. Only ODNs with 4 or 5 Gs showed tetramer formation; 3 Gs did not show the typical multimer formation seen in tetramer complexes.

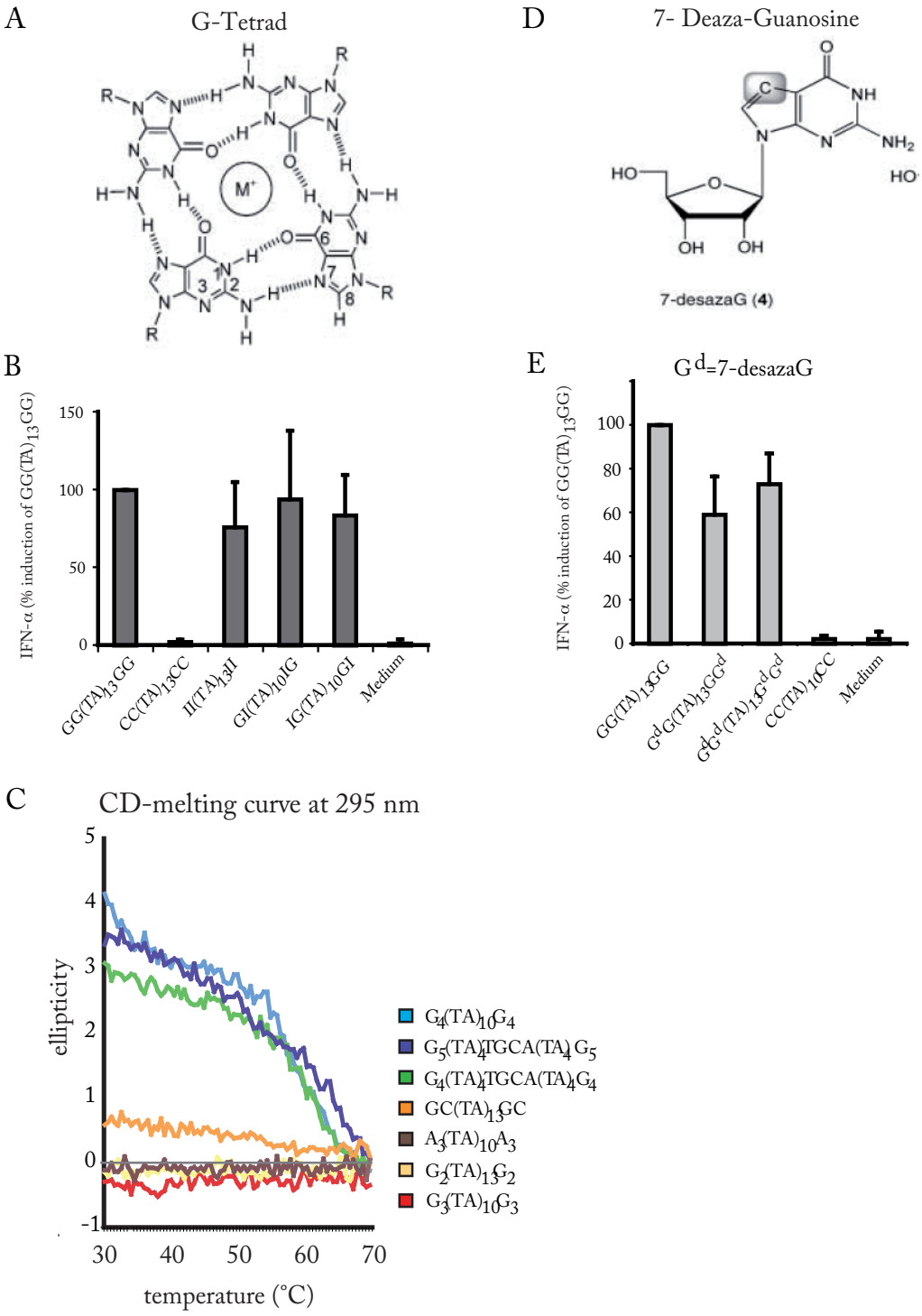

Fig. 3.15: IFNα-inducing characteristics and CD melting curves of G-ended and deaza-G-ended ODNs. CD spectra were used for observation of G tetrad formation in G-ended barbell ODNs. A) Arrangement of a G tetrad. B) IFNα induction in CQ-blocked PBMCs after transfection with deaza-G containing ODNs. C) CD measurement. ODNs were resuspended in a buffer using physiological pH and salt concentrations, then melted over a temperature course from 30 to 70°, with their CD spectra measured at 295nm D) Structure of deaza-G. N7 has been replaced by a C-H group. E) CQ-blocked PBMCs were transfected with G-ended ODNs, one of them containing deaza-G instead of G. No difference of IFN induction could be observed.

3.1.8. ODN are degraded in the cytosol

If the reason for different IFNα response to bar-bell ODNs does not lie in a polymerizing structural motif such as a G tetrad, maybe the key to the difference between G_3 ODNs and their counterparts, such as A_3, T_3 and C_3-ended ODNs, lies in their processing once they reach the cytosol. There are various DNases in mammalian cells, both endo and exonucleases. It could therefore be due to their delayed processing of G-ended ODNs.

Characterization of $G_3(TA)_{10}G_3$ vs $C_3(TA)_{10}C_3$ treatment

ODNs containing the G_3-ended nonpalindromic core sequence were used with a 5'- fluorescent FAM molecule, as well as a quenching 3' molecule. The idea was that the fluorescence would only be visible once cytosolic DNases had digested part of the sequence, thus freeing the FAM from the quencher. (see **Fig 3.16**). The assay was performed in 96-well plates; THP-1 cells were transfected with the ODNs, then incubated for different time points. In order to ascertain a transfection efficiency-independent readout, cells were also transfected with a Cy5-tagged control ODN, albeit at 1/10th the concentration of the nonpalindromic ODN of interest.

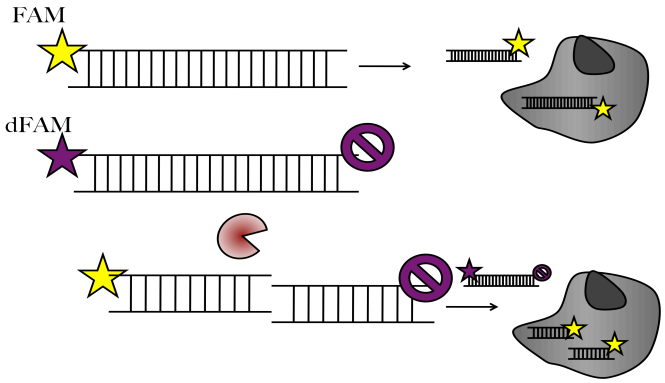

Fig. 3.16: Principle of the FAM-ODN transfection. A simple, FAM-tagged ODN would fluoresce regardless of its location. Coupling the FAM tag with a quencher on the 3' end of the ODN ensures fluorescence only when inside the target cell and enzyme activity separated the FAM molecule from the quenching molecule, an indication of intracellular localization of the ODN.

THP-1 cells were then investigated via FACS analysis, as well as measuring their fluorescence in the Perkin-Elmer luminometer. (see **Fig 3.17A, C, D** and **3.18C**). The percentage of Cy5 and FITC-positive cells were entered into a table. No significant difference between C_3 and G_3- ended sequences could be observed up to 6 hours' post transfection time (**Fig. 3.17A**). G_3-nonpalin ODNs were still capable of inducing and IFN response when transfected as a double strand (**Fig. 3.17B**.)

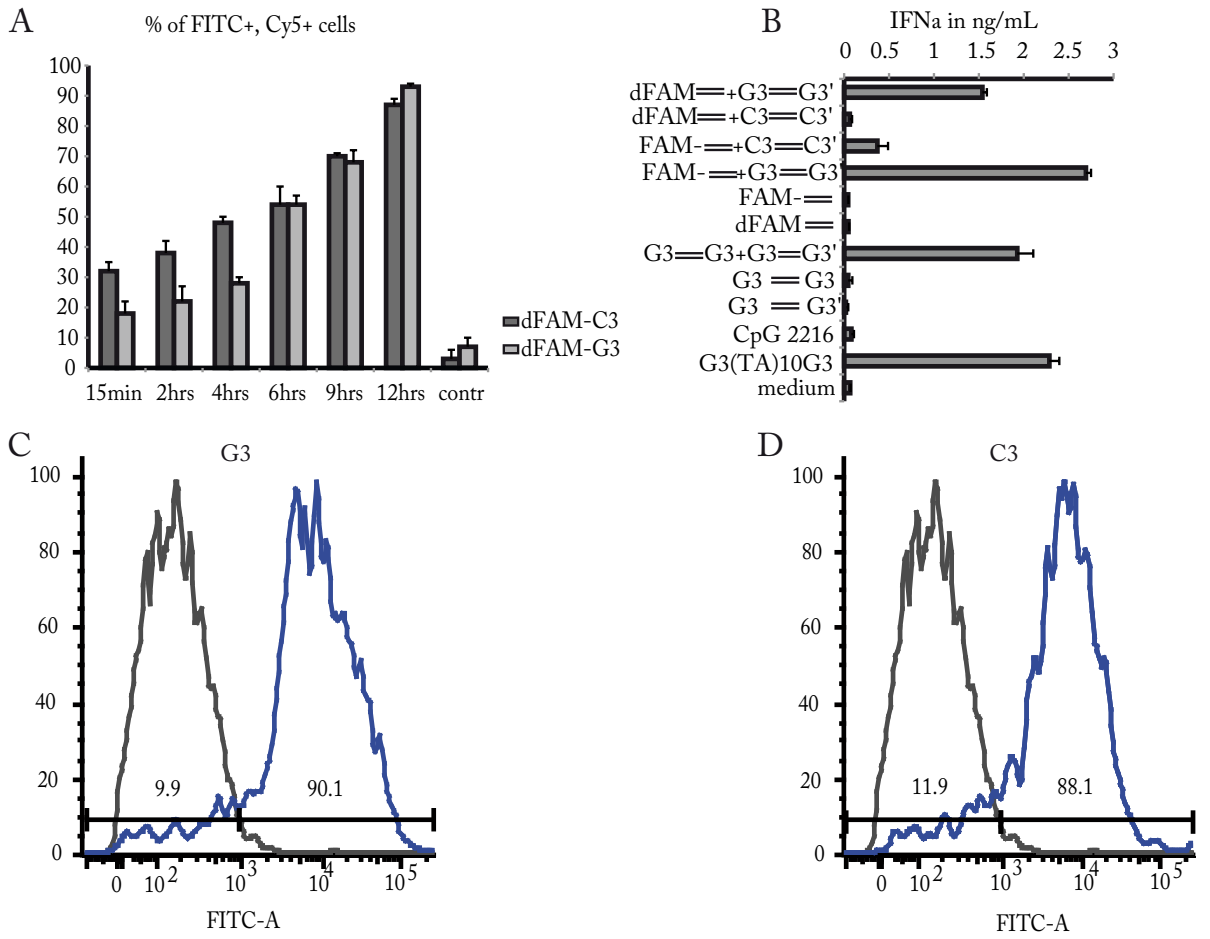

Fig 3.17: Fluorescence and IFNα induction of FAM-tagged ODNs. A) Percentage of FITC, Cy5 positive cell population over time. The percentage of positive cells steadily increases with time over the 12-hour timecourse. B) IFNα ELISA of CQ-blocked PBMCs. FAM-tagged ODNs possess no IFNα induction properties when transfected alone, only when tranfected as a double strand. FACS analysis of FAM fluorescence 12 hours after transfection with FAM-tagged ODNs hybridized with C) G_3 or D) C_3 strands.

There is no sequence specificity concerning transfection efficiency with nonpalindromic ODNs. (**Fig. 3.17C, D**) ODNs with barbell or blunt ends were transfected into THP-1 cells, with fluorescence measured via FACS analysis. All cells showed comparable transfection efficiencies 12 hours after transfection (**Fig. 3.17C, D**). There was also only a slight sequence specificity concerning fluorescence induction at early time points; all sequences were similarly fluorescent at later time points (**Fig. 3.17A**). Barbell sequences containing one FAM-tagged strand induce IFNα in CQ-blocked PBMCs. Single-stranded 314 was transfected into PBMCs, as well as the barbell combination of 314+111 and the blunt-ended dsODN of 314+313. Of the three sequences, only the barbell dsODN could induce type I IFN. All together, these date implicate a G3-dependent recognition of dsODN which does not depend on dsODN translocation into or stability in the cytosol of cells.

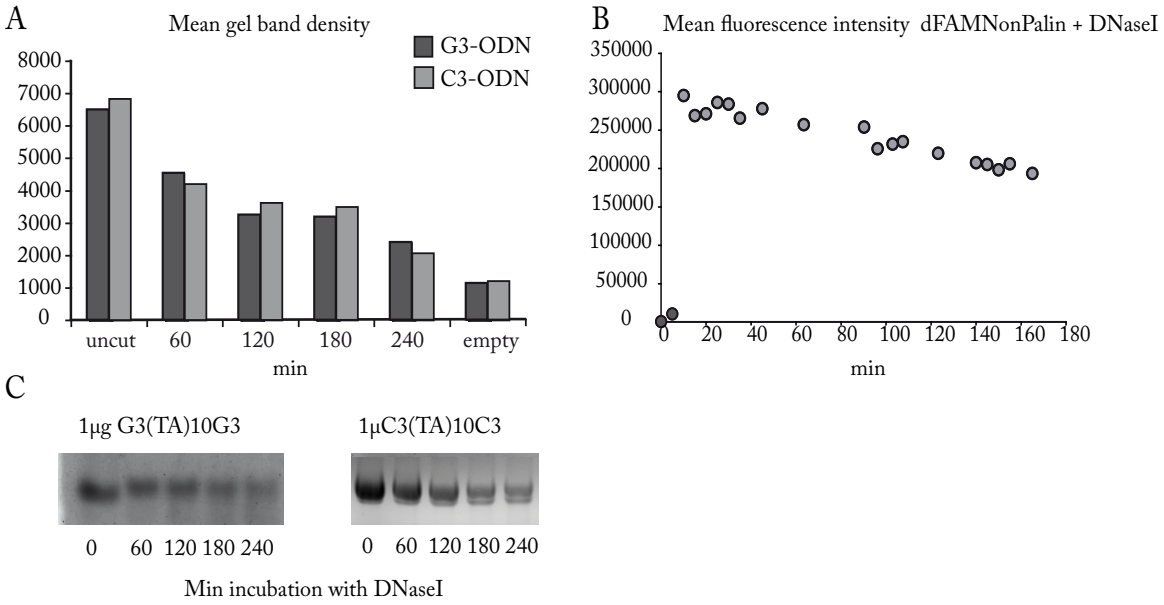

Fig. 3.18: Properties of FAM-tagged ODNs A) Mean density of gel bands of G- and C-ended ODNs incubated in PBMC lysate. PBMCs were lysed and incubated for the indicated timepoints with 10µg ODNs. Density of the gel bands in B) were then measured with gel analysis software. B) PAGE-gel of PBMC lysate incubated with G-ended and C-ended ODNs for the indicated timepoints. Gel band density decreases over time. C) FAM-tagged ODNs coupled with a quenching molecule fluoresce when incubated with DNase I. 1µg DNA was resuspended in 9µL DNAse I buffer and 2U DNaseI, then incubated at 37° for time spans from 30sec to 8 hours and fluorescence was measured in a Perkin-Elmer luminometer. Fluorescence sharply increased within the first five minutes after addition of the DNase, then slowly decreased over time. As a proof of principle, this shows that digestion of the DNA sequences does indeed enable unquenched fluorescence.

3.1.9 ODN induce IFN only if in cytosol

In order to visualize internalization of fluorescent ODNs into THP-1 cells and monocytes, fluorescent ODNs were complexed with either Lipofectamine or poly-L-arginine, then transfected into the abovementioned cells.

Cells were incubated with the ODNs for 2 hours, then fixed, permeabilized and stained for DAPI. ODNs transfected with poly-L-arginine showed punctate green fluorescence coinciding with endosomal delivery of the ODNs. Using Lipofectamine for transfection delivers the ODNs into the cytosol of the cells. As can be seen below (**Fig. 3.19**), Lipofectamine-complexed ODNs resulted in a fluorescent staining of the whole cytosol, while poly-L-arginine transfection of ODNs did not show this fluorescence.

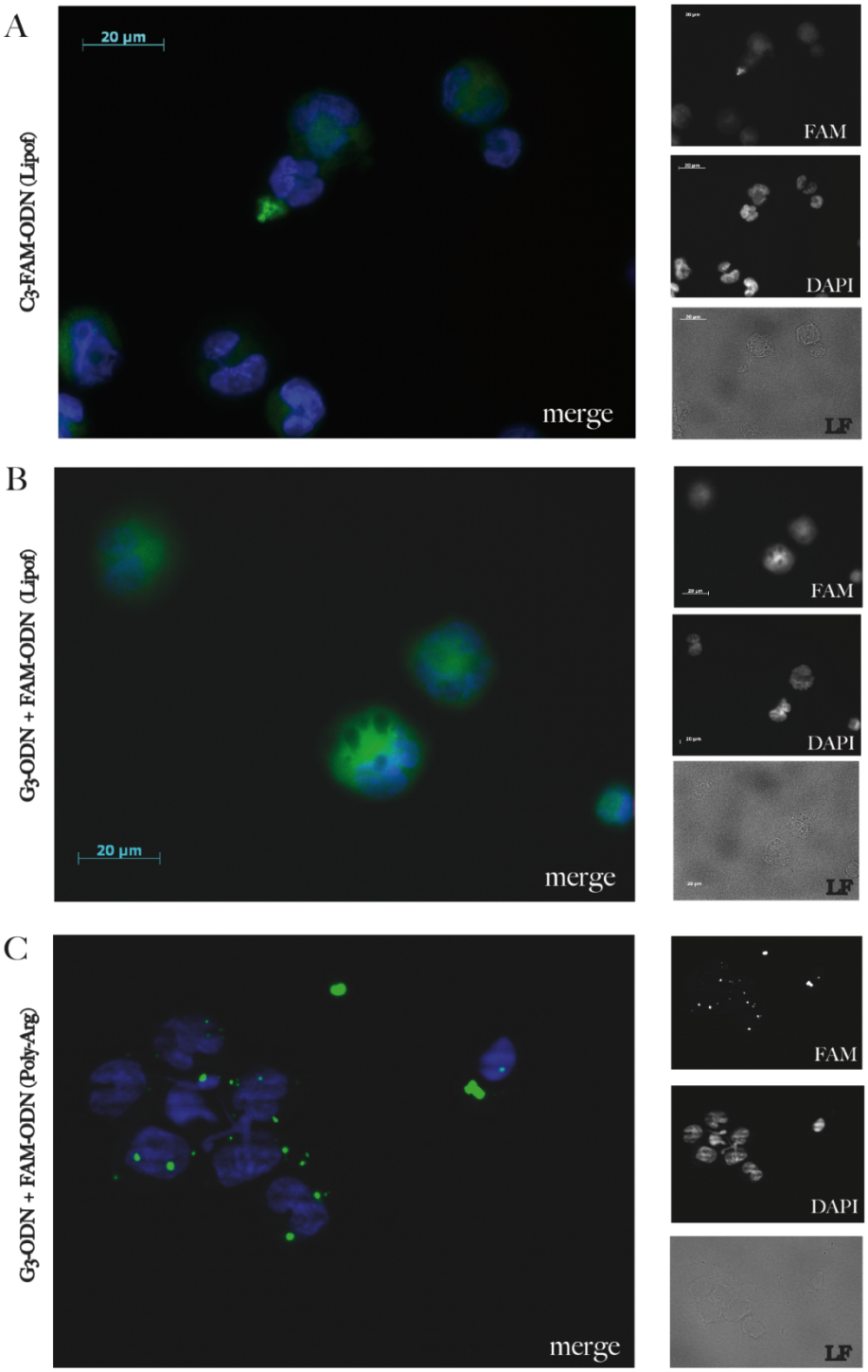

Fig. 3.19: Fluorescence microscopy images of FAM-tagged ODNs Monocytes were seeded at 200 000 cells per well of a 96-well plate, then transfected with Lipofectamine complexed to DNA ODN with either A) C_3 or B) G_3 ends, then washed and stained with DAPI after two hours' incubation. C) Monocytes were transfected with 0.2µg DNA complexed to 0.18µL poly-L-arginine. After two hours, cells were washed, incubated with DAPI, then resuspended in mounting medium and pipetted under a coverslip. Only punctate green specks are visible. An equally diffuse green staining is visible for both G_3 and C_3 sequence combinations.

3.2. MITA- or autophagy- dependent type I IFN response

MITA, or STING contains multiple transmembrane domains and colocalizes with the RIG-I adaptor protein IPS-1 (Ishikawa and Barber 2008; Zhong, Yang et al. 2008). Originally found to interact with IPS-1, it was also mentioned that the IFN response to cytosolic dsDNA was abrogated when MITA was inhibited. Further publications then cemented the necessity of MITA presence for cytosolic dsDNA-induced IFN (Ishikawa, Ma et al. 2009). It is not involved in the TLR pathway (Ishikawa and Barber 2008) and is critical for virus-induced activation of IRF 3 (Zhong, Yang et al. 2008). IFNα production in MITA-deficient MEFs is abrogated in response to ODN dsDNA, viral DNA and *L. monocytogenes* (Ishikawa, Ma et al. 2009).

The localization of MITA between the ER and the mitochondria would imply MITA to be a junction point linking RIG-I and dsDNA-mediated innate immune responses. This way it could detect viral RNAs in translation in addition to DNAs, inducing antiviral immunity via TBK1. A MITA/TBK1 complex is formed following transfection with DNA and then shuttled to endosomal compartments leading to a robust innate immune response (Ishikawa and Barber 2008; Zhong, Yang et al. 2008; Ishikawa, Ma et al. 2009).

Using adenoviral-induced knockdown of MITA, shRNA-mediated knockdown was accomplished in THP-1 cells and the cytokine responses to lipofection of ODNs observed (**Fig. 3.20B**).

3.2.1. The role of MITA in the type I IFN response

THP-1 cells were infected with a lentivirus encoding for MITA-shRNA, then stimulated with ODNs proven to induce a type I IFN response in CQ-blocked PBMCs. Type I IFN response is similar to the CQ-blocked PBMC response, with the added advantage of THPs being a cell line, not primary cells, and therefore not subject to the donor-induced variations normally found in PBMC-based experiments.

As can be seen in **Fig. 3.20A**, CQ-blocked PBMCs and THP-1 cells responded to DNA stimuli in a comparable manner. Both cell types induced type I IFN in response to $G_3(TA)_{10}G_3$, but not to ODNs with A, C or T ends. THP-1 cells were then transduced with lentivirus containing shRNA with a scrambled sequence, knocking down MITA, or left untreated. The type I IFN response to RNA did not greatly differ between conditions. The reaction of THP-1 cells treated with MITA-shRNA to cytosolic DNA stimuli such as $G_3(TA)_{10}G_3$, genomic DNA from *Listeria* and plasmid DNAand THP-1 cells left untreated did, however, differ.

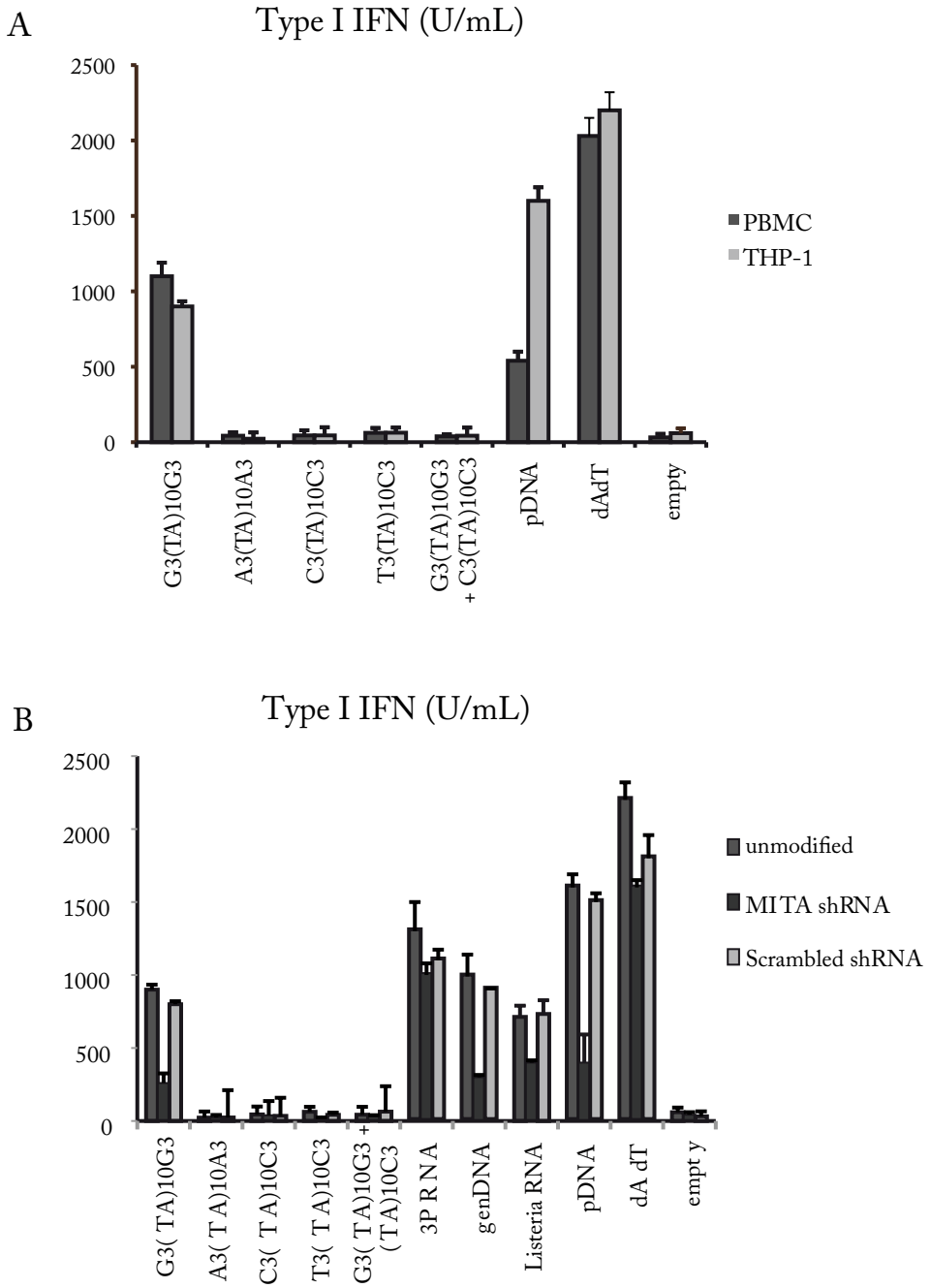

Fig. 3.20: Role of MITA in the Type I IFN response to DNA. A) Type I IFN response of PBMCs and THP-1 cells to various ODN combinations, pDNA and dAdT. PBMCs and THP-1 cells react in a comparable way to DNA stimuli. B) Transfection of RNA and DNA stimuli in THP-1 cells. THP-1 cells were either left unmodified or transduced with lentivirus carrying MITA or scrambled shRNA. Once MITA has been knocked down with lentiviral shRNA transduction, the type I IFN response to DNA stimuli was reduced in THP-1 cells. Transfection with dAdT resulted in similar type I IFN responses, which demonstrated the MITA-dependent recognition of cytosolic DNA stimuli. pDNA, plasmid DNA. genDNA, genomic DNA from *Listeria*.

THP-1 cells not transduced or transduced with scrambled shRNA lentivirus retained their ability to induce type I IFN production in response to $G_3(TA)_{10}G_3$, genDNA and pDNA, in contrast to THP-1 cells transduced with MITA shRNA lentivirus (see **Fig. 3.20B**).

3.2.2. The role of autophagy in the type I IFN response

The cellular mechanism of autophagy shuttles cytoplasmic components to the lysosome. The autophagosome, a double-membraned structure, becomes an amphisomes. The pH of the vesicle is lowered, enabling hydrolase-mediated degradation (reviewed in (Mizushima, Ohsumi et al. 2002). Autophagy has been implicated in the innate and adaptive immune responses: It degrades intracellular microbes in autolysosomes and can present cytosolic microbial products to PRRs.

Although type I IFNs are not thought to induce autophagy (Delgado, Elmaoued et al. 2008), the influence of autophagy on TLR and RLR signaling is not to be neglected. TLR7 interacts with autophagy to recognize the vesicular stomatitis virus; without Atg5 expression, IFN induction is abrogated (Lee, Lund et al. 2007). The Atg5-Atg12 complex inhibits RIG-I activation by blocking RIG-I from binding to IPS-1 (Jounai, Takeshita et al. 2007). This already enmeshed signaling between autophagy and the innate immune response does suggest an involvement of cytosolic DNA recognition. Recently, it has been found that Atg9 influences dsDNA-induced MITA translocation. Saitoh et al (Saitoh, Fujita et al. 2009) describe the translocation of MITA and TBK-1 after dsDNA sensing. MITA was shown to colocalize with autophagy proteins LC3-II and Atg9 after dsDNA stimulation. Once Atg9 was inhibited, the innate immune response was enhanced, suggesting Atg9 to function as a regulator of dsDNA sensing (Saitoh, Fujita et al. 2009). In this thesis, the role of autophagy-related genes, inhibitors and inducers in dsDNA stimulation and IFN response will be investigated for monocytes and monocyte-derived cell lines.

Preliminary results show a wortmannin-dependent IP-10 response to DNA stimuli in THP-1 cells (**Fig. 3.21**). THP-1 cells were either left untreated, incubated with wortmannin or rapamycin. THP-1 cells with a lentiviral knock-down of MITA, autophagy-associated protein Atg5, or the control scrambled shRNA sequence were also transfected with DNA and RNA stimuli. Wortmannin is used as an autophagy inhibitor (Blommaart, Krause et al. 1997), rapamycin is used to upregulate autophagy (Kamada, Funakoshi et al. 2000). Application of wortmannin, rapamycin and shRNA against Atg5 can give an approximation to autophagy induction or inhibition. In **Fig 3.21**, wortmannin diminished the IP-10 response to DNA stimuli G3(TA)10G3 and pDNA, but not to dAdT and the RNA stimulus 3P-dsRNA. As wortmannin functions as a PI3K inhibitor, the decrease of the IP-10 response could also be due to wortmannin interference in other cellular pathways. Application of rapamycin did not increase the IP-10 response. Interactions between MITA, autophagy, and the type I IFN

response to intracellular pathogens or cytosolic nucleic acids promise to be an interesting endeavour.

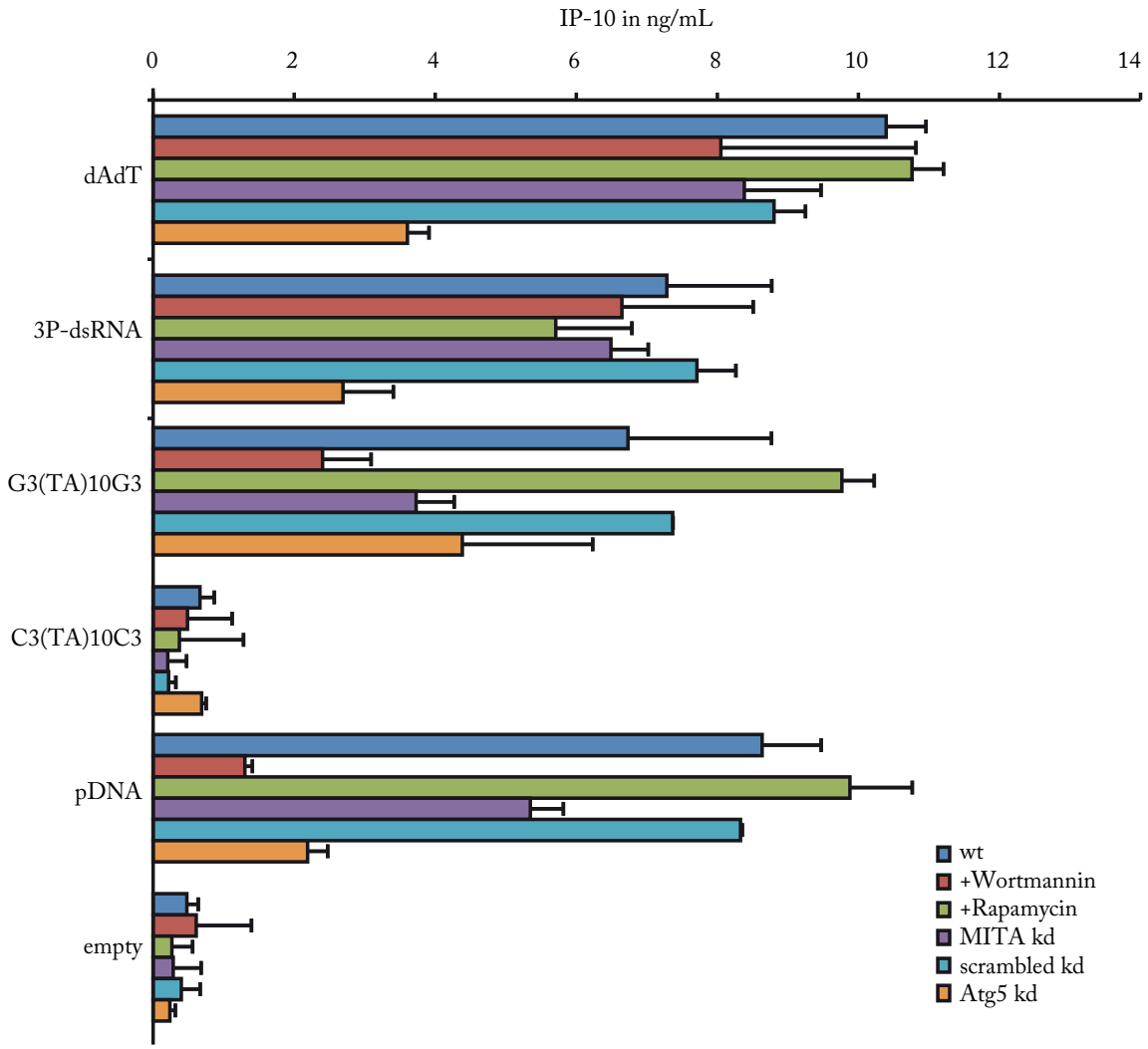

Fig. 3.21: IP-10 Elisa of THP-1 cells treated with autophagy-associated molecules. $8x10^5$ THP-1 cells were either left untreated (wt), incubated with 0.1 µM autophagy inhibitor wortmannin, 0.1µM autophagy inducer rapamycin, transduced with shRNA for MITA, Atg5 or a scrambled shRNA. Cells were then transfected with dAdT, 3P-dsRNA, $G_3(TA)_{10}G_3$, $C_3(TA)_{10}C_3$, plasmid DNA (pDNA) or left untransfected (empty).

3.3. The *Listeria*-induced IFN response

Listeria monocytogenes is a facultative intracellular bacterium that is the causative agent of Listeriosis. It is a foodborne pathogen and especially dangerous for immunocompromised individuals, such as the elderly, the young, or pregnant women (Ramaswamy, Cresence et al. 2007).

Primarily, *Listeria* infects the host via the intestinal epithelium where the bacteria invade non-phagocytic cells. Induction of uptake occurs by the binding of listerial internalins (Inl) to host cell adhesion factors such as E-cadherin. *L. monocytogenes* uses internalins only for invasion of non-phagocytic cells; invasion of macrophages, their preferred host cell, does not require

internalin use. Secretion of LLO creates holes in the vacuolar membrane and allows the bacterium to escape into the cytoplasm, where it can reproduce (Reviewed in (Kayal and Charbit 2006)).

Elucidating the host response to *Listeria* had been though to have been explained in 2006, when Decker *et al* described an IPS-1 independent response to *Listeria*. They used siRNA-mediated knock-down in macrophages to show that IFNβ synthesis in response to intracellular dsRNA decreased in absence of IPS-1. In their case, it was shown that *Listeria* infection targeted the IFNβ gene without detectable IPS-1 requirement (Soulat, Bauch et al. 2006). Later on in the same year, Medzhitov *et al* identified an IRF-3 dependent response to *Listeria* infection. They presented evidence that cytosolic DNA could induce a potent type I interferon response to *Listeria*. This activation of type I interferons was TLR independent and required IRF3 but occurred without detectable activation of NF-κB and MAP kinases (Stetson and Medzhitov 2006). However, evidence exists to suggest that *Listeria*, like *Legionella*, also take the RIG-I pathway. Maybe not uniquely, but RNA definitely plays a role in the innate immune response of A549 cells. In this section, the innate immune response to *Listeria* in phagocytic and non-phagocytic cells will be investigated.

3.3.1. *Listeria* induce various cytokine responses in monocytes and THP-1 cells

Bacterial RNA of various species induces a type I IFN response in chloroquine-blocked PBMCs

PBMCs were isolated and blocked with CQ in order to eliminate TLR9-dependent recognition. Bacterial RNA was isolated from different species by lysozyme treatment and according to manufacturer's instructions (Qiagen). RNA was treated with DNAse for 30 min at 37°C, then complexed with Lipofectamine and transfected into PBMCs. Bacterial DNA from the same species was also isolated and transfected into CQ-blocked PBMCs. Treatment with DNaseI did not impact IFNα induction by bacterial RNA (**Fig. 3.21A**). Bacterial RNA from various species was incubated with CIAP and then transfected into CQ-blocked PBMCs. 3P-dsRNA was used as a control. As soon as the bacterial RNA was treated with CIAP, a sharp decrease of the IFNα response could be observed. (**Fig 3.21B**) This shows that all bacterial RNA, regardless of strain or species, is capable of inducing a type I IFN response in a phosphorylation-dependent manner. *Listeria monocytogenes* infection has been linked to cytosolic nucleic acid sensor-dependent type I IFN induction. *Listeria* represents a well-characterized model organism for intracellular host-bacteria interaction; it is an opportunistic bacterium responsible for infections leading to meningitis and miscarriages. In this thesis, cell

lines used as target cells for *Listeria* infection were chosen because of their involvement in *Listeria* infections in vivo.

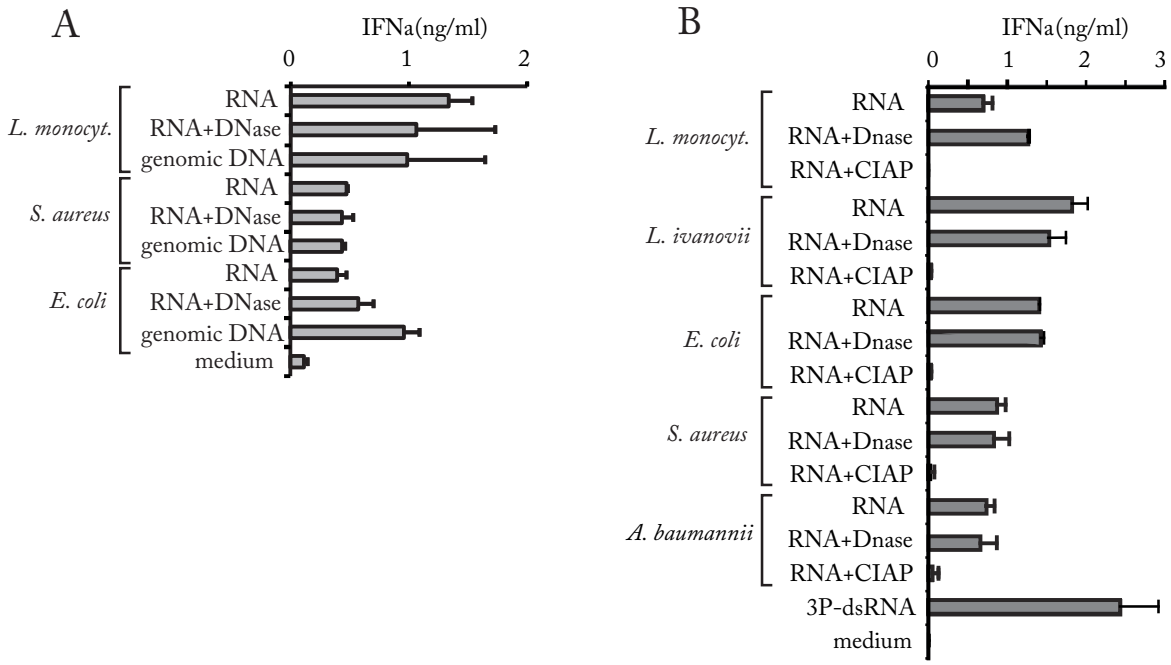

Fig. 3.22: Type I IFN response to bacterial RNA in PBMCs. A) RNA from the pathogens *S. aureus*, *E.coli* and *L. monocytogenes* was isolated and treated with DNase. Genomic DNA was also isolated and transfected into CQ-blocked PBMCs. DNase treatment did not lessen the IFNα response. B) RNA isolated from the indicated bacteria species was treated with DNase and CIAP, then transfected into CQ-blocked PBMCs. Only the treatment with CIAP abrogated the IFNα response, indicating that the phosphorylation state of the RNA was the key factor for the IFNa induction. RNA from Gram positive and negative bacterial strains showed the same IFN induction pattern.

Cytokine responses of THP1 and CD14⁺ monocytes occur in a localization-dependent manner

Listeria monocytogenes wt and Δhly strains were used at different MOIs in order to infect CD14⁺ monocytes and the THP-1 monocytic cell line, the supernatants removed after 20 hours and cytokine leves measured. MTT assays for viability could not be performed because the MTT reaction also gives a false positive in the presence of bacteria.

MOI titrations of MOI from 0.25 to 50 were carried out; MOIs higher than 20 tended to abrogate the cytokine response in monocytes and THP-1 cells, most likely due to cell death in response to microbe overload.

In **Fig 3.22**, CD14⁺ cells were isolated from PBMCs and then infected with *Listeria monocytogenes* wt and Δhly at the indicated MOI. The IFNα response corresponded to the MOI used for infection as long as bacteria were used that could express LLO in order to escape into the cytosol (*L. monocytogenes* wt). When the Δhly mutant was used, only a small amount of IFNα could be induced regardless of MOI applied, indicating that the cytokine response was due to the bacterial presence outside of the lysosome (**Fig. 3.22A**) and inside the cytosol. The

supernatants from CD14⁺ cells were then also used to measure IL-1β and IL-6, both proinflammatory cytokines (**Fig 3.22B, C**). The IL-6 response was very robust even at quite low MOIs, indicating that the pathogen induced IL-6 both when in the cytosol and constrained to the lysosome.

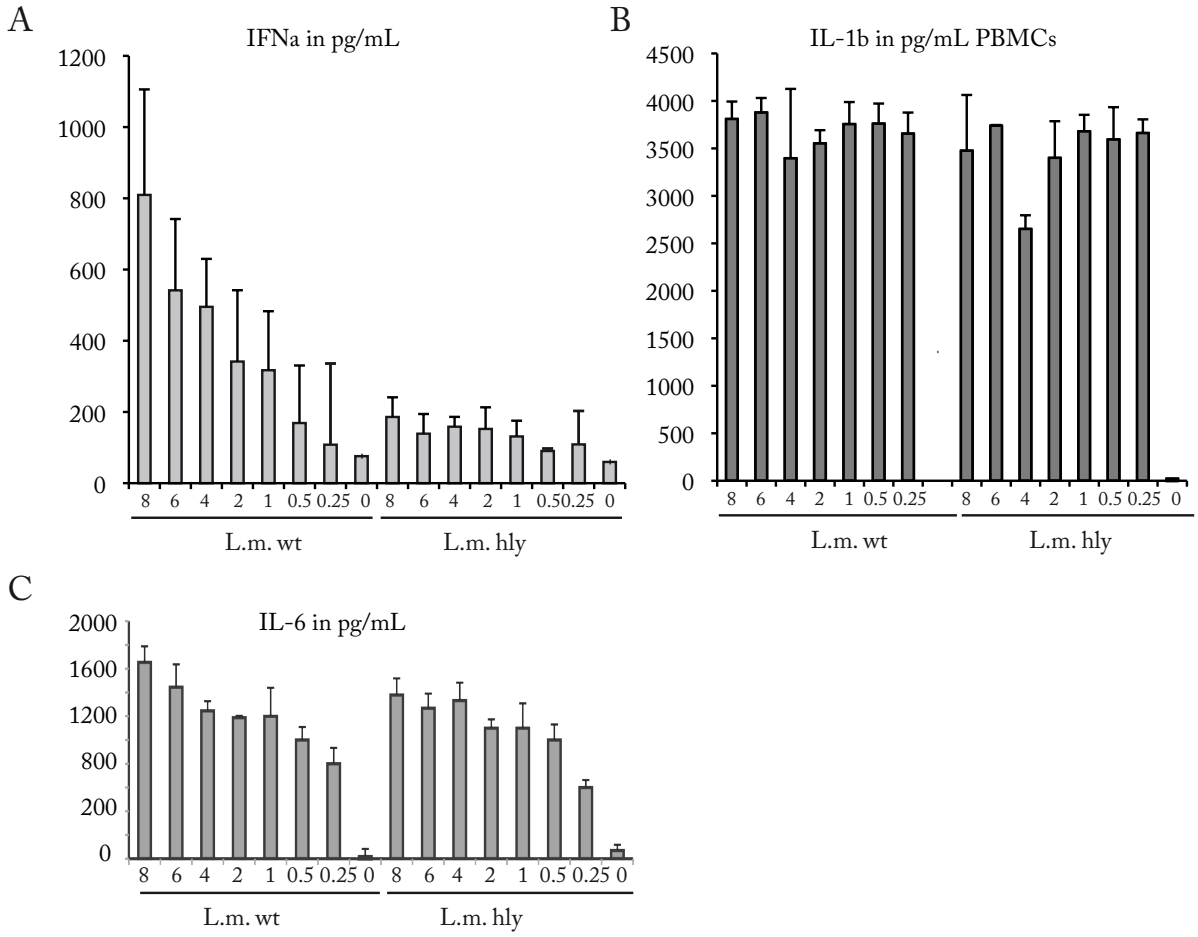

Fig. 3.23: Cytokine responses to *Listeria* infection. Monocytes were infected at the indicated MOIs (8, 6, 4, 2, 0.5, 0,25) with *Listeria* wt and Δhly. Supernatants were collected after 20h (for IFNα and IL-6 ELISAs) and 6h (IL-1β ELISAs). A) IFNα ELISA of monocytes infected with *Listeria monocytogenes*. The cytokine response was cellular localization-dependent, as the Δhly mutant induced a subdued IFNα response. B) IL-1β ELISA of monocytes infected with Listeria. No difference could be observed between wt and Δhly mutants. C) IL-6 ELISA of monocytes infected with *Listeria*. The IL-6 response is highly sensitive, as a robust response could be observed at MOI 0.25.

Induction of IL-1β, while not dependent of cellular localization of the bacteria, did correspond to the amount of bacteria used for infection, indicating that IL-6 can serve as a sign for pathogen infection. Monocytes were purified from healthy donor buffy coats by MACS beads for CD14, then infected with either wt *L. monocytogenes* or the Δhly mutant. The supernatants were removed after 6 hours (for IL-1β measurement) or 20 hours (for IL-6 and IFNα measurements). THP-1 cells were infected at rising MOIs, using RIG-I ligand 3P-dsRNA, RIG-I and DNAR dAdT and DNAR ODN 122 as positive controls. The IFNα response

occurred in a MOI- and mutant-dependent manner, with the response to Δhly-*Listeria* infection abrogated in comparison to the wt cytokine response. The IL-6 levels were the same for both *Listeria* types, indicating that the IL-6 response occurs independently from pathogen localization in the host cell.

THP-1 cells were also infected with wt and Δhly *Listeria* strains at the indicated MOI (**Fig. 3.23A-C**). The IP-10 response to wt *Listeria* corresponded to the MOI of the pathogens used up to MOI 5. The tapering off of the IP-10 response at higher MOIs indicates that IP-10 is not an adequate tool for measuring the immune response to *Listeria* infection (**Fig. 3.23A**). IL-1β induction after *Listeria* infection was not localization dependent in THP-1 cells, similar to the response observed in PBMCs (**Fig. 3.23B**). The IL-6 response to *Listeria* showed a slight correlation to MOI for both wt and Δhly infections (**Fig. 3.23C**);

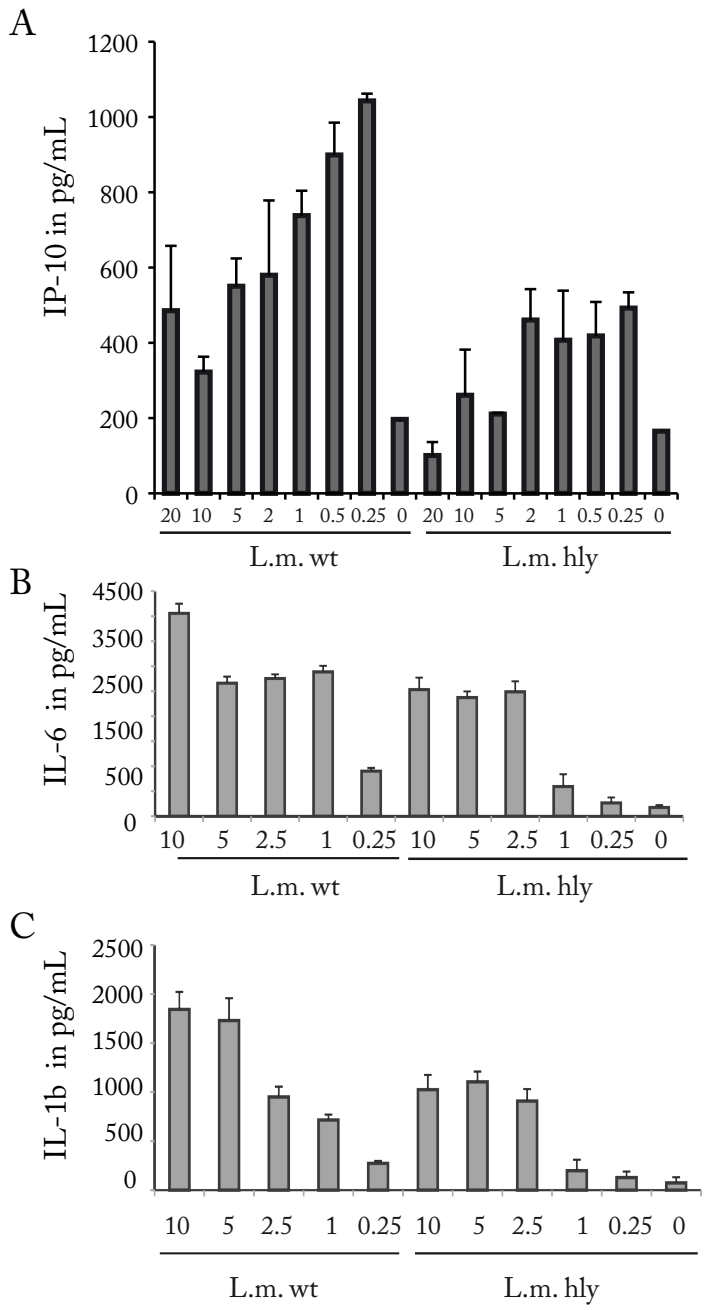

Fig. 3.24: THP-1 cytokine responses to *Listeria* infection. 10^5 THP-1 cells were infected with *Listeria* wt and Δhly and then IL-1β, IL6 and IP-10 responses measured. A) THP-1 cells were infected with *Listeria* at the MOI indicated and IP-10 production analyzed. The signal tapered off at higher MOIs. B) IL-6 ELISA of THP-1 cells infected with wt and Δhly *Listeria*. Cells infected with both *Listeria* strains produced IL-6. C) IL-1β ELISA of THP-1 cells infected at the indicated MOI with wt and Δhly *Listeria*. Both *Listeria* strains induced an IL-1β response, indicating a localization-independent response for both IL-6 and IL-1β.

3.3.2. Cytosolic *Listeria* induce IP-10 and type I IFN in A549 cells

A549 lung carcinoma cells are routinely used as host cells for *Legionella* infection. In infants and immunocompromised individuals, *Listeria* can populate and infect host alveolar macrophages via the lung (reviewed in (Campbell 1993), (Munder, Zelmer et al. 2005)). A549 cells were infected with *Listeria* in rising MOI concentrations, as well as the RIG-I ligands IVT2, IVT4,

and the DNAR- and RIG-I ligand dAdT. As controls, DNAR ligands ODN 122, pDNA, genDNA, as well as *Listeria* RNA were used.

As can be seen in **Fig 3.24A**, A549 cells do not react to the DNA stimulus genomic DNA. They do react to 3P-dsRNA and live *Listeria*. This would indicate that in A549 cells, the DNAR is not a component of the IFN pathway, as can be found in monocytes and monocytic cell lines.

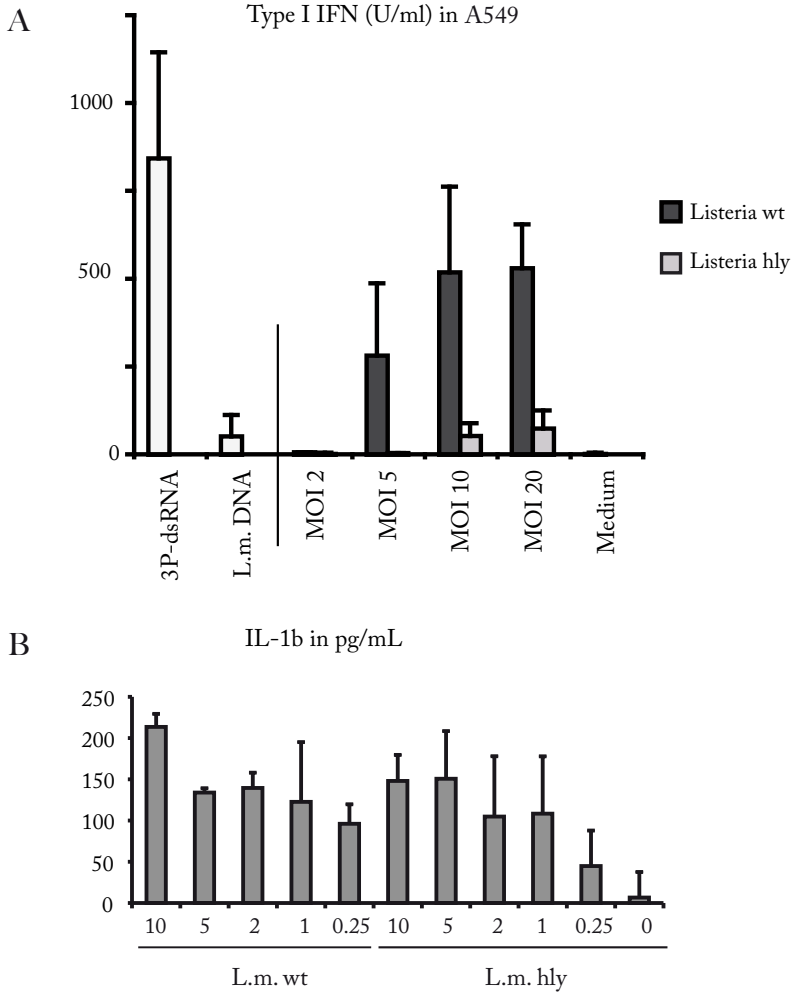

Fig. 3.25: Type I IFN and IL-1β responses to infection by *Listeria* wt and Δhly. A) There was a strong A549 type I IFN response to known RIG-I ligand 3P-dsRNA transfected into the cytosol by lipofection. The type I IFN response to wild type *Listeria* showed a definite difference between wt *Listeria* and the Δhly mutant. B) IL-1β ELISA of A549 cells shows no localization-dependent distinction of the IL-1β response.

A549 cells were infected with live *Listeria* from wt and Δhly strains. As was the case for the type I IFN response in THP-1 cells, Δhly *Listeria* did not induce a type I IFN response in A549 cells. As wt *Listeria* infection did result in production of type I IFN, this demonstrates a localization-dependent type I IFN response (**Fig. 3.24A**).

Supernatants from infected A549 cells were also used to measure IL-1β induction. In contrast to the type I IFN response, both *Listeria* strains were able to induce IL-1β, showing that IL-1β is a sign of infection, but not an indication of pathogen localization (**Fig. 3.24B**).

FACS of FITC-Listeria infection in THPs

In order to determine if *Listeria* elicited the cytokine responses due to their presence in the cytosol, FITC-tagged *Listeria* were added to THP-1 cells and A549 cells. The cells were washed after 1 and 4 hours of infection, then fixed and permeabilized with PFA. FACS analysis showed a fluorescence shift in all infected cells, irrespective of the *Listeria* type used. This assay confirmed equal uptake of Listeria into the host cells.

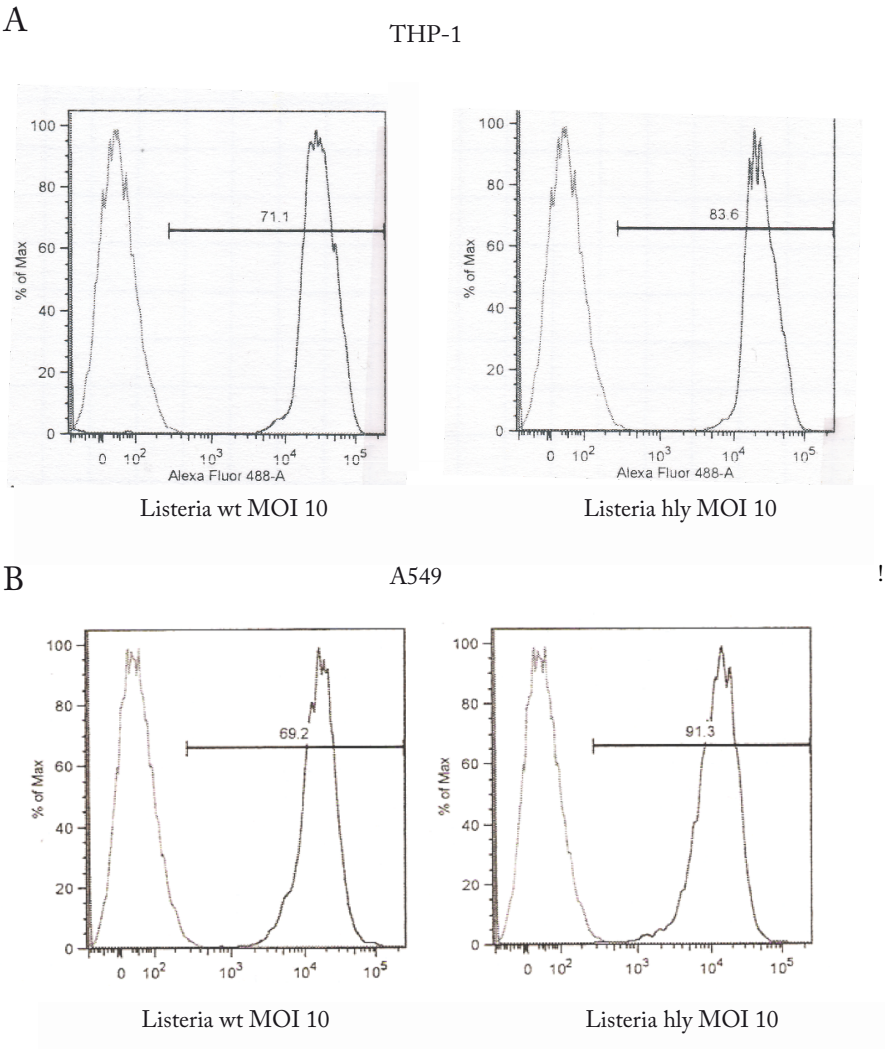

Fig. 3.26: FACS of A549 and THP1 infection with *Listeria* wt and Δhly. A) THP-1 cells were infected with *Listeria* wt and Δhly at the MOIs indicated. No difference in internalization can be seen between the uptake of wt and Δhly. B) A549 cells were infected with *Listeria* wt and Δhly at the MOIs indicated. *Listeria* were opsonized with human serum incubation for 30min at 37°C. Both *Listeria* types were equally internalized.

Listeria enter the cytosol of host cell, with listeria wt polymerizing actin

Listeria could still induce an innate immune response by clinging to the cell membrane and *Listeria* cell wall components binding to TLR receptors on the host cell membrane. THP-1 cells were infected with *Listeria*, then stained for phalloidin in order to visualize actin strands. (see **Fig. 3.26A**). Z-stacks were photographed in 1.6µm increments. FITC-stained *Listeria* were visible not only on the outside of the cell, but also inside the cell, showing polymerization with actin strands and presence in the same plane as the THP-1 nuclei.

As can be seen in the figures below (**Fig 3.27B**), actin colocalization with FITC-stained *Listeria* occurred only with wt *Listeria*, showing that *Listeria* did indeed enter the host cells cytosol and proceed with the infection cycle. *Listeria* with the Δhly mutation showed no colocalization with the phalloidin staining. Type I IFN responses after *Listeria* infection can therefore be considered to occur due to receptor interaction in the cytosol.

A

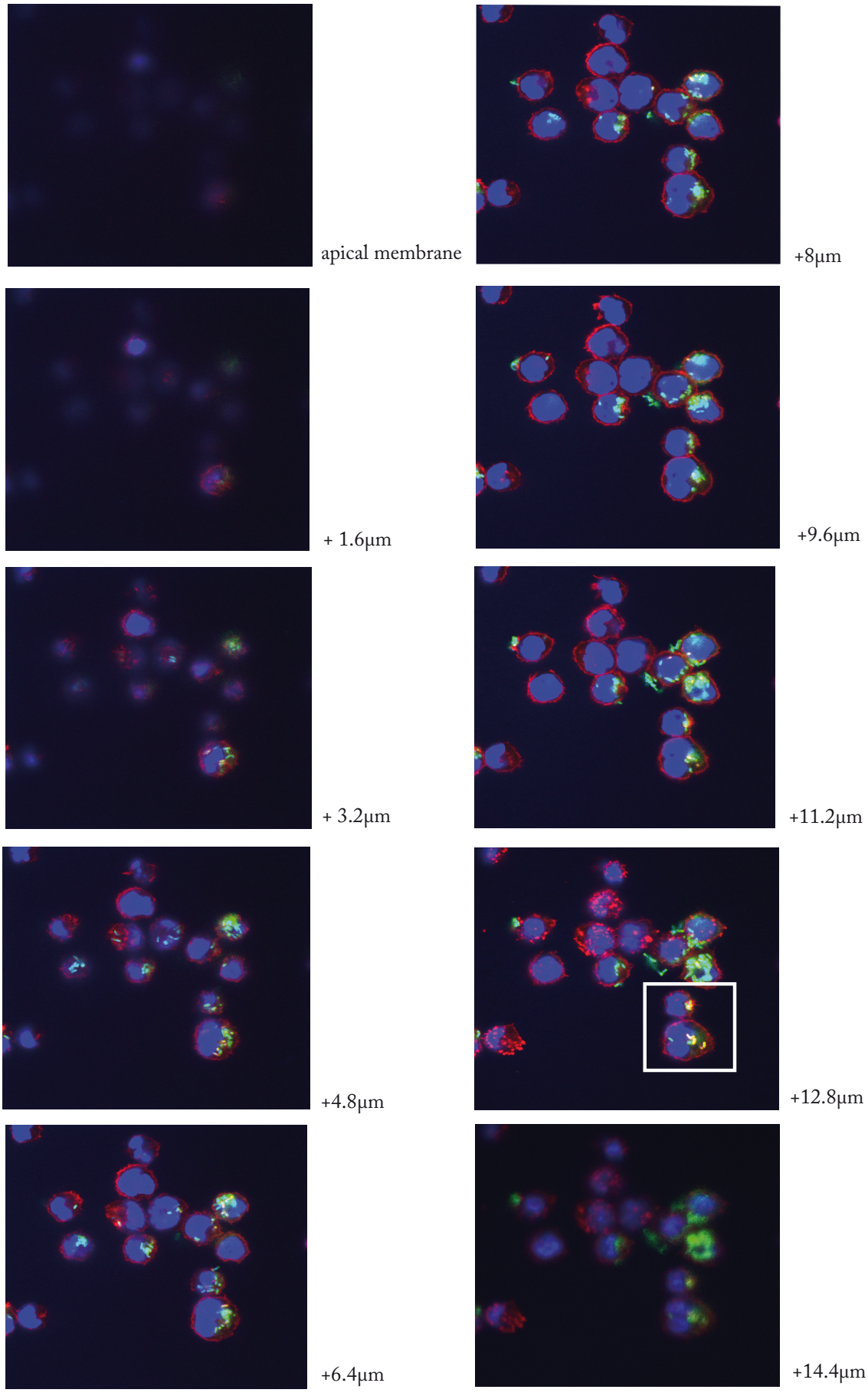
apical membrane
+8µm
+ 1.6µm
+9.6µm
+ 3.2µm
+11.2µm
+4.8µm
+12.8µm
+6.4µm
+14.4µm

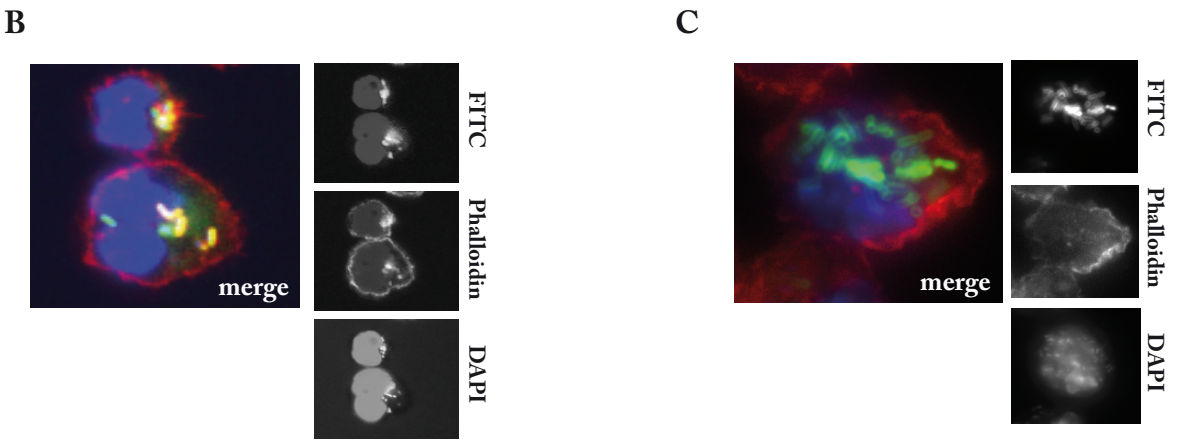

Fig 3.27: Z-stack images of *Listeria*-infected THP-1 cells. THP-1 cells were treated with PMA for four hours, adhered to coverslips and then infected with either wt or Δhly *Listeria* for 2 hours. Cells were then washed and fixed with 4% PFA, actin stained with phalloidin and observed under fluorescence microscopy. A) Images were taken, starting at the apical side of the cells, every 1.6µm, travelling towards the basal side until cell membranes were no longer in focus. *Listeria* show colocalization with phalloidin staining at multiple points. B) Zoom image of wt-Listeria infected THP1 cells at 12.8µm and C) Zoom image of hly-Listeria infected THP-1 cells.

3.3.3. *Listeria* – dependent induction of type I IFN is RIG-I dependent

A RIG-I knock-down using lentiviral delivery of RIG-I shRNA into A549 was used to observe the dependency of RIG-I presence for type I IFN response to *Listeria* infection. Using lentiviral knockdown ensured the genesis of a cell line that demonstrated knock down of RIG-I for upwards of 10 cell passages. Unmodified and knockdown cells were infected with wild-type and Δhly *Listeria*, 3P-dsRNA, dAdT, RNA gained from *Listeria* and RNA isolated from *E.coli* (**Fig. 3.28A**). The IP-10 ELISA showed no cytokine induction in response to *Listeria* or *E.coli* RNA. The response to live wt and Δhly *Listeria* was also reduced in RIG-I k.d. cells. The IP-10 response to both wt and Δhly *Listeria* in unmodified A549 cells is due to IP-10 not being a the sole indicator for type I IFN induction, which is why type I IFN assays were performed as well (**Fig. 3.28B**). THP-1 cells were also knocked down using the lentivirally-mediated shRNA system. Both A549 and THP-1 cells were transfected with 3P-dsRNA, *Listeria* RNA, *Listeria* DNA, and different MOIs of *Listeria* wt as well as Δhly. As can be seen in **Fig. 3.28B**, RIG-I knock-down in THP-1 cells reduced the type I IFN response to 3P-dsRNA and *Listeria* RNA, but only slightly lessened the type I IFN response to live *Listeria* infection. This differed from the changes in the type I IFN response between unmodified and RIG-I knocked down A549 cells, in which the induction of type I IFN after *Listeria* infection was sharply reduced. As THP-1 cells possess both cytosolic RNA and DNA receptors leading to induction of type I IFN, it is possible that *Listeria* are recognized by both pathways. This is not the case in A549

cells, as they do not respond to cytosolic DNAR stimuli and would therefore rely solely on cytosolic RNA as a type I IFN inducer.

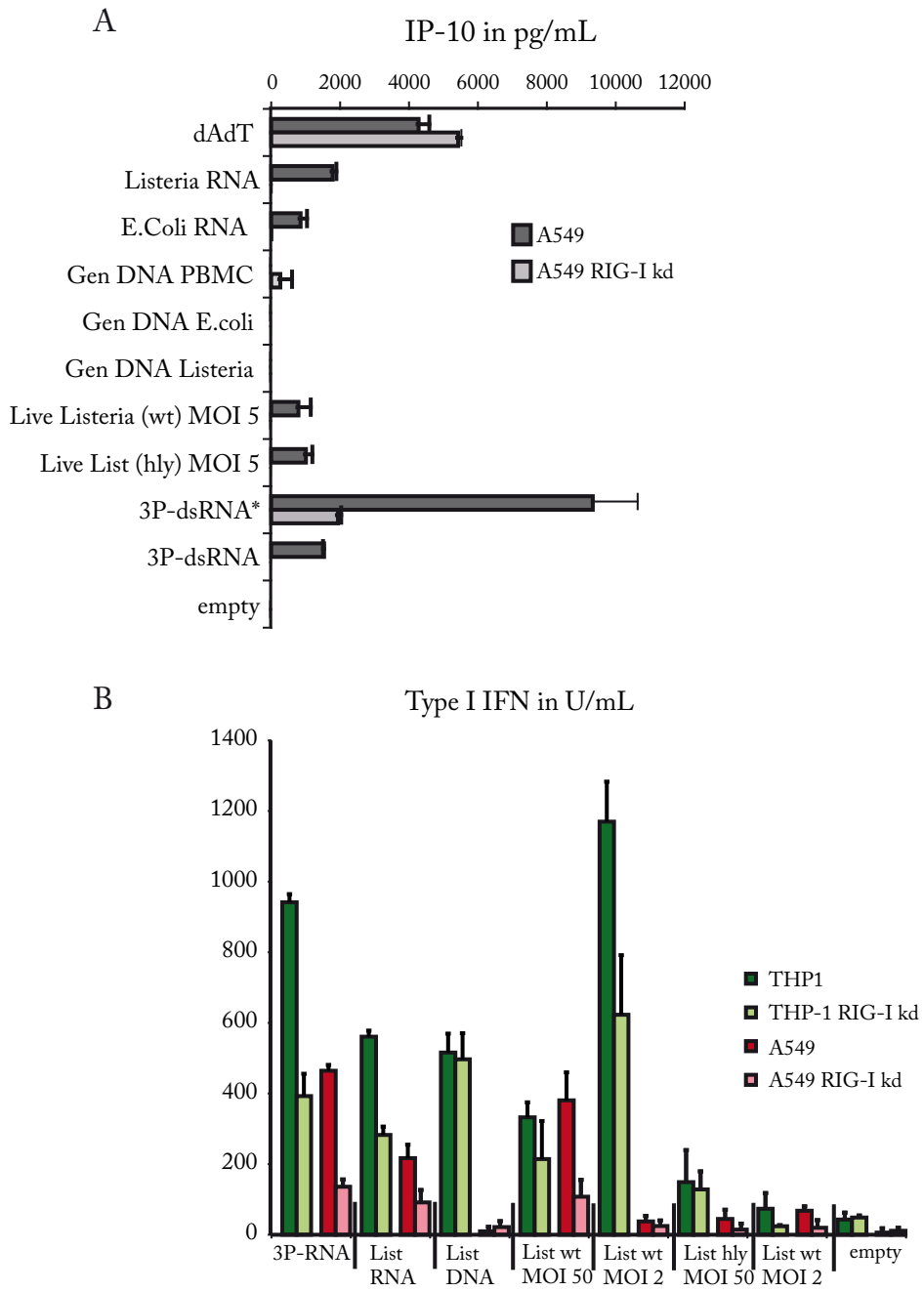

Fig. 3.28: Lentiviral knockdown of RIG-I in A549 and THP-1 cells. Cells were transfected with the indicated stimuli or live *Listeria* at various MOI. Antibiotics were added 4 hours post infection and supernatants removed after 20 hours incubation. A) IP-10 ELISA of A549 cells. Cells were transfected with bacterial RNA, genomic DNA, 3P-dsRNA and dAdT. Knock-down of RIG-I resulted in a decreased signal in response to RNA and bacterial stimuli. B) Lentiviral knockdown comparison of A549 cells with THP-1 cells, also with RIG-I lentiviral knockdown. Cells were transfected with 3P-dsRNA, *Listeria* RNA, *Listeria* DNA, live *Listeria* of wt and Δhly strains. The RIG-I-dependent type I IFN response to live *Listeria* was more pronounced in A549 cells than THP-1 cells.

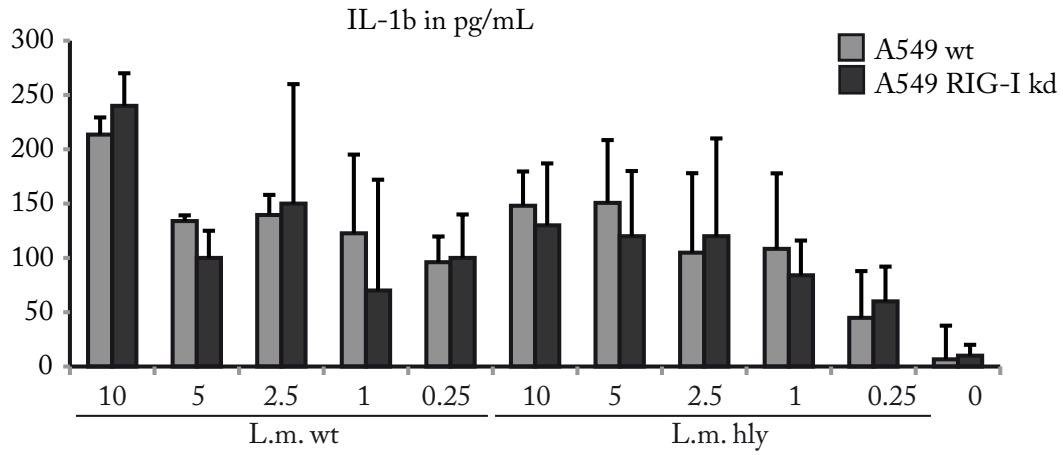

Fig. 3.29: IL-1β Elisa of A549 lentiviral kd of RIG-I. IL-1β ELISA showed no k.d. effect between the A549 wt and A549 RIG-I k.d., suggesting that the IL-1β induction pathway is not influenced by signals from the RIG-I pathway in response to *Listeria* infection.

The supernatants from infected A549 cells were also used for analysis of IL-1β response, but no difference could be observed, either between *Listeria* wt and Δhly or between A549 wt and A549 RIG-I k.d. (**Fig. 3.29**). This would indicate that Δhly are capable of inducing an immune response, just not type I IFN, and that A549 RIG-I k.d. is capable of producing an immune response, just not via RIG-I.

Because lentiviral knockdown of RIG-I was not performed for proteins in the RLR pathway, notably IPS-1 and IRF3, siRNA-mediated knockdown of A549 cells was attempted in order to have a comparable protocol between proteins. As can be seen, the knock-down extent is similar in lentivirally abrogated RIG-I and siRNA-mediated inhibition of RIG-I (**Fig 3.28A, B** and Fig. **3.30**). Cells were transfected with dAdT, *Listeria* RNA, 3P-dsRNA, and infected with both wt and Δhly *Listeria*. Positive controls that would elicit the same type I IFN response in both wt and kd cells would be difficult to come up with, as A549 cells do not react to DNA with type I IFN production, and the cytosolic response to RNA seems to go only via RIG-I. The Hiperfect-mediated siRNA knock-down of RIG-I necessitated a protocol in order to determine the best amounts of siRNA and Hiperfect reagent. Knock-down in A549 cells was greatest 48 hours after transfection and using 0.1μg RNA with 1.5μL Hiperfect (**Fig 3.30A**). A549 cells were treated with siRNA against RIG-I, IPS-1, Luciferase and a double knock-down of both RIG-I and IPS-1. After 48h, the cells were infected with *Listeria* wt and Δhly at different MOIs or transfected with 3P-RNA, *Listeria* RNA, and *Listeria* DNA. Both RIG-I and IPS-1 decreased the type I IFN response to 3P-dsRNA, wt *Listeria* and *Listeria* RNA. A cumulative effect was not always discernible in the cells subjected to a double knock-down.

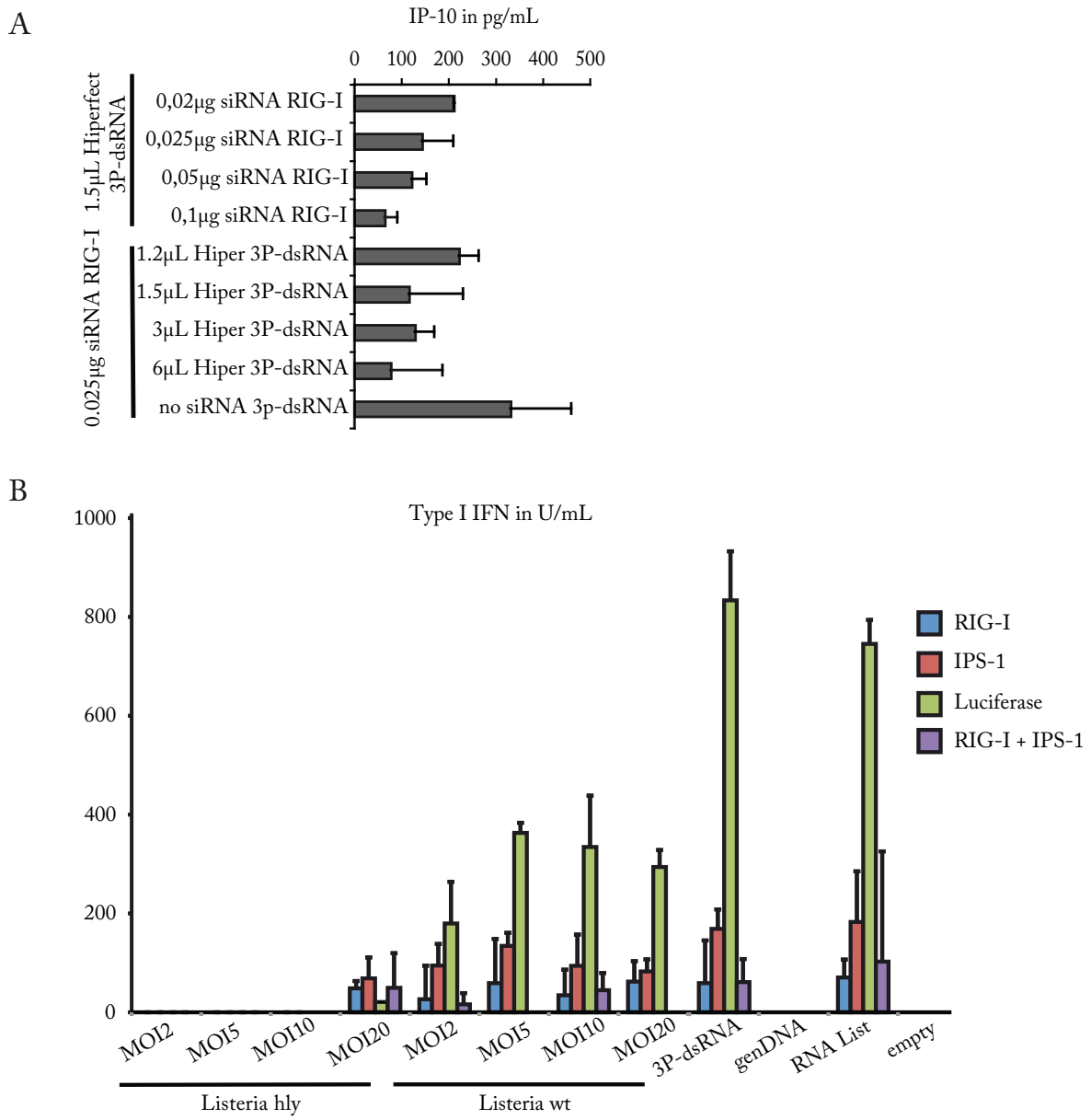

Fig. 3.30: A549 cells with siRNA mediated knockdown of RIG-I and cytokine responses of type I IFN. A) Titration of Hiperfect and siRNA in A549 cells. The best results were obtained after 48h incubation with siRNA+Hiperfect, using 0.1µg siRNA and 1.5µL Hiperfect. B) siRNA-mediated knock-down of A549 cells using siRNA against RIG-I, IPS-1, Luciferase and a double knock-down of RIG-I and IPS-1. Reduction in the type I IFN response to wt *Listeria* and cytosolic RNA stimuli could be seen in the knock downs of RIG-I, IPS-I, RIG-I+IPS-1, but not Luciferase.

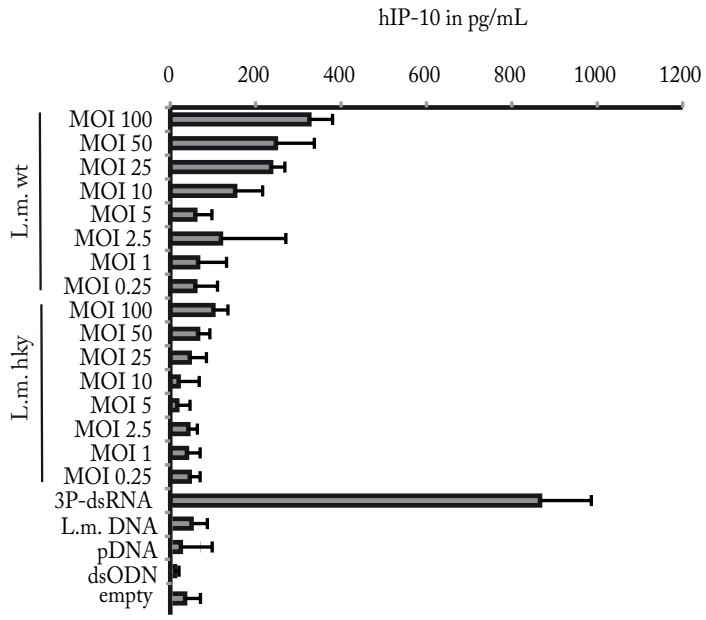

Fig. 3.31: HepG2 cytokine responses to *Listeria* infection. A) HepG2 cells were incubated with antibiotic-free medium for 24 hours prior to infection, then infected with different MOIs of *Listeria* wt and Δhly. A robust type I IFN response was only visible for MOI>25. Δhly did not induce a strong type I IFN response.

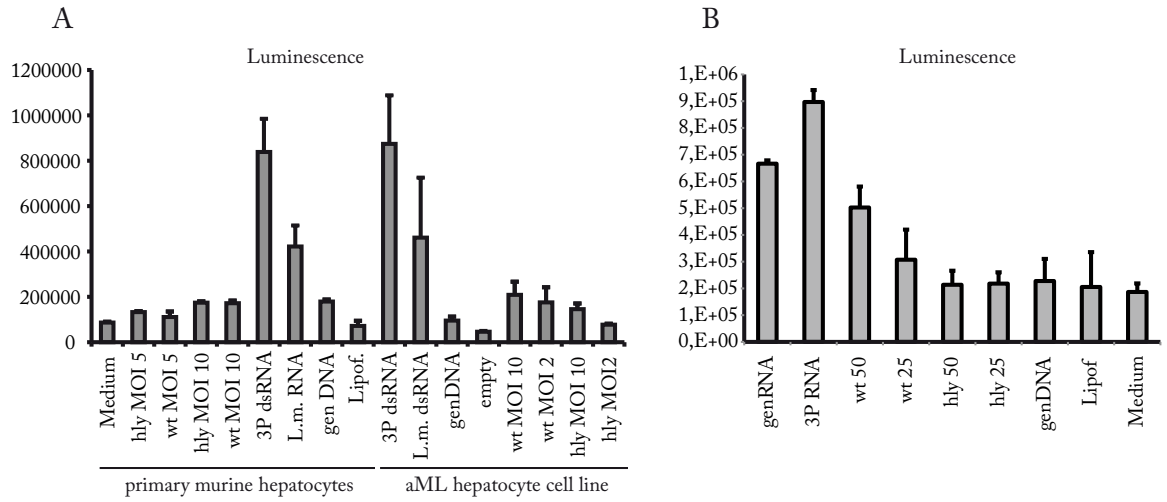

Fig. 3.32: Relative luminescence units in primary mouse hepatocytes and the αML mouse hepatocyte cell line. Primary mouse hepatocytes were isolated and infected with *Listeria*, as well as transfected with different RNA stimuli. The murine hepatocyte cell line αML was treated in a similar manner. Supernatants from both experiments were given to L929 cells expressing IFNβ-Luciferase and total luminescence then measured.

With this comparison, HepG2 cells were transfected and infected with known RNA and DNA stimuli, as well as different MOIs of *Listeria*, both wt and Δhly (**Fig. 3.31A**). HepG2 cells did not respond as readily to *Listeria* as THP-1 cells, which is to be expected; HepG2 cells showed a type I IFN response only at MOI > 25. They did not react to lower concentrations of 3P-dsRNA, nor did they respond to DNA stimuli like plasmid DNA, genomic DNA, or ODNs shown to induce type I IFN in THP-1 cells and PBMC (**Fig. 3.31B**). Due to the

inavailability of primary human hepatocytes, C57BL/6 mice were sacrificed and hepatocytes isolated, then kept in culture for 3 days to allow for differentiation. αML cells, a murine hepatocyte cell line, were used as well. Both types of cells were transfected with different types of RNA/DNA stimuli; *Listeria* RNA, 3P-dsRNA, genDNA and only Lipofectamine as a control. Both hepatocyte cell types reacted to 3P-dsRNA and bacterial RNA, but not genDNA. Luminescence could be observed only at high MOIs>25, a characteristic also true of the human HepG2 cells.

3.3.4. *Listeria* RNA present in the cytosol after infection

After having demonstrated that *Listeria* not only enter the cell, but also induce type I IFN in a localization-dependent manner, a system for visualizing the *Listeria* RNA in the host cell cytosol was implemented.

In order to visualize transfer of bacRNA into the cytosol of cells a recently developed sensitive, non-radioactive but non-toxic method was used to label RNA in living cells (Jao and Salic 2008) (**Fig. 3.33**): 5-ethynyluridine (EU) was shown to be incorporated into RNA transcripts generated by RNA polymerases I, II and III in mammalian cells but not into DNA (Jao and Salic 2008). *Listeria* were grown in medium containing EU and labeled with FITC. The host cells were then infected with labeled bacteria. One or four hours post infection, host cells containing *Listeria* in the cytosol were fixed, permeabilized and incubated with fluorescence dye coupled to a reactive azide group (Alexa594-azide). In this setting, the azide selectively couples to the ethynyl group of EU incorporated into the bacRNA. Whole *Listeria* are labeled green with FITC and RNA is visible as red fluorescence (Alexa594), nuclei are stained by DAPI (blue). As evident from fluorescence images, the cytosol of THP-1 cells was clearly labeled for EU-containing RNA when infected with wild type (wt) *Listeria monocytogenes* (**Fig. 3.33A** left and middle panel) but not when infected with a mutant lacking LLO (Δhly) (**Fig. 3.33A** right panel) which is not able to escape from the endosome. Bacterial RNA accumulated in the cytosol host cells upon prolonged infection time with wt *L. monocytogenes* (**Fig. 3.33A**, left and middle panel). In concordance with findings from THP-1 cells, similar results were obtained with epthelial (A549, **Fig. 3.33B**) and hepatocarcinoma cell lines (HepG2, **Fig. 3.33C**).

Labeled RNA was absent within *Listeria* because Alexa594-azide either cannot penetrate the cell wall or is inactivated within *Listeria*, as direct labeling of *Listeria* from bacterial culture is not possible (data not shown). By contrast, direct labeling of RNA from gram negative *E. coli* and from *L. monocytogenes* protoplasts, which lack the cell wall, was possible (**Fig. 3.34A, B**). Therefore, during *Listeria* infection only cytosolic bacRNA could be detected. The absence of

labeled RNA in the host cell nucleoli, the site of ribosomal RNA production, excluded transfer of EU nucleotides from *Listeria* with subsequent incorporation into the host. In fact, direct labeling of cells in conditioned culture medium led to strong staining of the nucleoli (**Fig. 3.35**, left panel). Of note, EU labelings were performed in starvation medium that allows the incorporation of EU. Indeed, EU is not quantitatively incorporated in standard culture medium (**Fig. 3.34**, right panel). Since we used standard medium during infection, we additionally excluded the possibility that host cell RNA is stained by non-incorporated EU diffusing from *Listeria*. Altogether, we conclude from the data that during infection significant amounts of bacRNA are transferred into the cytosol of cells where it is accessible for cytosolic immune receptors.

As Listeria appeared to be intact, we wondered, if occurrence of bacterial RNA in the cytosol of cells might be a result of an active release process. As a preliminary experiment it was examined if such a release could be provoked by stress conditions. *Listeria* were incubated in either full media, Fraser Half Medium (FHM), or starvation media (HTM). Supernatants were collected and nucleic acids isolated via phenol-chloroform precipitation. These were then incubated with either DNase, RNase, or left untreated and loaded on agarose gels. As can be seen in **Fig. 3.36**, a band appeared when bacteria were grown in starvation media. This band is RNase-sensitive, although the entire band is not gone after RNase incubation. This could be due to protein contamination of the supernatant, i.e. bacterial proteins binding to the RNA and encumbering RNase activity or presence of bacterial DNA. By contrast, incubation with DNase did not degrade any nucleic acid visible in the gel. This finding suggests an active release of bacteria RNA from *Listeria*. However, it is unclear, if RNA is released because of cell death leading to limited perforation of the bacteria membrane and “secretion” of small but large molecules. To estimate this scenario the identity of RNAs and the viability of *Listeria* need to be examined.

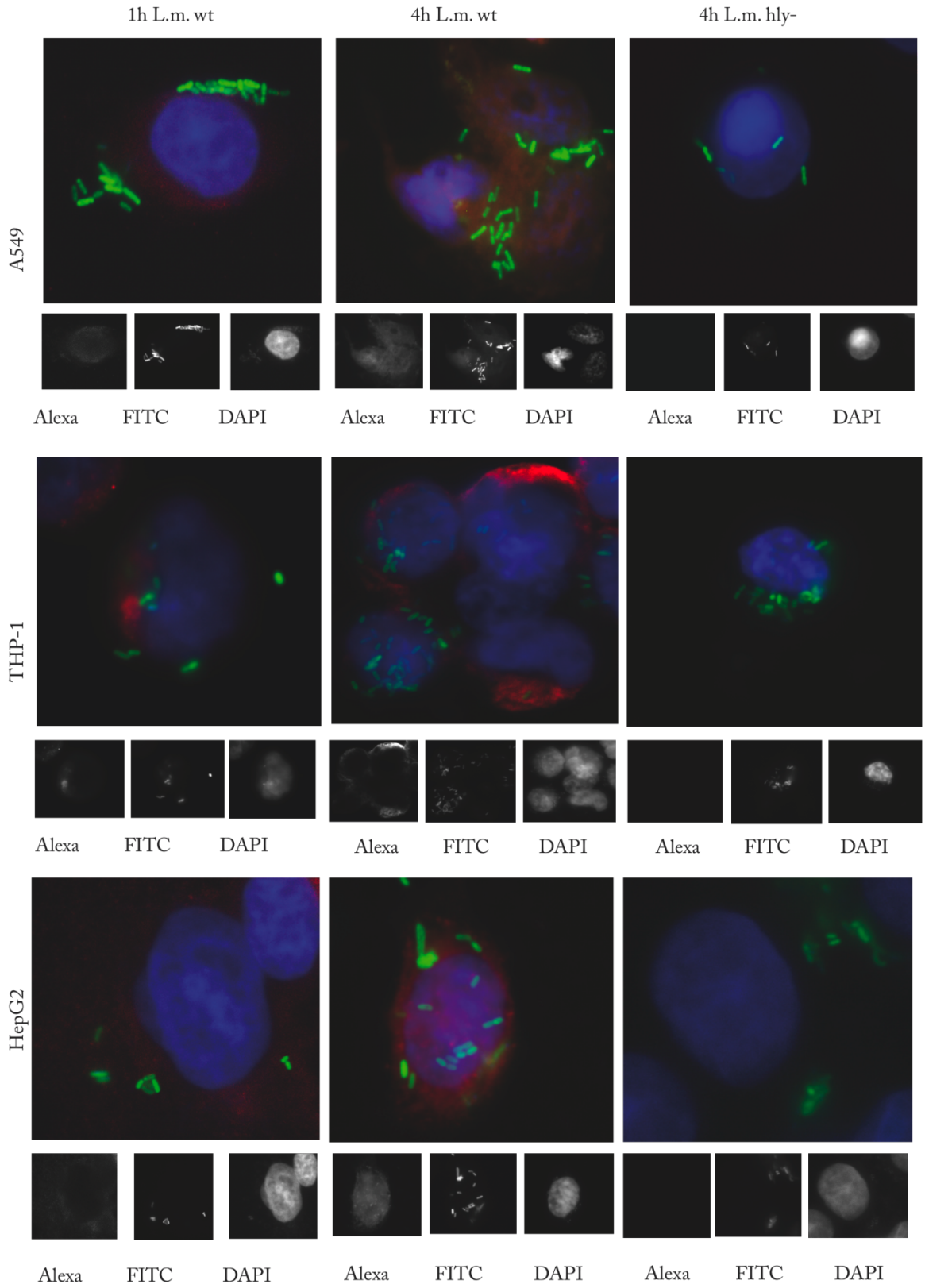

Fig. 3.33: EU staining of *Listeria* RNA after infection in A549 cells. Cells were infected with FITC-labeled and EU-incorporated *Listeria* for either 1 or 4 hours, then fixed and stained with DAPI and Alexa 594. The red staining of *Listeria* RNA can be seen to increase over time. THP-1 cells were infected with wt FITC-tagged *Listeria* for 1 and 4 hours, then fixed and stained with DAPI and Alexa 594. Due to their phagocytic nature, THP-1 cells manage to incorporate more *Listeria* than non-phagocytic cells such as A549 and HepG2 cell

infection of *Listeria*. HepG2 cells were infected with wt *Listeria* for 1 and 4 hours. A very slight red staining could be seen after 1 hour of *Listeria* infection. *Listeria* had been internalized after opsonization with human serum for 30 min at 37°C. Δhly *Listeria* infection of HepG2, A549 and THP1 cells, showing no red fluorescence of EU staining with alexa 594.

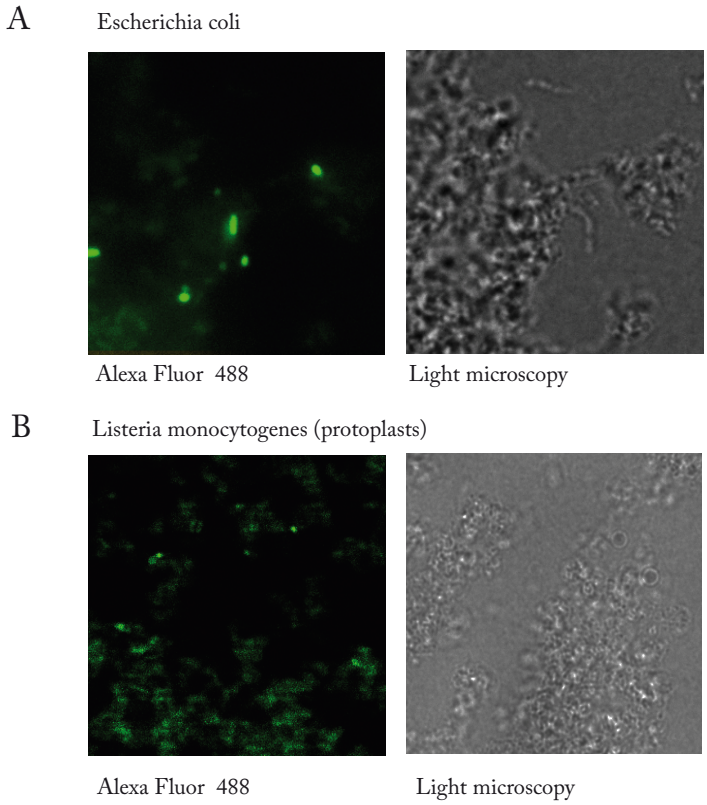

Fig. 3.34: EU stain in *E.coli* and *L.monocytogenes* protoplasts. A) *E.coli* and B) *L.monocytogenes* protoplasts were incubated with EU for 2 to 4 hours during log phase growth, pelleted, fixed and stained with Alexa fluor 488. *E.coli* readily showed EU staining during log phase, while *L.monocytogenes* had to be incubated in starvation medium or cultured as protoplasts for successful EU-Alexa azide staining.

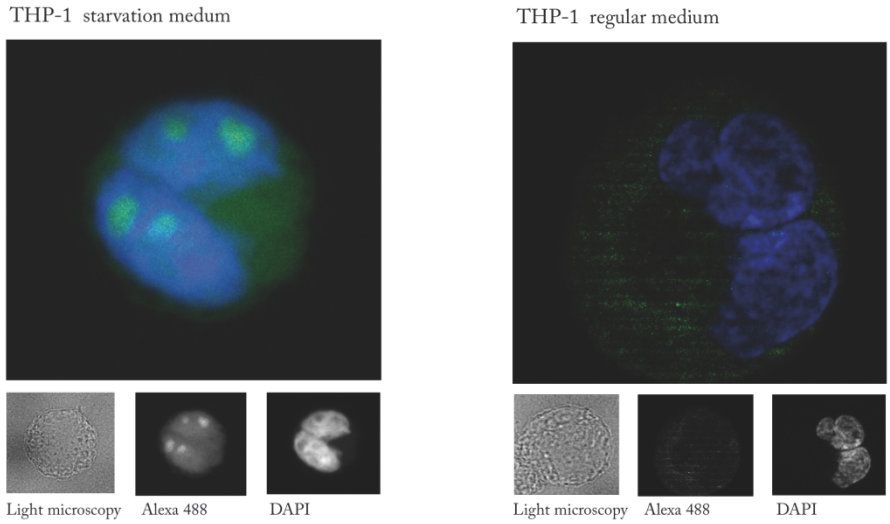

Fig. 3.35: EU incorporation into the host cell. THP-1 cells were incubate with EU for 4 hours, then fixed and stained with DAPI and Alexa 488. Only cells grown in starvation medium incorporated the EU into their own machinery (left), while cells grown in full RPMI medium showed only weak fluorescence (right).

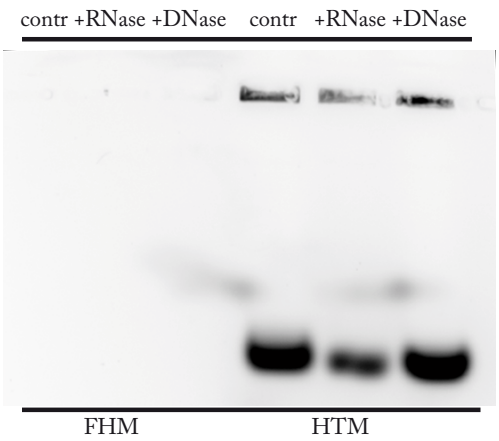

Fig. 3.36: Agarose gel of *Listeria* supernatant. *Listeria* were incubated in either full (FHM) or starvation (HTM) media. Supernatants were precipitated and treated with DNAse, RNAse, or left untreated then loaded on agarose gels. The band only appeared in HTM-grown *Listeria* and was RNase sensitive.

4. Discussion

4.1. Cytosolic recognition of DNA

Pathogen-derived nucleic acids are a highly important PAMP and play a central role during the innate immune response. TLR9 recognizes unmethylated CpG dsDNA located in the endosome of PDCs. In a healthy cell, DNA should not be present in the endosome. In the cytosol, the exact mechanism of dsDNA recognition is not yet fully elucidated and a bit more complicated. This is why a minimal DNA motif is of such interest; using a short well-defined dsODN in order to investigate the characteristics of the DNAR guarantees reproducible results. In this thesis, recognition motifs of short dsDNA ODNs were analyzed in monocytes, murine BM-DCs and assorted cell lines. Two classes of immune stimulatory ODNs could be determined. This is of great clinical interest because of the therapeutic options made available once PRR ligands can be accurately determined. With the possibility of activating the innate immune system without pathogen implementation, an immune response can be mounted resulting in induction of only specific cytokines.

4.1.1. PBMCs recognize DNA dependent of its localization

Once thought to be the gold standard of cytosolic DNA recognition, poly dAdT was recently determined to be a ligand for RIG-I (Ablasser, Bauernfeind et al. 2009). In this paper, dAdT was shown to serve as a template for the formation of an endogenous RIG-I ligand via RNA polymerase III. The TLR9-independent type I IFN response to random long dsDNA molecules, however, still induced type I IFN without involvement of RIG-I: dsDNA molecules in the size range of dAdT still induced a type I IFN response in human MoDC in which RIG-I was silenced. In **Fig. 3.2**, PBMCs were either left untreated, treated with CQ, which inhibits endosomal acidification, or alternatively depleted of PDCs, the main TLR9-expressing cell population. The three cell populations were then transfected with CpG 2216, genomic DNA from PBMCs, plasmid DNA, dAdT and a Lipofectamine control. CpG 2216, a well-known ligand for TLR9, failed to induce an IFNα response in all cell populations except in untreated PBMCs, where the endosomes were allowed to mature and PDCs had not been depleted. Together with the results from **Fig. 3.3** and **3.4**, this demonstrates that the main part of the cytosolic dsDNA-induced type I IFN response is produced by monocytes. Although PDCs are considered as the main IFNα producing cell population, this holds true only for endosomal

stimuli of TLR9. This is of great importance as the percentage of monocytes in the peripheral blood cells is much higher than that of PDCs (15 to 1%, respectively). Targeting monocytes for cytokine production with a monocyte-specific recognition mechanism would therefore be much more promising for therapeutic approaches.

4.1.2. Tandem dsODN are recognized by the DNAR in a length, then sequence-dependent manner

With the knowledge that PBMCs treated with CQ show a cytokine pattern derived almost exclusively from the monocyte response to stimuli, further experiments were carried out with PBMCs blocked with CQ. Building on results obtained in the murine system, ODNs of different lengths were designed in order to deduce the minimal length requirement needed to induce an IFNα response in monocytes (Stetson and Medzhitov 2006). Medzhitov et al. had established a dsODN that, when transfected as a single strand, did not induce an IFN response in murine macrophages. Transfected as a double strand, however, induced a robust type I IFN response. This dsODN was dubbed IFNstimulatory DNA, or ISD. Working from this length, ladders were designed in order to determine the minimal length requirement for human monocytes. The mIFNα response to dsODNs, however, was much more sensitive, reacting to dsODNs at much shorter lengths than in human monocytes. Our findings show that ISD only mildly induces type I IFN response in human monocytic cells (**Fig. 3.11A**). As could be seen in **Fig 3.10 C**, blunt-ended dsODN only induced an IFN response in human monocytes and monocytic cell lines, but not in cell lines derived from other cell populations, i.e. HEK293T, Hela, FaDu, A549, A498 or HepG2. This indicates that the ability to recognize dsODNs is restrained to cells of the immune system, both primary and cell line-derived. Because of this, further experiments to determine the DNAR ligand were carried out in THP-1 cells or primary monocytes in PBMCs.

Once the minimal length had been determined for monocytes/PBMCs, concatemerizing ODNs were designed. This way, each ODN by itself would not fulfill the minimal length requirement, while both together would hybridize into longer dsDNA strands (**Fig 3.6**). ODNs possessed switched corresponding sequences, so that once hybridized together, they would not form blunt-ended dsDNA but rather a self-multimerizing dsDNA strand with half the sequence always an overhang. When transfected into CQ-blocked PBMCs, the single strands indeed did not induce an IFNα response, while both strands hybridized together and transfected could elicit a very strong IFNα response. This principle was applied to various ODN including AT-poor

sequences (**Fig. 3.10A**), with the same cytokine induction pattern as a result. This would mean that for long dsODN sequences, the sequence is not relevant for cytokine induction, an effect that could also be seen for transfected plasmid DNA, where the signal was only partly abrogated after endosomal blockage by addition of CQ. This sequence vagueness is possibly due to the fact that healthy cells do not display any cytosolic DNA, so a cytosolic DNA receptor would need to respond to all types of DNA it encounters, no matter the methylation or PTO status. One of the concatemerizing double-stranded ODNs designed possessed a G-ended sequence which, surprisingly, induced IFNα when transfected as a single strand. This GG(TA)13GG ODN was used as a template sequence to better determine the reason for the IFNα inducing characteristics of this short ODN (**Fig. 3.7**). Working with the different permutations of the base construction of the ODN, C-ended ODNs were also developed, this time with G-rich sequences in the middle of the ODNs. Interestingly, these G-rich core sequences failed to induce hIFNα but induced quite a lot of mIFNα when transfected into murine BM-DCs. Analysis by PAGE revealed that this G-rich core sequence could polymerize into a band that was quite a bit higher than its ssDNA length. This would mean that G-rich core sequences induced IFNα only in the murine system and G-rich end sequences could induce IFNα in both human and murine systems.

A new basic sequence was designed, with the (TA) amount cut down and more Gs added on the ends in order to assure the same ODN length. This basic sequence was then modified with different nucleotides added to the ends in order to guarantee the same basic barbell structure, only alternating barbell components (**Fig. 3.10B**). Only the G-ended barbell ODNs could induce an IFNα response in CQ-blocked PBMCs, indicating a highly sequence-specific induction motif. This significantly facilitates the directed induction of IFNα; a short, well-known ODN sequence has more therapeutic uses than a long dsDNA sequence with unknown structural possibilities and conformations. Although easy recognition of long dsDNA present in the cytosol is due to the fact that the mere presence of cytosolic DNA could be an indication for infection, the recognition motif of short, sequence-specific dsDNA ODNs has the advantage of easier handling.

Further experiments concerning the necessity of the $(TA)_{10}$ segment in the middle of the ODN sequence were performed, demonstrating that an unbroken (TA) length does not correlate with augmented IFNα induction (**Fig 3.10A**). Working with this finding, ODNs were designed containing G-ended barbells and varying lengths of (TA) sequences. There was no strong difference visible between sequences containing longer stretches of (TA) and those of a shorter

length, once the length-dependency was factored out: Sequences under 24bp elicited little type I IFN, but once the threshold of 26bp had been breached, no length-dependent difference in type I IFN induction could be observed (**Fig. 3.5**). This would indicate a prompt saturation of type I IFN induction.

Nonpalindromic DNA sequences were implemented in order to abolish the possibility that the dsODN strands were formed because the ssDNA segments folded in on each other. As shown in **Fig. 3.11A**, G-ended barbell sequences were ordered and transfected on CQ-blocked PBMCs. Each ODN transfected by itself could not induce IFNα; both ODNs transfected to a bar-belled dsDNA strand, however, could. PA gels were run to show that no multimerization had taken place. This of course raised the question that if a barbell formation was necessary for IFNα induction in CQ-blocked PBMCs, how much of a barbell could be removed before the induction potential was abrogated. In **Fig. 3.12**, ODN sequences containing reduced numbers of G ends were paired with the original nonpalindromic G-ended strands. This resulted in IFNα abrogation as soon as both ends of a barbell were missing. Having only half a barbell was sufficient for IFNα induction; having a complete barbell on one end of the double strand and no G overhang on the other side, however, was not. This indicates that it is merely the G-ended overhang that is crucial for recognition by the DNAR or an associated protein, and not the angle of the barbell formed when two G overhangs are opposite each other. PA-gel analysis showed gel bands traveling at a unified height, demonstrating that the strand combinations were not different in their IFNα-induction potential because of varying structural characteristics.

4.1.3. G-ended bar-bell ODN are active as monomers

Although the bar-bell formation had been tested for A3, C3, T3 and G3 overhangs, only G-ended dsODNs had elicited an IFNα response. A possible explanation for this was thought to lie in the unique capacity of guanosine to interact via intermolecular G-quadruplex interplay. G-tetrad structures are present especially in telomeres and gene promoters (Huppert 2008), which would indicate that cytosolic G tetrads are potential recognition motifs. G quadruplexes are formed due to the array of 4 guanosine bases in a nearly planar field. They are more resistant to DNase digestion and have higher melting points than their counterparts composed of other bases. G quadruplexes are held together via their phosphodiester backbone and further stabilized due to their monovalent ion binding (reviewed in (Lane, Chaires et al. 2008)). Gels run with dsODNs containing G-ended overhangs of varying length showed a propensity for tetramer formation in dsODNs possessing 4 or 5 Gs in their bar-bell sequence (**Fig. 3.14**). Hybridizing

the dsODNs and transfecting them with Lipofectamine on CQ-blocked PBMCs showed a robust type I IFN response irrespective of the amount of Gs present on the bar-bell overhang. As there was no difference in induction between dsODNs shown to form tetramers on a PA gel and those presenting only a single molecular weight band, bar-bell dsODNs were analyzed using circular dichroism. CD spectroscopy measures the differential absorption of left- and right-handed circularly polarized light. It is known that G tetrads have unique melting curves at 295nm, so G-ended dsODNs were heated and absorbance at 295nm measured. As can be seen in **Fig. 3.15**, CD spectra showed the characteristic G-tetrad melting curve for dsODNs with 4 and 5-long G ended overhangs, and no melting curve for dsODNs containing 3 or less Gs in their bar-bell formation. The final indication against quadruplex formation, even inside the cytosol, occurred when dsODNs were designed containing N7-deaza-guanosine in their bar-bell overhangs. Due to the replacement of a nitrogen at position 7 by a C-H group, G-quadruplexes could no longer be formed. ODNs containing deaza-G ends, however, induced an equal amount of IFNα as G ended dsODNs, showing that G quadruplex formation, while an interesting phenomenon, was not the source of IFNα induction.

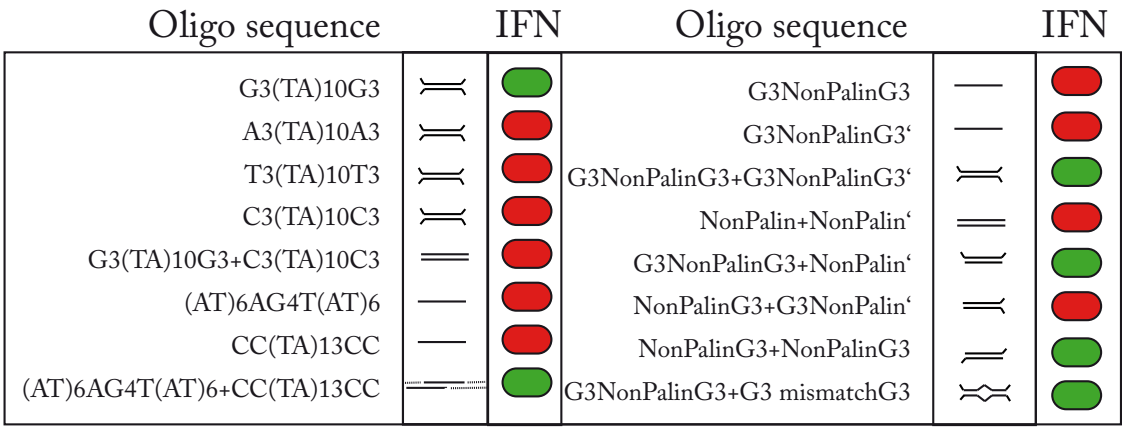

Fig. 4.1: Overview of stimulating ODN structures and sequences. In this thesis, various IFN-inducing ODN properties were investigated. In summary, G-ended ODNs with G barbells induce type I IFN irrespective of tetramer formation. At least two G ends had to be present on the dsODN for type I IFN induction to occur. In the case of concatemerizing ODNs, presence of G ends was not a factor in type I IFN induction, as the length was enough to trigger a response. Mismatches in G-ended ODN sequences did not abrogate the type I IFN response.

4.1.4. ODN are degraded in the cytosol irrespective of their overhangs

Instead of structural differences, the reason G3-ended ODNs manage to induce an IFN response and A3/T3/C3-ended ODNs could lie in the processing that occurs once the ODNs enter the cytosol of the cell of interest. To this end, ODNs were developed containing fluorescent FAM molecules accompanied by a quenching molecule on the opposite end of the

single strand, which suppress the fluorescence of the FAM molecule. The theory was that the fluorescence could be measured by FACS analysis or by fluorescence input with a Perkin Elmer envision reader. Differences between the G3 and C3-ended ODNs would indicate a variation of ODN processing in the cytosol.

In order to obtain a transfection control and possess identical parameters for both sets of ODNs, a third ODN was constructed, carrying a Cy5-fluorescent molecule. This ODN was used as a transfection control and provided a convenient gating tool for FACS experiments.

Time course assays were performed to see when, if any, difference in ODN processing was visible. As shown in **Fig. 3.17**, ODN uptake was similar for both bar-bells after 6 hours; C ends did, however, show a nearly twofold higher degradation than G for the first six hours post transfection. This difference in degradation in the first hours of ODN transfection into cells, however is unlikely to explain the IFNα induction ability of the G_3-ODN and the lack of IFNα induction of the C_3-ODN. IFNα is measured after 20-24 hours' incubation with the stimulus in question, and as degradation levels for both ODNs were equal in the later time points, any disparity from the first six hours would have evened out. The complete inability of the C_3-ODN to induce type I IFN is in no proportion to the uptake variation in comparison to the G_3-ODN. The heightened fluorescence that was observed over time can be explained with the compounded transfection rate of the ODNs. The FAM-tagged ODNs were transfected onto CQ-blocked PBMCs and showed a similar induction rate to the untagged ODNs, indicating that the presence of FAM did not influence the cytokine response of the cells. Incubating the ODNs with cytosolic lysate and then loading them onto a gel further demonstrated no disparity between barbell sequences and their rate of digestion. So although the ODNs are indeed processed and digested once present in the cytosol, it was not the rate of uptake and digestion nor their localization that resulted in the different IFNα response. This signifies that an as yet unknown processing mechanism, not dependent on ODN uptake nor localization, recognizes short dsDNA in a sequence-dependent manner and induces type I IFN induction in monocytes and monocyte-derived cell lines.

There have been many attempts to identify the cytosolic DNA receptor. In recent years, an inflammasome-associated cytosolic DNAR had been identified (Burckstummer, Baumann et al. 2009; Hornung, Ablasser et al. 2009), which did not, however, explain the IFNα induction after transfection with dsODNs, as AIM2 induces pro-IL-1β cleavage. For a while, DAI/ZBP-1 was thought to be the cytosolic DNA receptor (Takaoka, Wang et al. 2007). ZBP-1 deficient mice did not present any immunocompromised phenotype, therefore excluding ZBP-1 from the

continuing search for the cytosolic DNAR (Lippmann, Rothenburg et al. 2008). IFI16 has been traded as a potential cytosolic DNAR (Bowie 2010). Beyond the IFI16 DNA binding domain coprecipitating with 70bp DNA, shorter DNA sequences need to be shown to bind to IFI16 in order to give it the title of cytosolic type I IFN inducing DNAR. Knowing the minimal recognition motif also enables further therapeutic approaches, such as exploiting type I IFN responses of the body to aid the body's innate immune response in Hepatitis B and C therapies or for the treatment of Multiple Sclerosis ((Di Bisceglie, Martin et al. 1989; Di Bisceglie 1995).

4.2. MITA-dependent DNA recognition and the role of autophagy in the type I IFN response

MITA-dependent DNA recognition

Other approaches to the DNAR identification yielded, the adaptor protein MITA (Ishikawa and Barber 2008; Zhong, Yang et al. 2008). It is a membrane protein that could activate IRF3 and, therefore, induce a type-I IFN response to viral infection.

In order to investigate the role of MITA in PBMCs, specifically monocytes, MITA knock-down was performed using shRNA in lentiviral vectors, as well as siRNA assays (**Fig. 3.20**). MITA knockdown did reduce the cytokine response to DNA stimuli, such as pDNA, $G_3(TA)_{10}G_3$, and genDNA. RNA stimuli such as 3P-RNA and bacterial RNA, however, did not induce a MITA-dependent IFN response. Various publications had also associated cytokine induction in response to pathogens such as *Listeria monocytogenes* with MITA signaling (Ishikawa, Ma et al. 2009; Nakhaei, Hiscott et al. 2009). MITA knockdown in THP-1 cells was therefore also used in order to observe possible interaction of MITA with *Listeria* RNA, discussed further down. MITA interaction with *Listeria*-derived PAMPs has been shown in MEFs; this influence could also be seen in THP-1 cells knocked down using an shRNA lentiviral vector targeting MITA. This merits further study, not least because of the species divergence already seen in TLR9 expression.

The role of autophagy in the type I IFN response

Autophagy is a mechanism to deliver cytoplasmic components to the lysosome. In autophagy, cytoplasmic constituents are surrounded by a sac, which engulfs them and turns into a double-membraned structure called the autophagosome. (reviewed in (Mizushima, Ohsumi et al. 2002).

Autophagy, next to its well-known role in cell growth, homeostasis, and development, also has been shown to have an increasingly important role in the innate and adaptive immune responses: It helps to directly eliminate intracellular microbes by digesting them in autolysosomes, delivers cytosolic microbial products to PRRs and is an anti-microbial effector in TLR and RLR signaling.

Until recently, it had been considered that autophagy was a cellular process more beneficial to the pathogen than to the host cell, because the mechanisms of host defense via autophagy had not been wholly elucidated. Various pathogens do, indeed, use or block autophagy for their own purposes. HSV-1 produces a protein ICP34.5 that interferes with autophagy; *Shigella* becomes susceptible to autophagy as soon as it loses one of its motility proteins IscB, and *Listeria* can block phagosome maturation with LLO, forming pores in the membrane (Ogawa, Yoshimori et al. 2005; Birmingham, Canadien et al. 2007; Orvedahl, Alexander et al. 2007).

THP-1 cells (**Fig. 3.21**) cells were treated with autophagy inhibitor wortmannin (Blommaart, Krause et al. 1997), or autophagy inducer rapamycin (Kamada, Funakoshi et al. 2000) and then transfected with DNA stimuli. The IP-10 response occurred in a wortmannin-dependent manner. Other parameters included using THP-1 cells with MITA, Atg5, or a control scrambled shRNA sequence knocked down using a lentiviral system. Atg5 was considered a protein specifically required for autophagy in complex with Atg12, labeling the outer membranes of autophagic vacuoles. (Mizushima, Sugita et al. 1998) Newer findings show non autophagy-related functions for Atg5 (Codogno and Meijer 2006; Sanjuan, Dillon et al. 2007). The only definitive measure for autophagy, therefore, is the documentation of double-membrane autophagosomes in cells using electron microscopy. The usage of Atg5 knock-down, wortmannin, or rapamycin, however, can still be used as an estimation for autophagy involvement in cytokine reponses.

In **Fig 3.21**, the THP-1 IP-10 response to DNA stimuli G3(TA)10G3 and pDNA, but not to dAdT and the RNA stimulus 3P-dsRNA, was reduced in cells pretreated with wortmannin. Of course, as wortmannin is a PI3K inhibitor, this decrease could also attributed to interference in other pathways dependent on PI3K. On the inductory side of autophagy, rapamycin also was added to THP-1 cells in order to observe if this could have an additive effect on the IP-10 response. This could not be observed. This could be because upregulation of autophagy does not automatically deliver more stimuli to the appropriate receptor. THP-1 cells with lentivirally knocked down MITA showed a decreased IP-10 response to DNA stimuli, but not dAdT or RNA stimuli. Knock-down of Atg5 showed a general decline of the IP-10 response, but as Atg5

has an essential role in cell housekeeping (Hara, Nakamura et al. 2006), the diminished IP-10 response in Atg5 knock-down cells may be due to general impairment of cell homeostasis. In general, this experiment indicated a partially autophagy-dependent IP-10 response to DNA and, in the case of Atg5 knock down, also RNA stimuli. The interaction of MITA and autophagy in the pathogen-dependent immune response remains to be investigated.

4.3. The *Listeria*-induced IFN response

RNAs are outfitted with a 5'triphosphorylated nucleotide when transcribed. This aids in processing and regulation of mRNA translation in eukaryotes, where the 5' end is modified to a structure called "CAP". In bacteria, however, one third of mRNA remains 5'triphosphorylated (Bieger and Nierlich 1989). The ligand for 5'triphosphorylated RNA has been shown to be the cytosolic helicase RIG-I, which is activated upon binding (Hornung, Ellegast et al. 2006; Pichlmair, Schulz et al. 2006). The recognition of various negative and positive strand RNA viruses is accomplished via RIG-I (reviewed in (Schlee and Hartmann)). The mechanisms, if any, of the interaction of RIG-I with bacterial RNA remain less widely elucidated. It has been demonstrated that phagosomal, but not cytosolic bacteria are able to induce IFN in dendritic cells in a TLR7-dependent manner (Mancuso, Gambuzza et al. 2009). The cytosolic recognition of DNA from intracellular bacteria has been well documented (Stetson and Medzhitov 2006). Recognition of bacterial RNA in the cytosol, however, is not as clear-cut. It has been proposed that *Listeria*-mediated IFN induction occurs in an IPS-1 independent manner (Soulat, Bauch et al. 2006; Sun, Sun et al. 2006). Even so, IPS-1 was demonstrated to be involved in the pathway resulting in IFNβ induction in *Legionella*-infected lung epithelial cells (Opitz, Vinzing et al. 2006). This was followed up by a study showing transfected crude *Legionella* RNA to be recognized in a RIG-I-dependent manner (Monroe, McWhirter et al. 2009). It is to be noted that these experiments were performed in murine macrophages which are equipped with multiple type I IFN-inducing receptor systems, not least of which one responsible for DNA recognition. This would implicate a certain redundancy for immunrecognition of intracellular bacteria in macrophages. Analyzing the part RIG-I plays in the type I IFN response would be easier in cells not possessing both branches, DNA and RNA, of the cytosolic nucleic acid recognition pathway (Monroe, McWhirter et al. 2009).

The facultative intracellular bacterium *Listeria monocytogenes* is a widespread pathogen. As the causative agent for listeriosis, it endangers immunocompromised individuals including pregnant women. The *Listeria* infection pathway usually commences in the intestinal epithelium, where

the bacteria invade using listerial internalins to induce uptake into non-phagocytic cells such as hepatocytes. Originally, it had been thought that, similar to *Listeria monocytogenes, Legionella* DNA was the PAMP that initiated the host response to infection. Recent findings, however, suggest a recognition pathway involving the RNA, instead: Monroe *et al* found that the RIG-I/MDA5 pathway, thought primarily to detect viruses, is also involved in the innate immune response to an intracellular bacterial pathogen, *Legionella pneumophila* (Monroe, McWhirter et al. 2009). The RIG-I pathway was required for the response to *L. pneumophila* RNA, but not for the response to *L. pneumophila* DNA. It could be, therefore, that *L. pneumophila* RNA may access the host cell cytosol, where it triggers the RIG-I/MDA5 pathway. An unexpected finding, since bacteria have not previously been shown to translocate RNA into host cells. It was also found that *L. pneumophila* encodes a secreted bacterial protein, SdhA (Monroe, McWhirter et al. 2009), which suppresses the RIG-I/MDA5 pathway, thus explaining the supposed redundancy of multiple bacterial proteins for the same function, inhibiting the host response. Multiple viral repressors of the RIG-I/MDA5 pathway have been published, but bacterial inhibitors of RIG-I/MDA5 had not been, as yet, isolated.

4.3.1. *Listeria* induce cytokines in a localization-dependent manner

Listeria monocytogenes invade not only phagocytic cells but can also enter epithelial cells via the interaction of the listerial protein internalin and E-cadherin on the surface of epithelial cells. The invasin internalin is necessary for successful *Listeria* invasion of non-phagocytic cells such as enterocytes, hepatocytes, fibroblasts, epithelial cells and endothelial cells (Gaillard, Berche et al. 1991; Mengaud, Ohayon et al. 1996). The immune response has developed its own receptors to deal with bacterial invasion. The macrophage type I scavenger receptor recognizes lipoteichoic acid from gram positive bacteria (Dunne, Resnick et al. 1994). TLRs 2 and 5, both situated on cell membranes, are thought to be involved in *Listeria* recognition (Hayashi, Smith et al. 2001; Seki, Tsutsui et al. 2002). Obviously, bacteria can trigger type I IFN responses through stimulation of TLR4 on the cell surface or TLR9 in the endosomal compartment. A coactivator of the type I IFN pathway in macrophages, LRRFIP1, is also thought to be involved in *Listeria* recognition (Yang, An et al.). Investigations in the labs of Decker and Portnoy suggested TLR independent pathways leading to induction of type I IFN in mouse macrophages infected with *Listeria monocytogenes* (O'Riordan, Yi et al. 2002; Stockinger, Materna et al. 2002). NOD2 and NALP3 recognize intracellular *Listeria* (reviewed in (Zenewicz and Shen 2007)). However, type I IFN induction depended on cytosolic localization of the bacteria (O'Riordan, Yi et al.

2002; Stockinger, Materna et al. 2002) but was shown to be NOD2 independent (Stockinger, Reutterer et al. 2004). IL-1β is an indicator for *Listeria* infection; blocking the IL-1R exacerbates murine listeriosis (Havell, Moldawer et al. 1992).

RNA was isolated from different bacteria species and transfected onto PBMCs after treatment with phosphatase (CIAP) or DNase. As can be seen in **Fig. 3.22**, the IFNα signal was abrogated in all RNA samples after treatment with CIAP. Live *Listeria* of wt and Δhly strains were then used in order to infect monocytes at varying MOIs. Surprisingly, the IFNα, but not IL-6 and IL-1β response, was localization dependent, indicating at receptor systems not dependent on cytosolic presence of the pathogen.

Listeria in possession of LLO induced a type I IFN response in monocytes, while the Δhly was only able to induce a rudimentary IFNα response (**Fig. 3.23**). Since monocytes are non-proliferating primary cells and it is therefore rather difficult to perform knock-down experiments with them, the monocytic cell line THP-1 was used instead. However, both THP-1 cells and monocytes possess a cytosolic DNAR, so a clinically relevant cell line only in possession of a cytosolic RNA recognition mechanism and not expressing a DNAR was investigated.

A549 cells represent a well established infection system for intracellular bacteria (Chi, Mehl et al. 1991; Jones, Beveridge et al. 1996; Talbot, Paton et al. 1996). Therefore A549 cells were used for infection and transfection experiments. Cells were infected with varying MOIs of *Listeria* wt and Δhly, then tested for cytokines IP-10 and IL-1β. **Fig 3.24** shows the cytokine response of A549 cells. There was no reaction to DNA stimuli, with a very robust A549 hIP-10 response to RNA stimuli. Having established A549 cells as a system without a cytosolic DNAR, experiments were performed to see if *Listeria* induced an IP-10 response independent of DNA stimuli.

Listeria, wt and Δhly, were then labeled with FITC and infected host cells of both THP-1 and A549 strains. These were then investigated with fluorescence microscopy and FACS analysis, demonstrating that the bacteria did indeed enter the host cell cytosol (in the case of the wt strain).

4.1.3. *Listeria*-dependent induction of IFN is RIG-I dependent

Both THP-1 and A549 cell lines were then infected with a lentiviral vector in order to knock down RIG-I expression. This method was later amended using siRNA knock-down instead of lentivirus-mediated shRNA knock-down. A549 cells with impeded RIG-I expression did not mount a hIP-10 response to wt *Listeria* infection, while wt A549 cells could respond to *Listeria*

infection with secretion of hIP-10 (**Fig. 3.27**). The secretion of IL-1β, however, did not increase or decrease with RIG-I knockdown, indicating that *Listeria* activate various pathways of the innate immune response, one of them being the RIG-I pathway, in A549 cells. This would mean that even if the RIG-I dependent type I IFN response is not initiated, the IL-1β response still sounds the alarm. Knocking down RIG-I with siRNA yielded comparable results.

Conventionally, *Listeria* invade through the gastrointestinal tract, where they subvert epithelial cell actin cytoskeleton in order to reach the bloodstream. *Listeria* then migrate to the spleen and the liver, where they infect liver macrophages as well as hepatocytes (reviewed in (Hamon, Bierne et al. 2006)) *Listeria* invasin internalin B (InlB) binds to Hepatocyte Growth Factor (HGF) receptor Met (Dramsi, Biswas et al. 1995). Once bound, InlB activates the Ras-MAPK pathway, leading to cytoskeletal rearrangements and internalization of *Listeria* (Shen, Naujokas et al. 2000). HepG2 cells are known to secrete type I IFNs in response to pathogen infections (Guan, Lu et al. 2007). They are derived from hepatocytes which represent one common in vivo target of *Listeria* infection. HepG2 cells exhibited to be less sensitive to transfection of *Listeria* RNA and infection than THP-1 cells. Even though THP-1 cells secreted type I IFN at very low bacterial load, HepG2 cells only started demonstrating cytokine responses beyond MOI 25. The responses were, however, localization-dependent, allowing a deduction transfer from the A549 cell system (**Fig. 3.29**).

As HepG2 cells are carcinoma-derived, the same experiment was carried out in primary murine hepatocytes obtained from healthy C57BL/6 mice. Hepatocytes responded very well to 3P-RNA and RNA from *Listeria*, but only very sluggishly to *Listeria* infection – similar to infection of the hepatic carcinoma cell line HepG2, murine primary hepatocytes secreted type I IFNs only in response to MOIs greater than 30 (**Fig. 3.32**). This would indicate that the type I IFN response to *Listeria* is not the main defense mechanism of hepatocytes. With a localization-dependent immune response to *Listeria* deducible from ELISA and luminescence data, host cells were infected with FITC-tagged *Listeria* containing RNA which harbored incorporated ethynyl uridine. *Listeria* were allowed to infect the host cells. Cells were fixed and Alexa 594 molecules then bound to the ethynyl uridine present in the host cell cytosol. Because of fixing and permealization, single EU molecules are removed and only RNA incorporated EU molecules can be visualized.

EU staining increased over time in THP-1, A549 and HepG2 cells, indicating that the duration of *Listeria* infection correlated with the amount of EU visible in the cell. When Δhly *Listeria* were used to infect host cells, there was no EU staining visible, indicating that *Listeria* had to be

present in the cytosol for bacterial RNA secretion to take place. However, one could reason that Listeria simply imported EU which is then incorporated into host RNA. However, experimental settings excluded this scenario:

Host cells were incubated in normal RPMI or starvation media, then treated with EU for 2 hours. After fixation, EU strong fluorescence could only be seen in cells incubated in starvation media (**Fig. 3.35**). As host cells used in infection experiments with *Listeria* were grown in RPMI, EU uptake by host cells should be infringed. Additionally, *Listeria* were washed multiple times after incubation with EU; unincorporated EU molecules should be removed before *Listeria* are added to host cells. Azide staining of *Listeria*-incorporated EU in infected cells also showed exclusion of the nucleus (**Fig. 3.33**), indicating that EU-containing RNA was produced by *Listeria*.

With these experiments, it would seem that *Listeria* infect non-phagocytic cells by using their listerial internalins in order to induce uptake, then lyse their phagolysosomes with LLO and escape into the host cell cytosol. Recent findings have found that Group B streptococci (GBS) ssRNA, once present in the cytosol, activates macrophages by binding to components of the RIG-I like pathway and induce cytokine production in macrophages (Deshmukh 2010). As the cytosol is a potentially hostile environment, it is possible that *Listeria* secrete bacterial RNA as a stress signal. Starvation medium used for *Listeria* incubation loaded onto agarose gels showed a band of nucleic acids that was sensitive to RNase, but not DNase, degradation. The marine photosynthetic bacterium secretes RNAs of the size of fully mature tRNAs as well as 16S and 26S rRNA fragments (Ando, Suzuki et al. 2006). Secretion of DNA by *Streptococcus pneumoniae* and *Pseudomonas aeruginosa* has been tied to usage as donor material for bacterial gene transfer (Lorenz and Wackernagel 1994). This is a phenomenon that could well be transferred to *Listeria* behavior in the host cell cytosol; eukaryotic expression plasmid transfer from *Listeria* to host cells has already been documented (Hense, Domann et al. 2001). It is entirely possible that *Listeria* use this secreted RNA as a method of communication inside the cytosol, although this is an approach to the matter that must be thoroughly investigated. Very recent papers have described the recognition of cyclic-di-dAMP from *Listeria* in the host cell. Cyclic di-AMP is produced by bacteria and serves as a second messenger signaling DNA integrity (Woodward, Iavarone et al. ; Witte, Hartung et al. 2008). Further experiments establishing the extent of the involvement of cyclic-di-AMP in cell lines not possessing a cytosolic DNAR pathway would be of great interest.

E.coli overexpressing LLO and engineered to produce trans-kingdom shRNA were able to mediate RNAi in mammalian cells (Xiang, Fruehauf et al. 2006). In the course of this thesis, cytosolic transfer of endogenous intracellular bacterial RNA was visualized. siRNA-mediated

knock down of RIG-I in THP-1 cells only partially diminished *Listeria*-mediated type I IFN induction, indicating a redundant role of RIG-I in monocytic cells. A549 epithelial cells, however, showed RIG-I to be the main type I IFN inducer. As one possible explanation, *Legionella* recognition was suggested occurring via an indirect DNA template using the RNA polymerase III-dependent RIG-I pathway (Chiu, Macmillan et al. 2009). Genetic DNA from *Listeria*, however, failed to induce a type I IFN response in both A549 cells and the HepG2 hepatocyte cell line, excluding RNA polymerase III involvement. Epithelial cell lack of response to genetic DNA notwithstanding, bacterial RNA was shown to be directly recognized in a triphosphorylation-dependent manner, with RIG-I essential for type I IFN and IP-10 induction.

The 5' triphosphate end of RNA was determined to be associated with protection of mRNA from digestion by the bacterial RNase E (Celesnik, Deana et al. 2007). Regulation of the 5' phosphorylation status has been shown to be due to the pyrophosphatase RppH, which mediates mRNA decay (Deana, Celesnik et al. 2008; Celesnik, Deana et al. 2007). RppH has been demonstrated to preferentially interact with single-stranded triphosphorylated 5' nucleotides instead of base paired ends (Deana, Celesnik et al. 2008). Additionally, bacterial RNA could be stablilized by a 5' terminal stem-loop (Emory, Bouvet et al. 1992; Mackie 2000). This would characterize the bacterial RNA PAMP as base-paired and triphosphorylated. The 5'-terminal stem-loop RNAs can contain base-paired 5'-triphosphorylated ends, which has been shown to be the real ligand for RIG-I (Schlee, Roth et al. 2009).

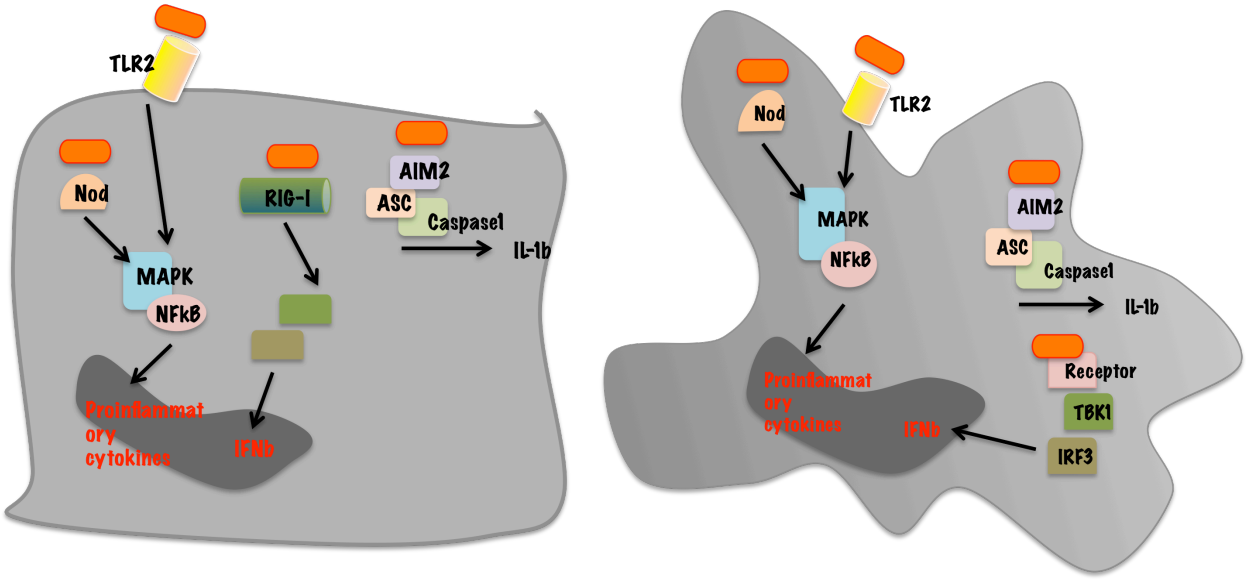

Fig. 4.2: *Listeria* recognition in epithelial cells and hepatocytes versus monocytic cells and macrophages. In epithelial cells and hepatocytes, the *listeria*-induced IFN response occurs in a RNA-dependent manner, implicating RIG-I and the IRF3 pathway. In monocytic cells and macrophages, DNA-dependent IFN induction also seems to play a role.

Essentially, the data in this thesis imply that the *Listeria*-mediated type I IFN and IP-10 response in cells without a DNAR mechanism such as A549 and HepG2 occurs via RIG-I (**Fig. 4.2.**). Various publications suggest type I IFN secretion to support *Listeria* infection; *Listeria* would therefore profit from RIG-I recognition of their RNA (Gregory, Barczynski et al. 1992) (Navarini, Recher et al. 2006). On the other hand, Mancuso et al showed type I IFN signaling to be crucial for host resistance to different pathogenic bacteria (Mancuso, Midiri et al. 2007). The murine system may not be the ideal experimental setup to investigate infection pathways, as murine E-cadherin does not bind *Listeria* internalin due to the mutation of one AA (Lecuit, Vandormael-Pournin et al. 2001). Mice are therefore highly resistant to oral *Listeria* infection, as *Listeria* do not invade the epithelial cells (Lecuit, Vandormael-Pournin et al. 2001). A host defense tactic against *Listeria* infection may be the secretion of the IFN-inducible CXC cytokine IP-10. It attracts phagocytic cells and can deliver defensin-like antibicriobial activity at high doses (Cole, Ganz et al. 2001). In order to further clarify the issue of the role RIG-I plays during *Listeria* infection, however, a humanized murine RIG-I knock-out model is necessary.

5. References

Ablasser, A., F. Bauernfeind, et al. (2009). "RIG-I-dependent sensing of poly(dA:dT) through the induction of an RNA polymerase III-transcribed RNA intermediate." Nat Immunol **10**(10): 1065-72.

Ablasser, A., H. Poeck, et al. (2009). "Selection of molecular structure and delivery of RNA oligonucleotides to activate TLR7 versus TLR8 and to induce high amounts of IL-12p70 in primary human monocytes." J Immunol **182**(11): 6824-33.

Ahmad-Nejad, P., H. Hacker, et al. (2002). "Bacterial CpG-DNA and lipopolysaccharides activate Toll-like receptors at distinct cellular compartments." Eur J Immunol **32**(7): 1958-68.

Akira, S. (2009). "Pathogen recognition by innate immunity and its signaling." Proc Jpn Acad Ser B Phys Biol Sci **85**(4): 143-56.

Akira, S., S. Uematsu, et al. (2006). "Pathogen recognition and innate immunity." Cell **124**(4): 783-801.

Alexopoulou, L., A. C. Holt, et al. (2001). "Recognition of double-stranded RNA and activation of NF-kappaB by Toll-like receptor 3." Nature **413**(6857): 732-8.

Ando, T., H. Suzuki, et al. (2006). "Characterization of extracellular RNAs produced by the marine photosynthetic bacterium Rhodovulum sulfidophilum." J Biochem **139**(4): 805-11.

Andriani, A., M. Bibas, et al. (1996). "Autoimmune hemolytic anemia during alpha interferon treatment in nine patients with hematological diseases." Haematologica **81**(3): 258-60.

Barchet, W., V. Wimmenauer, et al. (2008). "Accessing the therapeutic potential of immunostimulatory nucleic acids." Curr Opin Immunol **20**(4): 389-95.

Barland, C. O., E. Zettersten, et al. (2004). "Imiquimod-induced interleukin-1 alpha stimulation improves barrier homeostasis in aged murine epidermis." J Invest Dermatol **122**(2): 330-6.

Barton, G. M. and R. Medzhitov (2002). "Toll-like receptors and their ligands." Curr Top Microbiol Immunol **270**: 81-92.

Basler, C. F. and G. K. Amarasinghe (2009). "Evasion of interferon responses by Ebola and Marburg viruses." J Interferon Cytokine Res **29**(9): 511-20.

Bauer, S. and H. Wagner (2002). "Bacterial CpG-DNA licenses TLR9." Curr Top Microbiol Immunol **270**: 145-54.

Bauernfeind, F. and V. Hornung (2009). "TLR2 joins the interferon gang." Nat Immunol **10**(11): 1139-41.

Bhatti, Z. and C. S. Berenson (2007). "Adult systemic cat scratch disease associated with therapy for hepatitis C." BMC Infect Dis **7**: 8.

Biggioggero, M., L. Gabbriellini, et al. "Type I interferon therapy and its role in autoimmunity." Autoimmunity **43**(3): 248-54.

Birmingham, C. L., V. Canadien, et al. (2007). "Listeria monocytogenes evades killing by autophagy during colonization of host cells." Autophagy **3**(5): 442-51.

Blommaart, E. F., U. Krause, et al. (1997). "The phosphatidylinositol 3-kinase inhibitors wortmannin and LY294002 inhibit autophagy in isolated rat hepatocytes." Eur J Biochem **243**(1-2): 240-6.

Boehmer, P. E. and I. R. Lehman (1997). "Herpes simplex virus DNA replication." Annu Rev Biochem **66**: 347-84.

Bonjardim, C. A., P. C. Ferreira, et al. (2009). "Interferons: signaling, antiviral and viral evasion." Immunol Lett **122**(1): 1-11.

Borgia, G., L. Reynaud, et al. (2001). "Myasthenia gravis during low-dose IFN-alpha therapy for chronic hepatitis C." J Interferon Cytokine Res **21**(7): 469-70.

Boule, M. W., C. Broughton, et al. (2004). "Toll-like receptor 9-dependent and -independent dendritic cell activation by chromatin-immunoglobulin G complexes." J Exp Med **199**(12): 1631-40.

Bourne, E. J., J. L. Dienstag, et al. (2007). "Quantitative analysis of HBV cccDNA from clinical specimens: correlation with clinical and virological response during antiviral therapy." J Viral Hepat **14**(1): 55-63.

Bowie, A. G. (2010). Novel components of Anti-Viral Pattern Recognition Receptor Pathways. Innate Immunity: Mechanisms linking with Adaptive Immunity. L. A. J. O'Neill. Dublin, Keystone Symposia. **1:** 68.

Buchs, N., F. S. di Giovine, et al. (2001). "IL-1B and IL-1Ra gene polymorphisms and disease severity in rheumatoid arthritis: interaction with their plasma levels." Genes Immun **2**(4): 222-8.

Burckstummer, T., C. Baumann, et al. (2009). "An orthogonal proteomic-genomic screen identifies AIM2 as a cytoplasmic DNA sensor for the inflammasome." Nat Immunol **10**(3): 266-72.

Campbell, P. A. (1993). "T cell involvement in resistance to facultative intracellular pathogens of the lung." Chest **103**(2 Suppl): 113S-115S.

Cannon, J. G. (2000). "Inflammatory Cytokines in Nonpathological States." News Physiol Sci **15**: 298-303.

Chazal, N. and D. Gerlier (2003). "Virus entry, assembly, budding, and membrane rafts." Microbiol Mol Biol Rev **67**(2): 226-37, table of contents.

Chen, C. A. and H. Okayama (1988). "Calcium phosphate-mediated gene transfer: a highly efficient transfection system for stably transforming cells with plasmid DNA." Biotechniques **6**(7): 632-8.

Chen, F., Y. Du, et al. (2008). "Syntenin negatively regulates TRAF6-mediated IL-1R/TLR4 signaling." Cell Signal **20**(4): 666-74.

Chi, E., T. Mehl, et al. (1991). "Interaction of Pseudomonas aeruginosa with A549 pneumocyte cells." Infect Immun **59**(3): 822-8.

Chow, L. T. and T. R. Broker (1994). "Papillomavirus DNA replication." Intervirology **37**(3-4): 150-8.

Codogno, P. and A. J. Meijer (2006). "Atg5: more than an autophagy factor." Nat Cell Biol **8**(10): 1045-7.

Colonna, M., A. Krug, et al. (2002). "Interferon-producing cells: on the front line in immune responses against pathogens." Curr Opin Immunol **14**(3): 373-9.

Cummins, M. J., A. Papas, et al. (2003). "Treatment of primary Sjogren's syndrome with low-dose human interferon alfa administered by the oromucosal route: combined phase III results." Arthritis Rheum **49**(4): 585-93.

Cusson-Hermance, N., S. Khurana, et al. (2005). "Rip1 mediates the Trif-dependent toll-like receptor 3- and 4-induced NF-{kappa}B activation but does not contribute to interferon regulatory factor 3 activation." J Biol Chem **280**(44): 36560-6.

Dalrymple, S. A., L. A. Lucian, et al. (1995). "Interleukin-6-deficient mice are highly susceptible to Listeria monocytogenes infection: correlation with inefficient neutrophilia." Infect Immun **63**(6): 2262-8.

De Trez, C., B. Pajak, et al. (2005). "TLR4 and Toll-IL-1 receptor domain-containing adapter-inducing IFN-beta, but not MyD88, regulate Escherichia coli-induced dendritic cell maturation and apoptosis in vivo." J Immunol **175**(2): 839-46.

Deigendesch, N., F. Koch-Nolte, et al. (2006). "ZBP1 subcellular localization and association with stress granules is controlled by its Z-DNA binding domains." Nucleic Acids Res **34**(18): 5007-20.

Delgado, M. A., R. A. Elmaoued, et al. (2008). "Toll-like receptors control autophagy." EMBO J **27**(7): 1110-21.

Der, S. D., A. Zhou, et al. (1998). "Identification of genes differentially regulated by interferon alpha, beta, or gamma using oligonucleotide arrays." Proc Natl Acad Sci U S A **95**(26): 15623-8.

Deshmukh, S. D. (2010). Macrophages recognize internalized streptococci via interaction of bacteria ssRNA with the IPS-1 pathway. Innate Immunity: Mechanisms Linking with Adaptive Immunity. L. A. J. O'Neill. Dublin, Ireland, Keystone Symposia. **1:** 86.

Di Bisceglie, A. M. (1995). "Long-term outcome of interferon-alpha therapy for chronic hepatitis B." J Hepatol **22**(1 Suppl): 65-7.

Di Bisceglie, A. M., P. Martin, et al. (1989). "Recombinant interferon alfa therapy for chronic hepatitis C. A randomized, double-blind, placebo-controlled trial." N Engl J Med **321**(22): 1506-10.

Diebold, S. S., T. Kaisho, et al. (2004). "Innate antiviral responses by means of TLR7-mediated recognition of single-stranded RNA." Science **303**(5663): 1529-31.

Dinarello, C. A. (1994). "The interleukin-1 family: 10 years of discovery." FASEB J **8**(15): 1314-25.

Dinarello, C. A. (2005). "An IL-1 family member requires caspase-1 processing and signals through the ST2 receptor." Immunity **23**(5): 461-2.

Dinarello, C. A. (2005). "Blocking IL-1 in systemic inflammation." J Exp Med **201**(9): 1355-9.

Dinarello, C. A. (2005). "Interleukin-1beta." Crit Care Med **33**(12 Suppl): S460-2.

Dinarello, C. A. (2005). "The many worlds of reducing interleukin-1." Arthritis Rheum **52**(7): 1960-7.

Dramsi, S., I. Biswas, et al. (1995). "Entry of Listeria monocytogenes into hepatocytes requires expression of inIB, a surface protein of the internalin multigene family." Mol Microbiol **16**(2): 251-61.

Du, X., A. Poltorak, et al. (2000). "Three novel mammalian toll-like receptors: gene structure, expression, and evolution." Eur Cytokine Netw **11**(3): 362-71.

Dubinski, A. and Z. Zdrojewicz (2007). "[The role of interleukin-6 in development and progression of atherosclerosis]." Pol Merkur Lekarski **22**(130): 291-4.

Dunne, D. W., D. Resnick, et al. (1994). "The type I macrophage scavenger receptor binds to gram-positive bacteria and recognizes lipoteichoic acid." Proc Natl Acad Sci U S A **91**(5): 1863-7.

Dykes, G. A. and M. Dworaczek (2002). "Influence of interactions between temperature, ferric ammonium citrate and glycine betaine on the growth of Listeria monocytogenes in a defined medium." Lett Appl Microbiol **35**(6): 538-42.

Dziarski, R. and D. Gupta (2000). "Role of MD-2 in TLR2- and TLR4-mediated recognition of Gram-negative and Gram-positive bacteria and activation of chemokine genes." J Endotoxin Res **6**(5): 401-5.

Fernandes-Alnemri, T., J. W. Yu, et al. (2009). "AIM2 activates the inflammasome and cell death in response to cytoplasmic DNA." Nature **458**(7237): 509-13.

Fitzgerald, K. A., S. M. McWhirter, et al. (2003). "IKKepsilon and TBK1 are essential components of the IRF3 signaling pathway." Nat Immunol **4**(5): 491-6.

Forsdyke, D. R. (1995). "The origins of the clonal selection theory of immunity as a case study for evaluation in science." FASEB J **9**(2): 164-6.

Franchi, L., T. Eigenbrod, et al. (2009). "The inflammasome: a caspase-1-activation platform that regulates immune responses and disease pathogenesis." Nat Immunol **10**(3): 241-7.

Fu, Y., N. Comella, et al. (1999). "Cloning of DLM-1, a novel gene that is up-regulated in activated macrophages, using RNA differential display." Gene **240**(1): 157-63.

Gaillard, J. L., P. Berche, et al. (1991). "Entry of L. monocytogenes into cells is mediated by internalin, a repeat protein reminiscent of surface antigens from gram-positive cocci." Cell **65**(7): 1127-41.

Gitlin, L., W. Barchet, et al. (2006). "Essential role of mda-5 in type I IFN responses to polyriboinosinic:polyribocytidylic acid and encephalomyocarditis picornavirus." Proc Natl Acad Sci U S A **103**(22): 8459-64.

Goldbach-Mansky, R., N. J. Dailey, et al. (2006). "Neonatal-onset multisystem inflammatory disease responsive to interleukin-1beta inhibition." N Engl J Med **355**(6): 581-92.

Guan, S. H., M. Lu, et al. (2007). "Interferon-alpha response in chronic hepatitis B-transfected HepG2.2.15 cells is partially restored by lamivudine treatment." World J Gastroenterol **13**(2): 228-35.

Gursel, I., M. Gursel, et al. (2003). "Repetitive elements in mammalian telomeres suppress bacterial DNA-induced immune activation." J Immunol **171**(3): 1393-400.

Haas, T., J. Metzger, et al. (2008). "The DNA sugar backbone 2' deoxyribose determines toll-like receptor 9 activation." Immunity **28**(3): 315-23.

Hacker, H., H. Mischak, et al. (1998). "CpG-DNA-specific activation of antigen-presenting cells requires stress kinase activity and is preceded by non-specific endocytosis and endosomal maturation." EMBO J **17**(21): 6230-40.

Hafler, D. A. (2004). "Multiple sclerosis." J Clin Invest **113**(6): 788-94.

Hahn, A. M., L. E. Huye, et al. (2005). "Interferon regulatory factor 7 is negatively regulated by the Epstein-Barr virus immediate-early gene, BZLF-1." J Virol **79**(15): 10040-52.

Hamon, M., H. Bierne, et al. (2006). "Listeria monocytogenes: a multifaceted model." Nat Rev Microbiol **4**(6): 423-34.

Hanninen, K., H. Katila, et al. (2008). "Interleukin-1 beta gene polymorphism and its interactions with neuregulin-1 gene polymorphism are associated with schizophrenia." Eur Arch Psychiatry Clin Neurosci **258**(1): 10-5.

Hara, T., K. Nakamura, et al. (2006). "Suppression of basal autophagy in neural cells causes neurodegenerative disease in mice." Nature **441**(7095): 885-9.

Harte, M. T., I. R. Haga, et al. (2003). "The poxvirus protein A52R targets Toll-like receptor signaling complexes to suppress host defense." J Exp Med **197**(3): 343-51.

Hartmann, G. and A. M. Krieg (2000). "Mechanism and function of a newly identified CpG DNA motif in human primary B cells." J Immunol **164**(2): 944-53.

Havell, E. A., L. L. Moldawer, et al. (1992). "Type I IL-1 receptor blockade exacerbates murine listeriosis." J Immunol **148**(5): 1486-92.

Hayashi, F., K. D. Smith, et al. (2001). "The innate immune response to bacterial flagellin is mediated by Toll-like receptor 5." Nature **410**(6832): 1099-103.

Heeg, K., T. Sparwasser, et al. (1998). "Bacterial DNA as an evolutionary conserved ligand signalling danger of infection to immune cells." Eur J Clin Microbiol Infect Dis **17**(7): 464-9.

Heil, F., P. Ahmad-Nejad, et al. (2003). "The Toll-like receptor 7 (TLR7)-specific stimulus loxoribine uncovers a strong relationship within the TLR7, 8 and 9 subfamily." Eur J Immunol **33**(11): 2987-97.

Heil, F., H. Hemmi, et al. (2004). "Species-specific recognition of single-stranded RNA via toll-like receptor 7 and 8." Science **303**(5663): 1526-9.

Hemmi, H., T. Kaisho, et al. (2003). "The roles of Toll-like receptor 9, MyD88, and DNA-dependent protein kinase catalytic subunit in the effects of two distinct CpG DNAs on dendritic cell subsets." J Immunol **170**(6): 3059-64.

Hemmi, H., O. Takeuchi, et al. (2000). "A Toll-like receptor recognizes bacterial DNA." Nature **408**(6813): 740-5.

Hense, M., E. Domann, et al. (2001). "Eukaryotic expression plasmid transfer from the intracellular bacterium Listeria monocytogenes to host cells." Cell Microbiol **3**(9): 599-609.

Hoebe, K., X. Du, et al. (2003). "Identification of Lps2 as a key transducer of MyD88-independent TIR signalling." Nature **424**(6950): 743-8.

Hoffman, H. M., S. Rosengren, et al. (2004). "Prevention of cold-associated acute inflammation in familial cold autoinflammatory syndrome by interleukin-1 receptor antagonist." Lancet **364**(9447): 1779-85.

Honda, K. and T. Taniguchi (2006). "IRFs: master regulators of signalling by Toll-like receptors and cytosolic pattern-recognition receptors." Nat Rev Immunol **6**(9): 644-58.

Honda, K., H. Yanai, et al. (2005). "IRF-7 is the master regulator of type-I interferon-dependent immune responses." Nature **434**(7034): 772-7.

Horng, T., G. M. Barton, et al. (2002). "The adaptor molecule TIRAP provides signalling specificity for Toll-like receptors." Nature **420**(6913): 329-33.

Hornung, J. A., C. Brase, et al. (2009). "First experience with a new titanium clip stapes prosthesis and a comparison with the earlier model used in stapes surgery." Laryngoscope.

Hornung, R. W., B. P. Lanphear, et al. (2009). "Age of greatest susceptibility to childhood lead exposure: a new statistical approach." Environ Health Perspect **117**(8): 1309-12.

Hornung, V., A. Ablasser, et al. (2009). "AIM2 recognizes cytosolic dsDNA and forms a caspase-1-activating inflammasome with ASC." Nature **458**(7237): 514-8.

Hornung, V., J. Ellegast, et al. (2006). "5'-Triphosphate RNA is the ligand for RIG-I." Science **314**(5801): 994-7.

Hornung, V., M. Guenthner-Biller, et al. (2005). "Sequence-specific potent induction of IFN-alpha by short interfering RNA in plasmacytoid dendritic cells through TLR7." Nat Med **11**(3): 263-70.

Hornung, V., S. Rothenfusser, et al. (2002). "Quantitative expression of toll-like receptor 1-10 mRNA in cellular subsets of human peripheral blood mononuclear cells and sensitivity to CpG oligodeoxynucleotides." J Immunol **168**(9): 4531-7.

Horwitz, M. A. and S. C. Silverstein (1980). "Legionnaires' disease bacterium (Legionella pneumophila) multiples intracellularly in human monocytes." J Clin Invest **66**(3): 441-50.

Hu, B., S. Wang, et al. (2003). "A nuclear target for interleukin-1alpha: interaction with the growth suppressor necdin modulates proliferation and collagen expression." Proc Natl Acad Sci U S A **100**(17): 10008-13.

Hu, J. L., G. Li, et al. (2009). "Genetic analysis of interleukin-1A C(-889)T polymorphism with Alzheimer disease." Cell Mol Neurobiol **29**(1): 81-5.

Huang, E. S. and R. A. Johnson (2000). "Human cytomegalovirus - no longer just a DNA virus." Nat Med **6**(8): 863-4.

Huppert, J. L. (2008). "Four-stranded nucleic acids: structure, function and targeting of G-quadruplexes." Chem Soc Rev **37**(7): 1375-84.

Isberg, R. R., T. J. O'Connor, et al. (2009). "The Legionella pneumophila replication vacuole: making a cosy niche inside host cells." Nat Rev Microbiol **7**(1): 13-24.

Ishii, K. J., C. Coban, et al. (2006). "A Toll-like receptor-independent antiviral response induced by double-stranded B-form DNA." Nat Immunol **7**(1): 40-8.

Ishii, K. J., T. Kawagoe, et al. (2008). "TANK-binding kinase-1 delineates innate and adaptive immune responses to DNA vaccines." Nature **451**(7179): 725-9.

Ishii, K. J., K. Suzuki, et al. (2001). "Genomic DNA released by dying cells induces the maturation of APCs." J Immunol **167**(5): 2602-7.

Ishikawa, H. and G. N. Barber (2008). "STING is an endoplasmic reticulum adaptor that facilitates innate immune signalling." Nature **455**(7213): 674-8.

Ishikawa, H., Z. Ma, et al. (2009). "STING regulates intracellular DNA-mediated, type I interferon-dependent innate immunity." Nature **461**(7265): 788-92.

Iwasaki, A. and R. Medzhitov (2004). "Toll-like receptor control of the adaptive immune responses." Nat Immunol **5**(10): 987-95.

Jao, C. Y. and A. Salic (2008). "Exploring RNA transcription and turnover in vivo by using click chemistry." Proc Natl Acad Sci U S A **105**(41): 15779-84.

Jones, A. L., T. J. Beveridge, et al. (1996). "Intracellular survival of Burkholderia pseudomallei." Infect Immun **64**(3): 782-90.

Jounai, N., F. Takeshita, et al. (2007). "The Atg5 Atg12 conjugate associates with innate antiviral immune responses." Proc Natl Acad Sci U S A **104**(35): 14050-5.

Kagan, J. C. and R. Medzhitov (2006). "Phosphoinositide-mediated adaptor recruitment controls Toll-like receptor signaling." Cell **125**(5): 943-55.

Kagan, J. C., T. Su, et al. (2008). "TRAM couples endocytosis of Toll-like receptor 4 to the induction of interferon-beta." Nat Immunol **9**(4): 361-8.

Kamada, Y., T. Funakoshi, et al. (2000). "Tor-mediated induction of autophagy via an Apg1 protein kinase complex." J Cell Biol **150**(6): 1507-13.

Karayel, E., T. Burckstummer, et al. (2009). "The TLR-independent DNA recognition pathway in murine macrophages: Ligand features and molecular signature." Eur J Immunol **39**(7): 1929-36.

Kato, H., O. Takeuchi, et al. (2008). "Length-dependent recognition of double-stranded ribonucleic acids by retinoic acid-inducible gene-I and melanoma differentiation-associated gene 5." J Exp Med **205**(7): 1601-10.

Kato, H., O. Takeuchi, et al. (2006). "Differential roles of MDA5 and RIG-I helicases in the recognition of RNA viruses." Nature **441**(7089): 101-5.

Kawai, T., O. Adachi, et al. (1999). "Unresponsiveness of MyD88-deficient mice to endotoxin." Immunity **11**(1): 115-22.

Kawai, T. and S. Akira "The role of pattern-recognition receptors in innate immunity: update on Toll-like receptors." Nat Immunol **11**(5): 373-84.

Kawai, T. and S. Akira (2006). "Innate immune recognition of viral infection." Nat Immunol **7**(2): 131-7.

Kawai, T., K. Takahashi, et al. (2005). "IPS-1, an adaptor triggering RIG-I- and Mda5-mediated type I interferon induction." Nat Immunol **6**(10): 981-8.

Kayal, S. and A. Charbit (2006). "Listeriolysin O: a key protein of Listeria monocytogenes with multiple functions." FEMS Microbiol Rev **30**(4): 514-29.

Kenneth Murphy, P. T., Mark Walport (2008). Janeway's Immunobiology. New York, Garland Science.

Krieg, A. M., G. Hartmann, et al. (2000). "Mechanism of action of CpG DNA." Curr Top Microbiol Immunol **247**: 1-21.

Kristiansen, O. P. and T. Mandrup-Poulsen (2005). "Interleukin-6 and diabetes: the good, the bad, or the indifferent?" Diabetes **54 Suppl 2**: S114-24.

Krug, A., G. D. Luker, et al. (2004). "Herpes simplex virus type 1 activates murine natural interferon-producing cells through toll-like receptor 9." Blood **103**(4): 1433-7.

Krug, A., S. Rothenfusser, et al. (2001). "Identification of CpG oligonucleotide sequences with high induction of IFN-alpha/beta in plasmacytoid dendritic cells." Eur J Immunol **31**(7): 2154-63.

Krug, A., A. Towarowski, et al. (2001). "Toll-like receptor expression reveals CpG DNA as a unique microbial stimulus for plasmacytoid dendritic cells which synergizes with CD40 ligand to induce high amounts of IL-12." Eur J Immunol **31**(10): 3026-37.

Lane, A. N., J. B. Chaires, et al. (2008). "Stability and kinetics of G-quadruplex structures." Nucleic Acids Res **36**(17): 5482-515.

Lee, H. K., J. M. Lund, et al. (2007). "Autophagy-dependent viral recognition by plasmacytoid dendritic cells." Science **315**(5817): 1398-401.

Lefort, S., A. Soucy-Faulkner, et al. (2007). "Binding of Kaposi's sarcoma-associated herpesvirus K-bZIP to interferon-responsive factor 3 elements modulates antiviral gene expression." J Virol **81**(20): 10950-60.

Leimeister-Wachter, M., C. Haffner, et al. (1990). "Identification of a gene that positively regulates expression of listeriolysin, the major virulence factor of listeria monocytogenes." Proc Natl Acad Sci U S A **87**(21): 8336-40.

Lerolle, N., J. R. Zahar, et al. (2002). "Pneumonia involving Legionella pneumophila and Listeria monocytogenes in an immunocompromised patient: an unusual coinfection." Respiration **69**(4): 359-61.

Li, T. and S. He (2006). "Induction of IL-6 release from human T cells by PAR-1 and PAR-2 agonists." Immunol Cell Biol **84**(5): 461-6.

Lippmann, J., S. Rothenburg, et al. (2008). "IFNbeta responses induced by intracellular bacteria or cytosolic DNA in different human cells do not require ZBP1 (DLM-1/DAI)." Cell Microbiol **10**(12): 2579-88.

Liu, L., I. Botos, et al. (2008). "Structural basis of toll-like receptor 3 signaling with double-stranded RNA." Science **320**(5874): 379-81.

Liu, Z., R. J. Simpson, et al. (1995). "Interaction of interleukin-6, tumour necrosis factor and interleukin-1 during Listeria infection." Immunology **85**(4): 562-7.

Lorenz, M. G. and W. Wackernagel (1994). "Bacterial gene transfer by natural genetic transformation in the environment." Microbiol Rev **58**(3): 563-602.

Lovell, D. J., S. L. Bowyer, et al. (2005). "Interleukin-1 blockade by anakinra improves clinical symptoms in patients with neonatal-onset multisystem inflammatory disease." Arthritis Rheum **52**(4): 1283-6.

Lund, J. M., L. Alexopoulou, et al. (2004). "Recognition of single-stranded RNA viruses by Toll-like receptor 7." Proc Natl Acad Sci U S A **101**(15): 5598-603.

Mancuso, G., A. Midiri, et al. (2007). "Type I IFN signaling is crucial for host resistance against different species of pathogenic bacteria." J Immunol **178**(5): 3126-33.

March, C. J., B. Mosley, et al. (1985). "Cloning, sequence and expression of two distinct human interleukin-1 complementary DNAs." Nature **315**(6021): 641-7.

Mazur, D. J. and F. W. Perrino (1999). "Identification and expression of the TREX1 and TREX2 cDNA sequences encoding mammalian 3'-->5' exonucleases." J Biol Chem **274**(28): 19655-60.

McCluskie, M. J. and A. M. Krieg (2006). "Enhancement of infectious disease vaccines through TLR9-dependent recognition of CpG DNA." Curr Top Microbiol Immunol **311**: 155-78.

Medzhitov, R. and C. Janeway, Jr. (2000). "The Toll receptor family and microbial recognition." Trends Microbiol **8**(10): 452-6.

Medzhitov, R., P. Preston-Hurlburt, et al. (1997). "A human homologue of the Drosophila Toll protein signals activation of adaptive immunity." Nature **388**(6640): 394-7.

Meylan, E., J. Curran, et al. (2005). "Cardif is an adaptor protein in the RIG-I antiviral pathway and is targeted by hepatitis C virus." Nature **437**(7062): 1167-72.

Mizushima, N., Y. Ohsumi, et al. (2002). "Autophagosome formation in mammalian cells." Cell Struct Funct **27**(6): 421-9.

Mizushima, N., H. Sugita, et al. (1998). "A new protein conjugation system in human. The counterpart of the yeast Apg12p conjugation system essential for autophagy." J Biol Chem **273**(51): 33889-92.

Monroe, K. M., S. M. McWhirter, et al. (2009). "Identification of host cytosolic sensors and bacterial factors regulating the type I interferon response to Legionella pneumophila." PLoS Pathog **5**(11): e1000665.

Morita, M., G. Stamp, et al. (2004). "Gene-targeted mice lacking the Trex1 (DNase III) 3'-->5' DNA exonuclease develop inflammatory myocarditis." Mol Cell Biol **24**(15): 6719-27.

Mosevitskaia, T. V. (1978). "[Repair mechanisms and mutagenesis in Escherichia coli bacteria irradiated with ultraviolet light]." Usp Sovrem Biol **85**(3): 340-59.

Munder, A., A. Zelmer, et al. (2005). "Murine pulmonary infection with Listeria monocytogenes: differential susceptibility of BALB/c, C57BL/6 and DBA/2 mice." Microbes Infect **7**(4): 600-11.

Murai, K., M. Yamanaka, et al. (1980). "Purification and properties of deoxyribonuclease II from human urine." J Biochem **87**(4): 1097-103.

Nakhaei, P., J. Hiscott, et al. (2009). "STING-ing the Antiviral Pathway." J Mol Cell Biol.

Neuhaus, O., J. J. Archelos, et al. (2003). "Immunomodulation in multiple sclerosis: from immunosuppression to neuroprotection." Trends Pharmacol Sci **24**(3): 131-8.

Ogawa, M., T. Yoshimori, et al. (2005). "Escape of intracellular Shigella from autophagy." Science **307**(5710): 727-31.

Oliveri, M., A. Daga, et al. (2001). "DNase I mediates internucleosomal DNA degradation in human cells undergoing drug-induced apoptosis." Eur J Immunol **31**(3): 743-51.

Orvedahl, A., D. Alexander, et al. (2007). "HSV-1 ICP34.5 confers neurovirulence by targeting the Beclin 1 autophagy protein." Cell Host Microbe **1**(1): 23-35.

Pamer, E. G. (2004). "Immune responses to Listeria monocytogenes." Nat Rev Immunol **4**(10): 812-23.

Pan, X., A. Luhrmann, et al. (2008). "Ankyrin repeat proteins comprise a diverse family of bacterial type IV effectors." Science **320**(5883): 1651-4.

Pauls, E., J. Senserrich, et al. (2007). "Induction of interleukins IL-6 and IL-8 by siRNA." Clin Exp Immunol **147**(1): 189-96.

Pestka, S. (2000). "The human interferon alpha species and receptors." Biopolymers **55**(4): 254-87.

Pestka, S. (2003). "A dance between interferon-alpha/beta and p53 demonstrates collaborations in tumor suppression and antiviral activities." Cancer Cell **4**(2): 85-7.

Petrilli, V., C. Dostert, et al. (2007). "The inflammasome: a danger sensing complex triggering innate immunity." Curr Opin Immunol **19**(6): 615-22.

Platanias, L. C. (2005). "Mechanisms of type-I- and type-II-interferon-mediated signalling." Nat Rev Immunol **5**(5): 375-86.

Poeck, H., M. Bscheider, et al. (2009). "Recognition of RNA virus by RIG-I results in activation of CARD9 and inflammasome signaling for interleukin 1beta production." Nat Immunol.

Popov, A., Z. Abdullah, et al. (2006). "Indoleamine 2,3-dioxygenase-expressing dendritic cells form suppurative granulomas following Listeria monocytogenes infection." J Clin Invest **116**(12): 3160-70.

Prins, K. C., W. B. Cardenas, et al. (2009). "Ebola virus protein VP35 impairs the function of interferon regulatory factor-activating kinases IKKepsilon and TBK-1." J Virol **83**(7): 3069-77.

Qian, Y., M. Commane, et al. (2001). "IRAK-mediated translocation of TRAF6 and TAB2 in the interleukin-1-induced activation of NFkappa B." J Biol Chem **276**(45): 41661-7.

Rahman, A. and D. A. Isenberg (2008). "Systemic lupus erythematosus." N Engl J Med **358**(9): 929-39.

Yasutomo, K., T. Horiuchi, et al. (2001). "Mutation of DNASE1 in people with systemic lupus erythematosus." Nat Genet **28**(4): 313-4.

Yoneyama, M., M. Kikuchi, et al. (2005). "Shared and unique functions of the DExD/H-box helicases RIG-I, MDA5, and LGP2 in antiviral innate immunity." J Immunol **175**(5): 2851-8.

Yoneyama, M., M. Kikuchi, et al. (2004). "The RNA helicase RIG-I has an essential function in double-stranded RNA-induced innate antiviral responses." Nat Immunol **5**(7): 730-7.

Zenewicz, L. A. and H. Shen (2007). "Innate and adaptive immune responses to Listeria monocytogenes: a short overview." Microbes Infect **9**(10): 1208-15.

Zhong, B., Y. Yang, et al. (2008). "The adaptor protein MITA links virus-sensing receptors to IRF3 transcription factor activation." Immunity **29**(4): 538-50.

Zhu, F. X., S. M. King, et al. (2002). "A Kaposi's sarcoma-associated herpesviral protein inhibits virus-mediated induction of type I interferon by blocking IRF-7 phosphorylation and nuclear accumulation." Proc Natl Acad Sci U S A **99**(8): 5573-8.

Ziegler-Heitbrock, L. (2007). "The CD14+ CD16+ blood monocytes: their role in infection and inflammation." J Leukoc Biol **81**(3): 584-92.

6. Appendix

6.1. Table of abbreviations

Table 6.1: Below is a table of abbreviations used in the course of this thesis, accompanied by their definitions.

Abbreviation	Definition
AIM-2	Absent in Melanoma 2
ASC	apoptosis-associated speck-like protein
Atg	Autophagy
ATP	Adenosine Triphosphate
BDCA-2	Blood Dendritic Cell Ag
BHI	Brain Heart Infusion
CARD	Caspase Recruitment Domain
CD	Circular Dichroism
CTL	Cytotoxic T Cells
DAI	DNA-dependent activator of IRFs
DMEM	Dulbecco's Modified Eagle's Medium
DMSO	dimethylsulfoxide
DNA	Desoxyribonucleic Acid
EAMG	experimental autoimmune myasthenia gravis
EDTA	Ethylenediaminetetraacetic Acid
EE1	early endosomal protein 1
eIF-2	Eukaryotic translation initiation factor 2
ELISA	enzyme-linked immunosorbent assay
FCS	fetal calf serum
FSC	Forward scatter
HRP	horseradish peroxidase
HSV	herpes simplex virus
HTM	Hsiang-Ning Tsai medium
IFN	interferon
IKB	inhibitor kappaB
IKKi	IKB kinase inhibitor
IL1	interleukin
IPS-1	IFN promoter stimulating factor-1
IRAK	IL-1R-associated kinase
IRF-3	Interferon Regulatory Factor
ISG	interferon-stimulated gene
LB	Luria Broth
LC-3	Light Chain 3
LRR	Leucine Rich Repeats
M-CSF	Macrophage colony stimulating factor
MACS	magnetic-activated cell sorting
MDC	Myeloid Dendritic Cells
MITA	mediator of IRF3 activation
MYD88	Myeloid differentiation primary response gene
NFkB	Nuclear Factor kB

NLPR3	NOD-LRRs containing pyrin domain 3
NOD	nucleotide-binding oligomerization domain
ODN	Oligonucleotide
Opti-MEM	Minimal Essential Medium
p:IC	poly Inosine-Cytosine
PAMP	Pathogen-Associated Molecular Patterns
PBMC	Peripheral Blood Mononuclear Cells
PDC	Plasmacytoid Dendritic Cells
PLC	Phospholipase C
PRR	Pattern Recognition Receptors
PYD	Pyrin Domain
RANKL	receptor activator of NFkB Ligand
RIG-I	Retinoic Acid Inducible Gene I
RIP	Receptor interacting protein
RNA	Ribonucleid Acid
RPMI	Roswell Park Memorial Institute Medium
SLE	Systemic Lupus Erythmatosus
SSC	Sidewards scatter
STAT	Signal Transducer and Activator of Transcription
STING	Stimulator of Interferon Genes
TAK	TGFß-activated kinase
TBE	Tris-Borate-EDTA
TBK-1	TANK-binding kinase 1
TIR	Toll-IL1 Receptor
TLR	Toll-Like-Receptor
TRAF	TNF-receptor-associated factor
TREX 1	3' Repair exonuclease 1
ZBP-1	Z-DNA Binding Protein

6.2. Figure index

Table 6.2: List of Figures, their definitions and page numbers

6.3. Table index

Table 6.3: List of tables, definitions and page numbers

6.4. Synthetic oligonucleotides used in the course of this dissertation

Table 6.4: The synthetic oligonucleotides used in this thesis are listed in table 2. They were chosen according to (TA) repetitions, CpG motifs, poly G or poly C ends, palindromic probability and/or structure formation.

Oligo Number	Oligo Name	Oligo sequence
1	GC(AC)10GC	GC(AC)10GC
2	GC(AT)20GC	GC(AT)20GC
3	GC(AT)30GC	GC(AT)30GC
4	GC(AT)340GC	GC(AT)340GC
5	(AT)7GG(AT)7	ATATATATATATATGGATATATATATATAT
6	C(AT)14C	C(AT)14C
7	(AC)7CC(AT)7	(AC)7CCATATATATATATAT
8	A4T8A4	A4T8A4
9	A4T8C4	A4T8C4
10	core C13	
11	core C6dUC6	
12	core C8TC6	
13	CG(TA)13GC	CGTATATATATATATATATATATATAGC
14	(AT)6ACGGCT(AT)6	ATATATATATATACGGCTATATATATATAT
15	GC(TA)13CG	GCTATATATATATATATATATATATACG
16	(AT)6AGCCGT(AT)6	ATATATATATATAGCCGTATATATATATAT
17	GC(AT)9CC(AT)9GC	GCATATATATATATATATCCATATATATATAT ATATATGC
18	GC(AT)9GG(AT)9GC	GCATATATATATATATATGGATATATATATAT ATATATGC
19	GC(AT)8GCCG(AT)8GC	GCATATATATATATATATGCCGATATATATATAT

		ATATGC
20	GC(AT)8CGGC(AT)8GC	GCATATATATATATATATCGGCATATATATATAT ATATGC
21	GC(AT)8CCCC(AT)8GC	GCATATATATATATATATCCCCATATATATATAT ATATGC
22	GC(AT)8GGGG(AT)8GC	GCATATATATATATATATGGGGATATATATATAT ATATGC
23	GC(AT)19GC-HPLC	
24	GC(AT)19GC-Kart	
25	GC(TA)13CG	GCTATATATATATATATATATATATATACG
26	(AT)6AGCCGT(AT)6	ATATATATATATAGCCGTATATATATATAT
27	(AT)6ACGGCT(AT)6	ATATATATATATACGGCTATATATATATAT
28	CG(TA)13GC	CGTATATATATATATATATATATATATAGC
29	CG(TA)13CG	CGTATATATATATATATATATATATATACG
30	(AT)4AGCCGT(AT)8	(AT)4AGCCGTATATATATATATAT
31	(AT)2AGCCGT(AT)10	(AT)2AGCCGTATATATATATATATATAT
32	AGCCGT(AT)12	AGCCGT(AT)12
33	CC(TA)13CC	CCTATATATATATATATATATATATATACC
34	GG(TA)13GG	GGTATATATATATATATATATATATATAGG
35	(AT)6ACCCCT(AT)6	ATATATATATATACCCCTATATATATATAT
36	(AT)6AGGGGT(AT)6	ATATATATATATAGGGGTATATATATATAT
37	GC(TA)10CG	GCTATATATATATATATATACG
38	(TA)5GCCG(TA)5	TATATATATAGCCGTATATATATA
39	CC(TA)13CC	CCTATATATATATATATATATATATATACC
40	(AT)6AGGGGT(AT)6	ATATATATATATAGGGGTATATATATATAT
41	CG(TA)13GC	CGTATATATATATATATATATATATATAGC
42	CC(TA)13CC	CCTATATATATATATATATATATATATACC
43	GG(TA)13GG	GGTATATATATATATATATATATATATAGG
44	(AT)6ACCCCT(AT)6	ATATATATATATACCCCTATATATATATAT
45	(AT)6AGCCGT(AT)6	ATATATATATATAGCCGTATATATATATAT
46	(AT)6ACGGCT(AT)6	ATATATATATATACGGCTATATATATATAT
47	(TA)6GGGGGG(TA)6	TATATATATATAGGGGGGTATATATATATA
48	CCC(TA)12CCC	CCCTATATATATATATATATATATATACCC
49	CC(TA)10CC	CCTATATATATATATATATATACC
50	(TA)5GGGG(TA)5	TATATATATAGGGGTATATATATA
51	CC(TA)5GGGG(TA)5CC	CCTATATATATAGGGGTATATATATACC

52	CC(TA)4GGGG(TA)4CC	CCTATATATAGGGGTATATATACC
53	GG(TA)13GG	GGTATATATATATATATATATATATATAGG
54	GG(TA)11GG	GGTATATATATATATATATATATAGG
55	GG(TA)10GG	GGTATATATATATATATATATAGG
56	GG(TA)9GG	GGTATATATATATATATATAGG
57	GG(TA)13	GGTATATATATATATATATATATATATA
58	C3(TA)4G6(TA)4C3	C3TATATATAG6TATATATAC3
59	C3(TA)3G6(TA)3C3	C3TATATAG6TATATAC3
60	C4(TA)11C4	CCCCTATATATATATATATATATATACCCC
61	A(TA)5G8(TA)5T	ATATATATATAGGGGGGGGTATATATATAT
62	CCC(TA)6	CCCTATATATATATA
63	CCC(TA)12	CCCTATATATATATATATATATATATATA
64	G4(TA)10G4	GGGGTATATATATATATATATATAGGGG
65	GG(TA)8GG	GGTATATATATATATATAGG
66	GG(TA)7GG	GGTATATATATATATAGG
67	GGG(TA)10GGG	GGGTATATATATATATATATATAGGG
68	C6(TA)12	CCCCCCTATATATATATATATATATATATA
69	GC(TA)13GC	GCTATATATATATATATATATATATATAGC
70	GG(TA)4GCGC(TA)4GG	GGTATATATAGCGCTATATATAGG
71	(GC)5(TA)10	GCGCGCGCGCTATATATATATATATATATA
72	C4(TA)3G8(TA)3C4	CCCCTATATAGGGGGGGGTATATACCCC
73	C5(TA)2G10(TA)2C5	CCCCCTATAGGGGGGGGGGTATACCCCC
74	G3(TA)10G3	GGGTATATATATATATATATATAGGG
75	G3(TA)4TGCA(TA)4G3	GGGTATATATATGCATATATATAGGG
76	G3(TA)4TCGA(TA)4G3	GGGTATATATATCGATATATATAGGG
77	G3(TA)4TTAA(TA)4G3	GGGTATATATATTAATATATATAGGG
78	G3(TA)4AATT(TA)4G3	GGGTATATATAAATTTATATATAGGG
79	G3(TA)4AGCT(TA)4G3	GGGTATATATAAGCTTATATATAGGG
80	G3(TA)4ACGT(TA)4G3	GGGTATATATAACGTTATATATAGGG
81	G3(TA)4ATAT(TA)4G3	GGGTATATATAATATTATATATAGGG
82	G3(TA)4GATC(TA)4G3	GGGTATATATAGATCTATATATAGGG
83	G3(TA)4GGCC(TA)4G3	GGGTATATATAGGCCTATATATAGGG
84	G3(TA)4GCGC(TA)4G3	GGGTATATATAGCGCTATATATAGGG
85	G3(TA)4GTAC(TA)4G3	GGGTATATATAGTACTATATATAGGG
86	G3(TA)4CATG(TA)4G3	GGGTATATATACATGTATATATAGGG
87	G3(TA)4CGCG(TA)4G3	GGGTATATATACGCGTATATATAGGG

88	G3(TA)4CCGG(TA)4G3	GGGTATATATACCGGTATATATAGGG
89	G3(TA)4CTAG(TA)4G3	GGGTATATATACTAGTATATATAGGG
90	C3(TA)5G6(TA)5C3	C3TATATATATAG6TATATATATAC3
91	G3(TA)4GC(TA)4G8	GGGTATATATAGCTATATATAG8
93	CpG 2216-AT	GGGGG(AT)3CGATCG(AT)3CG6
94	G3(TA)4TGCA(TA)4G3	GGGTATATATATGCATATATATAGGG
95	G3(TA)3T(GC)3A(TA)3G3)	GGGTATATAT(GC)3ATATATAGGG)
96	G3(TA)3(GC)4(TA)3G3	GGGTATATA(GC)4TATATAGGG
97	G3(TA)2(GC)6(TA)2G3	GGGTATA(GC)6TATAGGG
98	G3(TA)(GC)8(TA)G3	GGG(TA)(GC)8(TA)GGG
99	G3(GC)10G3	GGG(GC)10GGG
100	G3-CpG-AT	GGG(AT)3(CGAT)2(AT)2CGGGG
101	(TA)12C3	TATATATATATATATATATATATAC3
102	(TA)6C3	TATATATATATAC3
103	GFP A-B	CA3C2A3GA2TGG(CAT)2A3...
		(TA3)2GGGCAGAT2(GT)2GGAC
104	GFP B'-C	GTC(CA)3ATCTGC3T3AT3...
		A2GTGGAGAGGGTGA2GGTGA
105	GFP C'-D	TCAC2T2CAC3TCTC2ACT2...
		A3TGTTGGC2ATGGA2CAGGTAG
106	GFP D'-A	CTAC2TGT2C2ATGGC2A2...
		CAT3(ATG)2C2AT2CT3GGT3G
108	CpG-2216 AT	GGGGG(AT)3(CGAT)2(AT)2CG6
109	G3 CpG AT	GGG(AT)3CGATCG(AT)3CGGGG
110	G3-PTO	GGGTATATATATGCATATATATAGGG
111	G3NonPalin1G3	GGGCAATGGTCCTGCTGGAGTTCGGG
112	G3NonPalin1'G3	GGGGAACTCCAGCAGGACCATTGGGG
113	G3mixPalin1G3	GGGTTGAGCCACATGTGGCTCGTGGG
114	G3mixPalin1'G3	GGGACGAGCCACATGTGGCTCAAGGG
115	G3NonPalin2G3	GGGCAATGGACCTGCTGAAGTTCGGG
116	G3NonPalin2'G3	GGGGAACTTCAGCAGGTCCATTGGGG
117	G3Palin2-2'G3	GGGATGAGCCACATGTGGCTCATGGG
118	NonPal EGFP-5'	AGGGCGAGGAGCTGTTCA
119	NonPal EGFP-3'	GAACTCCAGCAGGACCATGT
120	Pal pBKS-5'	AAGGGAAGAAAGCGAAAGGA
121	Pal pBKS-3'	AATACGCAAACCGCCTCTC

122	G3(TA)10G3	GGGTATATATATATATATATATAGGG
123	A3(TA)10A3	AAATATATATATATATATATATAAAA
124	T3(TA)10T3	TTTTATATATATATATATATATATTT
125	C3(TA)10C3	CCCTATATATATATATATATATACCC
126	GFP A-C	CAAACCAAAGAATGGCATCATAAATAGTGGAGA GGGTGAAGGTGA
127	GFP C'-A'	TCACCTTCACCCTCTCCACTATTTATGATGCCAT TCTTTGGTTTG
128	GFP D'-B	CTACCTGTTCCATGGCCAACTAAATAAAGGGCA GATTGTGTGGAC
129	GFP B'-D	GTCCACACAATCTGCCCTTTATTTAGTTGGCCAT GGAACAGGTAG
130	(GATC)4	(GATC)4
131	(AGAGCTCT)2	(AGAGCTCT)2
132	(GAGCTC)3	(GAGCTC)3
133	(AGACT)3	(AGACT)3
139	(TA)6G6(TA)6	
140	C3(TA)12C3	
141	G3nonPalin1	GGGCA2TGGTC2TGCTGGAGT2C
142	NonPalin1G3	CA2TGGTC2TGCTGGAGT2CGGG
143	G3-3P	P- GGGTATATATATGCATATATATAGGG
144	3201-3P	P-(AT)12GC2GCGGC
145	GFP-C' 3P	P-TCAC2T2CAC3TCTC2ACTAT
146	GFP C'	TCAC2T2CAC3TCTC2ACTAT
147	GFP A'	T2(ATG)2C2AT2CT3GST3G
148	GFP A' 1	TATGATGC2AT2CT3GGT3G
149	GFP A' 2	(ATG)2C2AT2CT3GGT3G
150	G3-3P	GGGTATATATATGCATATATATAGGG -3P
151	D3201-3P	(AT)12GC2GCGGC-3P
152	GFP C' -3P	TCAC2T2CAC3TCTC2ACTAT 3P
153	GFP A'-C'	TATGATGCCATTCTTTGGTTTGTCACCTTCA CCCTCTCCACTATT
154	D3201	(AT)12GC2GCGGC
155	NonPalin1	CAATGGTCCTGCTGGAGTTC
156	NonPalin1'G3	GAACTCCAGCAGGACCATTGGGG
157	G3NonPalin1'	GGGGAACTCCAGCAGGACCATTG

158	NonPalin1'	GAACTCCAGCAGGACCATTG
159	GC(AT)10GC	GCATATATATATATATATATGC
160	N30TGGTCGGC	NNNNNNNNNNNNNNNNNNNNNNNNNNNNNT GGTCGGC
161	GCCGACCA	GCCGACCA
162	(AT)7A	ATATATATATATATA
163	POLY(AT)(+G+C)1	TATACATGTATACATG
164	POLY (AT)(+G+C)2	TGTATGTATACATACATA
165	POLY (AT)(+G+C)3	TATACGTATATACGTA
166	111G2NonPalin1G2	GGCAATGGTCCTGCTGGAGTTCGG
167	112G2NonPalin1'G2	GGGAACTCCAGCAGGACCATTGGG
168	141NonPalin1G2	GGCA2TGGTC2TGCTGGAGT2C
169	142G2NonPalin1G2	CA2TGGTC2TGCTGGAGT2CGG
170	155NonPalin1	CAATGGTCCTGCTGGAGTTC
171	156NonPalin1'G2	GAACTCCAGCAGGACCATTGGG
172	157G2NonPalin1'	GGGAACTCCAGCAGGACCATTG
173	158NonPalin1'	GAACTCCAGCAGGACCATTG
174	GFP A'-C' G3	GGGTATGATGCCATTCTTTGGTTTGTCACC TTCACCCTCTCCACTATTGGG
175	G3(TA)6TGCA(TA)6G3	GGGTATATATATATATGCATATATATATATAGG G
176	G3(TA)6GC(TA)6G3	GGGTATATATATATAGCTATATATATATAGGG
177	G3(TA)5TGCA(TA)5G3	GGGTATATATATATGCATATATATATAGGG
178	G3(TA)5GC(TA)5G3	GGGTATATATATAGCTATATATATAGGG
179	G3(TA)4TGCA(TA)4G3	GGGTATATATATGCATATATATAGGG
180	G3(TA)4GC(TA)4G3	GGGTATATATAGCTATATATAGGG
181	G3(TA)3TGCA(TA)3G3	GGGTATATATGCATATATAGGG
182	G3(TA)3GC(TA)3G3	GGGTATATAGCTATATAGGG
183	G3(TA)2TGCA(TA)2G3	GGGTATATGCATATAGGG
184	G4(TA)4TGCA(TA)4G4	GGGGTATATATATGCATATATATAGGGG
185	G5(TA)4TGCA(TA)4G5	GGGGGTATATATATGCATATATATAGGGGG
186	G3(TA)4TGGA(TA)4G3	GGGTATATATATGGATATATATAGGG
187	G3(TA)4TCCA(TA)4G3	GGGTATATATATCCATATATATAGGG
188	G3(TA)4CCCC(TA)4G3	GGGTATATATACCCCTATATATAGGG
198	G2(TA)13G2	GGTATATATATATATATATATATATAGG

199	XG(TA)13GX	DEAZAGTATATATATATATATATATATATATAGDEAZA
200	111-biotin	GGGCAATGGTCCTGCTGGAGTTCGGG
201	GA2(TA)10A2G	GAATATATATATATATATATAAAG
202	A2G(TA)10GA2	AAGTATATATATATATATATAGAA
203	GAG(TA)10GAG	GAGTATATATATATATATATAGAG
204	24mer Upper	ATGAGTAAAGGAGAAGAACTTTTC
205	24mer Lower	GAAAAGTTCTTCTCCTTTACTCAT
206	30mer Upper	ATGAGTAAAGGAGAAGAACTTTTCACTGGA
207	30mer Lower	TCCAGTGAAAAGTTCTTCTCCTTTACTCAT
208	44mer Upper	ATGAGTAAAGGAGAAGAACTTTTCACTGGAGTGGTCCCAGTTCT
209	44mer Lower	AGAACTGGGACCACTCCAGTGAAAAGTTCTTCTCCTTTACTCAT
210	64mer Upper	ATGAGTAAAGGAGAAGAACTTTTCACTGGAGTGGTCCCAGTTCTTGTTGAATTAGATGGCGATG
211	64mer Lower	CATCGCCATCTAATTCAACAAGAACTGGGACCACTCCAGTGAAAAGTTCTTCTCCTTTACTCAT
212	84mer Upper	ATGAGTAAAGGAGAAGAACTTTTCACTGGAGTGGTCCCAGTTCTTGTTGAATTAGATGGCGATGTT AATGGGCAAAAATTCTCT
213	84mer Lower	AGAGAATTTTTGCCCATTAACATCGCCATCTAATTCAACAAGAACTGGGACCACTCCAGTGAAAAGTTCTTCTCCTTTACTCAT
214	G5(TA)10G5	GGGGGTATATATATATATATATATAGGGGG
215	AGG(TA)4TGCA(TA)4GGA	AGGTATATATATGCATATATATAGGA
216	TGG(TA)4TGCA(TA)4GGT	TGGTATATATATGCATATATATAGGT
217	CGG(TA)4TGCA(TA)4GGC	CGGTATATATATGCATATATATAGGC
218	GG(TA)4TGCA(TA)4GG	GGTATATATATGCATATATATAGG
219	AGGGG(TA)4TGCA(TA)4GGGGA	AGGGGTATATATATGCATATATATAGGGGA
220	CGG(TA)4TGCA(TA)4GGC	CGGTATATATATGCATATATATAGGC
221	AG(TA)13GA	AGTATATATATATATATATATATATAGA
222	GAA(TA)4TGCA(TA)4AAG	GAATATATATATGCATATATATAAAG
223	GAA(TA)4TGCA(TA)4TTG	GAATATATATATGCATATATATATTG

224	TAA(TA)4TGCA(TA)4AAT	TAATATATATATGCATATATATAAAT
225	CAA(TA)4TGCA(TA)4AAC	CAATATATATATGCATATATATAAAC
226	GTT(TA)4TGCA(TA)4TTG	GTTTATATATATGCATATATATATTG
227	GCC(TA)4TGCA(TA)4CCG	GCCTATATATATGCATATATATACCG
228	NonPalin1 AAG	GAACAATGGTCCTGCTGGAGTTCAAG
229	G2(TA)10G2	GGTATATATATATATATATATAGG
230	G2(TA)13G2	GGTATATATATATATATATATATATATAGG
231	Deaza(TA)13geaza	XTATATATATATATATATATATATATAX
232	C2(TA)13C2	CCTATATATATATATATATATATATATACC
233	I2(TA)13I2 -inosin	IITATATATATATATATATATATATATAII
234	GI(TA)13IG	GITATATATATATATATATATATATATAIG
235	IG(TA)13GI	IGTATATATATATATATATATATATATAGI
236	I3(TA)13I3	IIITATATATATATATATATATATATATAIII
237	G3(TA)2GC(TA)2G3	GGGTATAGCTATAGGG
238	C3(TA)3TGCA(TA)3C3	CCCTATATATGCATATATAC3
239	G3TAGCATGCATGCTAG3	GGGTAGCATGCATGCTAGGG
240	G3TAGCTGCAGCTAG3	GGGTAGCTGCAGCTAGGG
241	GC(AT)4GC(AT)4GC	GCATATATATGCATATATATGC
242	111 1mm	GGGCAATGGTCCAGCTGGAGTTCGGG
243	111 2mm	GGGCAATGGTCCACCTGGAGTTCGGG
244	111 3mm	GGGCAATGGTCGACCTGGAGTTCGGG
245	111 4mm	GGGCAATGGTCGACGTGGAGTTCGGG
246	111 +5mm	GGGCTATGGTCCTGCTGGAGTTCGGG
247	111 +15mm	GGGCAATGGTCCTGCTGGAGTACGGG
248	111 28mer	GGGTGACCAATGGTCCTGCTGGAGTTCCAGTGGG
249	111 26mer	GGGTGACAATGGTCCTGCTGGAGTTCAGTGGG
250	111 24mer	GGGTGCAATGGTCCTGCTGGAGTTCGTGGG
251	111 22mer	GGGTCAATGGTCCTGCTGGAGTTCTGGG
252	111 18mer	GGGAATGGTCCTGCTGGAGTTGGG
253	111 16mer	GGGATGGTCCTGCTGGAGTGGG
254	111 14mer	GGGTGGTCCTGCTGGAGGGG
255	111 12mer	GGGGGTCCTGCTGGAGGG
256	112 28mer	GGGACTGGAACTCCAGCAGGACCATTGGTCAGGG
257	112 26mer	GGGACTGAACTCCAGCAGGACCATTGTCAGGG

258	112 24mer	GGGACGAACTCCAGCAGGACCATTGCAGGG
259	112 22mer	GGGAGAACTCCAGCAGGACCATTGAGGG
260	112 18mer	GGGAACTCCAGCAGGACCATTGGG
261	112 16mer	GGGACTCCAGCAGGACCATGGG
262	112 14mer	GGGCTCCAGCAGGACCAGGG
263	112 12mer	GGGTCCAGCAGGACCGGG
264	115i no G3	CAATGGACCTGCTGAAGTTC
265	116a G3 5'	GGGGAACTTCAGCAGGTCCATTG
266	116b G3 3'	GAACTTCAGCAGGTCCATTGGGG
267	GG(TA)13GG	GGTATATATATATATATATATATATAGG
268	GA(TA)13AG	GATATATATATATATATATATATATAAG
269	GT(TA)13TG	GTTATATATATATATATATATATATATG
270	GC(TA)13CG	GCTATATATATATATATATATATATACG
271	AG(TA)13GA	AGTATATATATATATATATATATATAGA
272	AA(TA)13AA	AATATATATATATATATATATATATAAA
273	AT(TA)13TA	ATTATATATATATATATATATATATATA
274	AC(TA)13CA	ACTATATATATATATATATATATATACA
275	TG(TA)13GT	TGTATATATATATATATATATATATAGT
276	TA(TA)13AT	TATATATATATATATATATATATATAAT
277	TT(TA)13TT	TTTATATATATATATATATATATATATT
278	TC(TA)13CT	TCTATATATATATATATATATATATACT
279	CG(TA)13GC	CGTATATATATATATATATATATATAGC
280	CA(TA)13AC	CATATATATATATATATATATATATAAC
281	CT(TA)13TC	CTTATATATATATATATATATATATATC
282	CC(TA)13CC	CCTATATATATATATATATATATATACC
283	IInonPalin26II	IIACTCAATGGTCCTGCTGGAGTTCACTII
284	GGnonPalin26GG	GGACTCAATGGTCCTGCTGGAGTTCACTGG
285	TTnonPalin26TT	TTACTCAATGGTCCTGCTGGAGTTCACTTT
286	AAnonPalin26AA	AAACTCAATGGTCCTGCTGGAGTTCACTAA
287	CCnonPalin26CC	CCACTCAATGGTCCTGCTGGAGTTCACTCC
288	IInonPalin26'II	IIAGTGAACTCCAGCAGGACCATTGAGTII
289	GGnonPalin26'GG	GGAGTGAACTCCAGCAGGACCATTGAGTGG
290	TTnonPalin26'TT	TTAGTGAACTCCAGCAGGACCATTGAGTTT
291	AAnonPalin26'AA	AAAGTGAACTCCAGCAGGACCATTGAGTAA
292	CCnonPalin26'CC	CCAGTGAACTCCAGCAGGACCATTGAGTCC
293	nonPalin26'	AGTGAACTCCAGCAGGACCATTGAGT

294	GGG(TA)10GGG	GGGTATATATATATATATATATAGGG
295	GGA(TA)10AGG	GGATATATATATATATATATATAAGG
296	GGT(TA)10TGG	GGTTATATATATATATATATATATGG
297	GGC(TA)10CGG	GGCTATATATATATATATATATACGG
298	GAG(TA)10GAG	GAGTATATATATATATATATATAGAG
299	GAA(TA)10AAG	GAATATATATATATATATATATAAAG
300	GAT(TA)10TAG	GATTATATATATATATATATATATAG
301	GAC(TA)10CAG	GACTATATATATATATATATATACAG
302	GTG(TA)10GTG	GTGTATATATATATATATATATAGTG
303	GTA(TA)10ATG	GTATATATATATATATATATATAATG
304	GTT(TA)10TTG	GTTTATATATATATATATATATATTG
305	GTC(TA)10CTG	GTCTATATATATATATATATATACTG
306	GCG(TA)10GCG	GCGTATATATATATATATATATAGCG
307	GCA(TA)10ACG	GCATATATATATATATATATATAACG
308	GCT(TA)10TCG	GCTTATATATATATATATATATATCG
309	GCC(TA)10CCG	GCCTATATATATATATATATATACCG
310	FAM-G3NonPalinG3 (111)	FAM-GGGCAATGGTCCTGCTGGAGTTCGGG
311	C3NonPalin1'C3 (112 w/C3)	CCCGAACTCCAGCAGGACCATTGCCC
312	G3NonPalin1'G3 (112)	GGGGAACTCCAGCAGGACCATTGGGG
313	C3NonPalin1C3 (111 w/ C3)	CCCCAATGGTCCTGCTGGAGTTCCCC
314	NonPalin1' (112, no G)	FAM-GAACTCCAGCAGGACCATTG-BHQ_